1986-12

Film condensation of steam on low-integral finned tubes with drainage strips

Cakan, Oguz

NAVAL POSTGRADUATE SCHOOL
Monterey, California

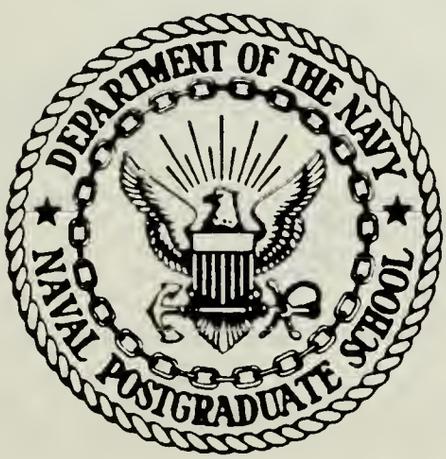

THESIS

FILMWISE CONDENSATION OF STEAM ON LOW
INTEGRAL-FINNED TUBES
WITH DRAINAGE STRIPS

by

Oguz Cakan

December 1986

Thesis Advisor P. J. Marto
Co-Advisor A. S. Wanniarachchi

Approved for public release; distribution is unlimited.

SECURITY CLASSIFICATION OF THIS PAGE

REPORT DOCUMENTATION PAGE

1a REPORT SECURITY CLASSIFICATION UNCLASSIFIED	1b. RESTRICTIVE MARKINGS
2a SECURITY CLASSIFICATION AUTHORITY	3 DISTRIBUTION/AVAILABILITY OF REPORT Approved for public release; distribution unlimited.
2b DECLASSIFICATION / DOWNGRADING SCHEDULE	
4 PERFORMING ORGANIZATION REPORT NUMBER(S)	5 MONITORING ORGANIZATION REPORT NUMBER(S)
6a NAME OF PERFORMING ORGANIZATION Naval Postgraduate School 6b OFFICE SYMBOL (If applicable) 69	7a NAME OF MONITORING ORGANIZATION Naval Postgraduate School
6c ADDRESS (City, State, and ZIP Code) Monterey, California 93943-5000	7b ADDRESS (City, State, and ZIP Code) Monterey, California 93943-5000
8a NAME OF FUNDING / SPONSORING ORGANIZATION National Science Foundation 8b OFFICE SYMBOL (If applicable)	9 PROCUREMENT INSTRUMENT IDENTIFICATION NUMBER
8c ADDRESS (City, State, and ZIP Code) Washington, DC 20550	10 SOURCE OF FUNDING NUMBERS PROGRAM ELEMENT NO / PROJECT NO / TASK NO / WORK UNIT ACCESSION NO

11 TITLE (Include Security Classification)

FILM CONDENSATION OF STEAM ON LOW-INTEGRAL FINNED TUBES WITH DRAINAGE STRIPS

12 PERSONAL AUTHOR(S)
Cakan, Oguz

13a TYPE OF REPORT	13b TIME COVERED	14 DATE OF REPORT (Year, Month, Day)	15 PAGE COUNT
Master's Thesis	FROM _____ TO _____	1986 December	106

16 SUPPLEMENTARY NOTATION

17 COSATI CODES			18 SUBJECT TERMS (Continue on reverse if necessary and identify by block number)
FIELD	GROUP	SUB-GROUP	Steam, Condensation, Filmwise, Condensate Retention Drainage Strips, Heat-Transfer Coefficient, Finned Tubes

19 ABSTRACT (Continue on reverse if necessary and identify by block number)

Heat-transfer measurements were made for filmwise condensation of steam under low pressure and at near-atmospheric pressure on horizontal finned tubes attached with bronze porous and solid drainage strips. The effects of drainage strip type, height and thickness were investigated. A total of sixteen drainage strips were manufactured and tested on two finned tubes each with a fin thickness and height of 1.0 mm and with a fin spacing of 0.5 mm and 1.0 mm.

The heat-transfer performance generally increased with increasing porous height up to a possible optimum value between 11 and 15 mm. Of the pore diameters tested (0.05-0.013 mm, 0.025-0.05 mm and 0.0025-0.013 mm), the strip with an average pore diameter of 0.025 -0.05 mm gave the best heat-transfer performance. This optimum strip type showed an optimum strip thickness of 5.2 mm. The solid strips showed an optimum strip thickness of 1.5 mm. The optimum porous strip gave a 9% and 17% greater steam-side

20 DISTRIBUTION / AVAILABILITY OF ABSTRACT ☒ UNCLASSIFIED/UNLIMITED ☐ SAME AS RPT ☐ DTIC USERS	21 ABSTRACT SECURITY CLASSIFICATION UNCLASSIFIED
22a NAME OF RESPONSIBLE INDIVIDUAL P. J. Marto	22b TELEPHONE (Include Area Code) 408-646-2586 22c OFFICE SYMBOL 69Mx

DD FORM 1473, 84 MAR 83 APR edition may be used until exhausted
All other editions are obsolete

SECURITY CLASSIFICATION OF THIS PAGE

19 Abstract (Continued)

enhancement than the optimum solid strip for low and atmospheric pressures, respectively. For the finned tube with a fin spacing of 0.5 mm, a maximum enhancement of about 1.6 was found when it was attached with 5.2-mm-thick and 8-mm-high porous strip having a pore diameter of 0.025-0.05 mm.

Approved for public release; distribution is unlimited.

Filmwise Condensation of Steam on Low integral-Finned Tubes with Drainage Strips

by

Oguz Çakan
Lieutenant JG, Turkish Navy
B. S., Turkish Naval Academy, 1980

Submitted in partial fulfillment of the
requirements for the degree of

MASTER OF SCIENCE IN MECHANICAL ENGINEERING

from the

NAVAL POSTGRADUATE SCHOOL
December 1986

ABSTRACT

Heat-transfer measurements were made for filmwise condensation of steam under low pressure and at near-atmospheric pressure on horizontal finned tubes attached with bronze porous and solid drainage strips. The effects of drainage strip type, height and thickness were investigated. A total of sixteen drainage strips were manufactured and tested on two finned tubes each with a fin thickness and height of 1.0 mm and with a fin spacing of 0.5 mm and 1.0 mm.

The heat-transfer performance generally increased with increasing porous strip height up to a possible optimum value between 11 and 15 mm. Of the pore diameters tested (0.05-0.013 mm, 0.025-0.05 mm and 0.0025-0.013 mm), the strip with an average pore diameter of 0.025-0.05 mm gave the best heat-transfer performance. This optimum strip type showed an optimum strip thickness of 5.2 mm. The solid strips showed an optimum strip thickness of 1.5 mm. The optimum porous strip gave a 9% and 17% greater steam-side enhancement than the optimum solid strip for low and atmospheric pressures, respectively. For the finned tube with a fin spacing of 0.5 mm, a maximum enhancement of about 1.6 was found when it was attached with a 5.2-mm-thick and 8-mm-high porous strip having a pore diameter of 0.025-0.05 mm.

TABLE OF CONTENTS

LIST OF TABLES

LIST OF FIGURES

ACKNOWLEDGEMENTS

The author would like to express his appreciation to Professor P. J. Marto and Dr. A. S. Wanniarachchi for their guidance and support in completing this work.

The author would also like to thank Mr. Tom McCord and his machine shop crew for their support.

I. INTRODUCTION

A. BACKGROUND

An investigation of the fundamental heat-transfer mechanisms which occur during film condensation on horizontal finned tubes can lead to improved condenser performance and can reduce construction cost and weight. In steam condensers, even though a large thermal resistance occurs on the cooling-water side, a significant improvement in overall heat transfer can still be accomplished by using integral-fin tubing on the steam side.

The theoretical treatment of steam condensation on horizontal finned tubes is very difficult due to the large number of controlling parameters, such as gravitational and surface tension forces, and fin spacing, height, thickness and shape, all of which leads to three-dimensional flow of condensate. Due to the complexity of the problem, any theoretical model requires simplifying assumptions, thus leading to questionnable results. Therefore, a large pool of reliable data, systematically covering all of the relevant variables, is essential in order to test simplified theoretical models or to arrive at a satisfactory correlation or to achieve both.

It is well known that during filmwise condensation on finned tubes, the condensate tends to collect in the interfin space on the lower portion of the tube. This phenomenon is referred to as condensate flooding or retention. Earlier investigators [Refs. 1,2,3] have demonstrated that the extent of flooding can be reduced considerably by attaching drainage strips at the bottom of horizontal finned tubes, and this should improve upon the finned-tube performance. Attaching such strips may be somewhat impractical for large condensers. However, the application of such drainage strips may be practical for small condensers containing, for example, only a few tubes.

Further, as discovered by Wanniarachchi et al. [Ref. 4], a copper finned tube having a fin spacing of 0.5 mm (with fin thickness and height of 1.0 mm) gave a significant steam-side enhancement even though this tube was fully flooded by condensate (i.e., water). In fact, this tube gave enhancement ratios (i.e., the steam-side coefficient of the finned tube to the smooth-tube value for constant heat flux) of about 2.4 and 4.0 under low and at atmospheric pressures, respectively. The area enhancement due to finning was about 2.4 for this tube. If pure conduction of heat is

assumed to occur within the liquid-filled grooves of the flooded portion, theoretical calculations were shown to underpredict the steam-side enhancement by a factor of 3 or more. Therefore, the mechanism occurring within the flooded portion of a finned tube is more than pure conduction and must include convective effects. As a consequence, data taken with and without drainage strips may help to understand the complex mechanisms involved, particularly those occurring in the flooded region of a finned tube. This thesis is an initial attempt to investigate the effect of drainage strips on finned tube performance.

B. OBJECTIVES OF THIS THESIS

Based on the foregoing discussion, the main objectives of this thesis are as follows:

1. Show repeatability of data with those reported by previous thesis students [Refs. 5,6,7],
2. Study the effect of different porous strip types and geometries on the heat-transfer performance of two copper finned tubes with rectangular fins, and
3. Study the effect of different solid strip geometries on the heat-transfer performance of the same finned tubes in item (2) above.

II. EARLIER INVESTIGATIONS ON HORIZONTAL FINNED TUBES

A. GENERAL OBSERVATIONS

When vapor condenses in a filmwise mode on smooth horizontal tubes, a condensate film always exists around the tube. The latent heat released by the vapor will eventually be absorbed by the coolant that flows through the tube. The condensate film provides a resistance to this heat flow because of the low conductivity of the liquid. This resistance increases as the film thickness increases. At the top of the tube, the condensate film thickness is small (the resistance is low) and it increases with increasing distance around the perimeter of the tube. Since the thermal resistance of the condensate limits the heat-transfer performance of the tube, to enhance heat transfer, it is necessary to reduce condensate film thickness. For horizontal tubes, thinning of the condensate film may be achieved by using a finned surface.

On a finned tube, the flow of condensate between the fins depends on the ratio of surface tension forces to gravity forces. The surface tension effect on the behavior of the condensate is composed of two factors. One is the effect of reducing the condensate film thickness on the fin flanks in the unflooded region of the tube, which leads to enhanced heat transfer. In this region, the condensate on the fin surface is driven by combined gravity and surface tension forces into the fin root where it is drained by gravity. The other factor is the effect of retaining condensate between the fins on the lower, flooded region of the tube, which leads to a decrease in effective surface area. The flooded portion of the tube is defined by the retention angle, (ψ) (i.e., the angle from the bottom of the tube to the highest position on the tube where the interfin space is still full of condensate) as shown schematically in Figure 2.1. Decreasing the retention angle increases the heat-transfer performance. Therefore, any means of reducing the retention angle is beneficial. One way to decrease the retention angle is by attaching a porous drainage strip at the lower part of the tube as shown schematically in Figure 2.1. If the condensate retention angle is large, a significant heat-transfer enhancement can be achieved by the use of a drainage strip.

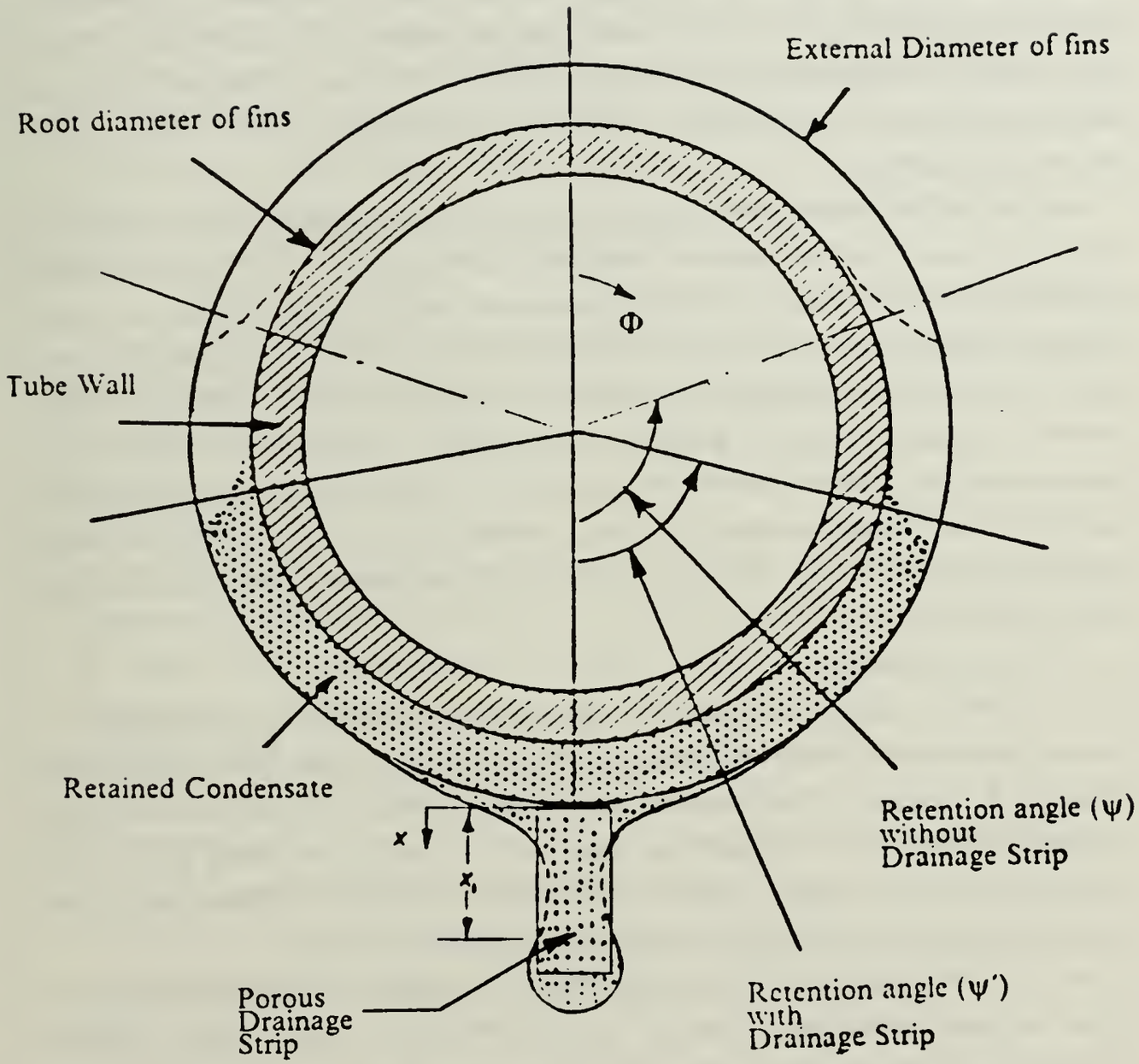

Figure 2.1 Schematic of Condensate Retention on a Finned Tube with and without a Porous Drainage Strip.

B. EXPERIMENTAL STUDIES

1. Condensate Retention Angle

In 1946, the first measurements of the condensate retention angle (i.e., the extent of 'flooding') on finned tubes were made by Katz et al. [Ref. 8]. These mesurements were made under static conditions (i.e., no condensation taking place), using water, aniline, acetone and carbon tetrachloride on a number of tubes with different fin densities (276 to 984 fins/m), and fin heights (1.2 to 5.7 mm). It was shown that condensate retention depended mainly on the ratio of surface tension to liquid density and on the fin spacing, and, in some circumstances, the condensate could flood the entire tube.

In recent years, various measurements of the condensate-retention angle, ψ, have been made both for static and condensing conditions. In 1981, Rudy and Webb [Ref. 9] made measurements of condensate-retention angles on finned tubes with three different fin densities (748, 1024, 1378 fins/m) using water, R-11, and n-pentane as test fluids. Their results showed that the retention angle increases with increasing surface tension to density ratio of the fluid. Honda et al. [Ref. 1] in 1983 reported measurements on finned tubes with ethanol and R-113 for both static and condensing conditions and found essentially the same results. Yau et al. [Ref. 2] also made measurements under static conditions for a range of fin densities using water, ethylene glycol and R-113.

2. Heat Transfer

In 1948, Beatty and Katz [Ref. 10] performed experiments with propane, n-butane, sulfur-dioxide, methyl chloride, and R-22 on single finned tubes with densities from 422 to 630 fins/m. They reported enhancements of up to 2.3 on the overall heat-transfer coefficient for the finned tubes compared to smooth tubes using R-22, with a water-side velocity of 6 ft/sec. However, they did not compare the enhancement on the outside heat-transfer coefficient, which would have been about six.

In 1971, Karkhu and Borovkov [Ref. 11] obtained data for condensation of steam at near-atmospheric pressure on four horizontal tubes having different configurations of trapezoidally shaped fins. They reported that, for transverse fins and with large Weber numbers (i.e., larger surface tension forces in relation to gravity forces), the average condensation heat-transfer coefficient increased by 50 to 100 percent over smooth-tube values whereas for low Weber numbers, there was little or no improvement.

In 1980, Carnavos [Ref. 12] tested a wide variety of finned tubes using R-11 and discovered gains in the heat-transfer coefficient as much as 5 times the smooth-tube result. Rudy and Webb [Ref. 9] in 1983 reported data for R-11 condensing on four tubes with different fin geometries. Their results indicated vapor-side coefficients exceeding Nusselt values by factors of about 7 to 9 (for constant temperature drop across the condensate film). Honda et al. [Ref. 1] in 1983 tested four low-fin tubes with different fin geometries using methanol and R-113 as condensing fluids. Vapor-side enhancements of 9 for R-113 and 6 for methanol were found. Yau et al. [Ref. 2] in 1984 reported heat-transfer coefficients for steam at atmospheric pressure condensing on thirteen tubes with rectangular-section fins for which the fin spacing was the only variable. They reported vapor-side enhancements (for the same heat flux) up to almost 4 for the tube with a fin spacing of 1.5 mm.

During the last four years, a wide variety of data has been obtained at the Naval Postgraduate School (NPS) for film condensation of steam on horizontal finned tubes under a grant from the National Science Foundation. The basic test apparatus was constructed by Krohn [Ref. 13]. Graber [Ref. 14] provided the instrumentation and took preliminary data as the system experienced problems with non-condensing gases and partial dropwise condensation on copper tubes. Poole [Ref. 15] made further improvements on the apparatus especially for leak tightness. He operated the apparatus both under low pressure and at atmospheric pressure, and tested a total of six finned tubes, with different fin spacings, as well as a smooth tube. Poole had problems due to the occurrence of partial dropwise condensation. Using this system, Georgiadis [Ref. 5] was able to obtain complete filmwise condensation on a smooth tube and on 21 finned copper tubes having rectangular-section fins. Based on both low pressure and atmospheric runs, Georgiadis reported an optimum fin spacing of 1.5 mm and an optimum fin thickness of 0.75 to 1.0 mm. Among the finned tubes with a fin height of 1.0 mm, the tube with a fin spacing of 1.5 mm and fin thickness of 1.0 mm provided the best heat-transfer performance. This tube resulted in a steam-side enhancement (i.e., the ratio of steam-side coefficient for the finned tube to the value for the smooth tube for the same heat flux) of about 4 and 5.7 at low pressure and at atmospheric pressure, respectively.

Flook [Ref. 6] tested 19 additional tubes. These tubes included two sets of four tubes with fin heights of 0.5 and 1.5 mm, respectively. He found an optimum fin spacing of about 2.0 mm for rectangularly-shaped fins with a fin thickness of 1.0 mm,

and fin height of 0.5 mm and 1.5 mm. He obtained maximum enhancements of about 4.8 and 6.9 at low and atmospheric pressures respectively.

Continuing with this investigation, Mitrou [Ref. 7] obtained data for 26 copper tubes with circular fins of rectangular, triangular, trapezoidal and parabolic cross sections, for spiral fins of triangular cross section and for wire-wrapped tubes. A near-parabolic fin shape that provides a gradually decreasing curvature from fin tip to fin root resulted in a 10 to 15 percent increase in steam-side heat-transfer coefficient over other fin shapes. Therefore, he concluded that fin shape does not appear to be as crucial a variable as fin spacing [Ref. 16].

Because of the low thermal conductivity of non-metallic liquids, heat transfer through the flooded portion of a finned tube should be considerably lower than that through the unflooded portion. However, as stated in Chapter I, Wanniarachchi et al. [Ref. 4] showed considerable enhancement for a finned tube with a fin spacing of 0.5 mm, which was fully flooded by condensate both at low and atmospheric pressures.

3. Effect of Drainage Strip

In 1983, Honda et al. [Ref. 1] tested four low-finned tubes attached with a porous drainage strips on the underside of the tubes. The enhancement ratio (i.e., the vapor-side coefficient of the finned tube to the smooth-tube value for constant heat flux) was found to be about 12 and 10 for R-113 and methanol, respectively. These ratios were 10 and 9 without the drainage strips. They also pointed out that condensate retention between the fins is considerably reduced by attaching porous strips.

In 1984, Yau, Cooper and Rose [Ref. 2] tested two low-finned tubes with solid copper drainage strips fitted to the lower edge of the tube. These two tubes had fin spacings of 1.5 and 2.0 mm, a fin height of 1.0 mm, a fin thickness of 0.5 mm, and a fin root diameter of 12.7 mm. They reported that the presence of the drainage strip resulted in vapor-side enhancement ratios of 3.6 and 4.4 (compared to 2.8 and 3.7 without the drainage strips) for tubes with fin spacings of 2.0 mm and 1.5 mm, respectively.

C. THEORETICAL MODELS

1. Condensate Retention Angle

Independent condensate retention studies by Rudy and Webb [Refs. 19,20], Owen et al. [Ref. 21] and Honda et al. [Ref. 1] have led essentially to the same result. For a finned tube, having fins of arbitrary shape, Rudy and Webb give:

$$\psi = \cos^{-1}(1 - R/W) \qquad \text{(eqn 2.1)}$$

where

$$R = 2\sigma[(t_t + 2\,e) - t_b]\,, \qquad \text{(eqn 2.2)}$$

$$W = D_o\rho_f g\,[(t_b + s_b)\,e - A_p]\,, \text{ and} \qquad \text{(eqn 2.3)}$$

where

A_p = profile area of fin over fin cross section,
D_o = fin-tip diameter,
e = fin height,
g = acceleration of gravity,
t_t = thickness of fin at tip,
s_b = spacing of fin at base,
t_b = thickness of fin at base,
ρ_f = density of condensate, and
ψ = retention angle measured from the bottom of the tube to the position at which the interfin space is just filled with condensate.

Honda et al. [Ref. 1] obtained ψ for the case where the fin flank is just wholly wetted

$$\psi = \cos^{-1}[1 - (4\sigma\cos\theta)/(D_o\rho_f g\, s_b)] \qquad \text{(eqn 2.4)}$$

where θ is the fin half-angle at the fin tip. Note that for rectangular-section fins, θ equals zero. Therefore, equations (2.1) and (2.4) are identical for tubes with rectangular-section fins. The final result of Owen et al. was also same as expressed by equation (2.4), except that they considered only rectangular-section fins (i.e., $\cos\theta$ = 1.0). Notice that the above equations predict an increase in retention angle as the surface tension to density ratio σ/ρ increases. Also, for a given fluid/tube combination, the retention angle will increase as fin spacing s_b decreases. A tube would be fully flooded if $s_b \leq 4\sigma/(D_o\rho_f g)$.

2. **Heat Transfer**

In 1948, Beatty and Katz [Ref. 10] developed a model to predict the heat-transfer coefficient for condensation on horizontal finned tubes, as shown in equation (2.5). This was essentially a combination of Nusselt equations for the vertical plane surfaces of the fin flanks and for the cylindrical surface of the tube in the interfin spaces. They did not take into account surface-tension effects for thinning the condensate along the fin height. They also neglected condensate retention, assumed gravity to be entirely responsible for the flow of condensate and modified the customary leading constant (0.728) found in the Nusselt equation to fit their experimental data. However, the result was simple and readily usable, and was found to give coefficients within 11% of measured values for a variety of non-aqueous (i.e., low-surface-tension) fluids.

$$h_{BK} = 0.689\ F^{1/4}\ \left(\frac{1}{\Delta T_{vf}}\right)^{1/4}\ \left(\frac{1}{D_e}\right)^{1/4} \qquad \text{(eqn 2.5)}$$

where

$$F = (k_f^3 \rho_f^2\ g\ h_{fg})/\mu_f\ ,$$

$$(D_e)^{-1/4} = A_r/A_{eff} D_r^{-1/4} + 1.3(\eta A_f/A_{eff}) x^{-1/4}\ ,$$

$$A_r = \pi\ D_r L\ , \qquad \text{(eqn 2.6)}$$

$$A_f = 0.5\pi(D_o^2 - D_r^2)\ N\ L\ , \qquad \text{(eqn 2.7)}$$

$$A_{eff} = A_r + \eta A_f\ , \text{and} \qquad \text{(eqn 2.8)}$$

$$x = 0.25\pi(D_o^2 - D_r^2)/D_o\ . \qquad \text{(eqn 2.9)}$$

where

h_{BK} = average vapor-side heat-transfer coefficient,
A_{eff} = effective area of finned tubes,
A_f = fin surface area,
A_r = surface area of tube at base of fins,
D_e = equivalent tube diameter,
D_r = root diameter of the finned tube,
D_o = fin-tip diameter,
h_{fg} = specific enthalpy of vaporization,
k_f = thermal conductivity of condensate,
η = fin efficiency (1.0 for low-finned copper tubes),
ΔT_{vf} = vapor-side temperature drop,
μ_f = viscosity of condensate,
L = tube length,
N = number of fins per unit length, and
x = mean effective height of fins.

More recent studies stem from the work of Gregorig [Ref. 18] for fluted surfaces. Gregorig drew attention to the significance of the pressure gradient in the condensate film resulting from surface tension in the presence of surface curvature. Thus, for the two-dimensional case,

$$dP/ds = \sigma\, d(r^{-1})/ds \qquad \text{(eqn 2.10)}$$

where P is pressure, s is distance along the surface and r is the radius of curvature of the liquid surface.

In 1971, Karkhu and Borovkov [Ref. 11], considering horizontal finned tubes, took the pressure gradient to be uniform over the fin flank and equal to the value given by estimates of the radii of curvature at the top and root of the fin, and they found an analytical expression for the heat-transfer coefficient as:

$$h_{av} = G\, h_{fg}/[F_s(T_s - T_r)] \qquad \text{(eqn 2.11)}$$

$$F_s = (s + b + e/\cos\theta)\, \pi R_r \qquad \text{(eqn 2.12)}$$

where

h_{av} = average heat-transfer coefficient,
G = condensate flow rate,
h_{fg} = specific enthalpy of vaporization,
F_s = effective condensation surface area,
s = fin spacing,
b = half of fin tip width,
e = fin height,
θ = fin semivertex angle,
R_r = root radius of the finned tube,
T_s = vapor saturation temperature, and
T_r = fin-root temperature.

They solved the heat conduction equation over the fin to find the temperature distribution over the fin height. They also found the vapor-side coefficients to be 50 to 100 percent greater than that for a smooth tube and reported that their predictions agreed to within ± 5% with their experimental data.

In 1980, Rifert [Ref. 22] analyzed condensation of vapor on horizontal finned tubes enhanced by the effect of surface-tension forces. In this analysis, he divided the tube into flooded and unflooded zones and solved a two-dimensional form of the energy equation for each zone. The mean heat flux was then determined by integration over each zone over the tube length. In cases where condensate is retained in more than half of the tube perimeter, Rifert indicated that a three-dimensional form of the energy equation must be used. Solutions to these equations revealed that, in most cases, the fin temperature is very nonuniform and it depends on the properties of the wall and the vapor and the heat flux. He stated that for a highly non-isothermal fin surface, the use of an average temperature drop from vapor to the outer wall temperature (ΔT) yields computed heat flux values that are very sensitive to ΔT. Since this is unacceptable, he recommended the use of the average heat flux for the computation.

Based on their study of condensate-retention measurements mentioned earlier [Ref. 9], Rudy and Webb [Ref. 19] proposed that the Beatty and Katz [Ref. 10] heat-transfer-coefficient equation (2.5) be modified to account for condensate retention, as shown below:

$$h = h_{BK}[(\pi-\psi)/\pi] \qquad \text{(eqn 2.13)}$$

Equation (2.13) neglects heat transfer through the flooded portion of the tube. As a result, this equation was shown to underpredict the heat-transfer coefficient of condensing R-11 by up to 30 percent. They recognized that the surface tension effect must be taken into account. Rudy and Webb [Ref. 23] later modified the above result after replacing h_{BK} in equation (2.13) by an expression which included surface tension. Once again, they assumed no heat transfer through the flooded portion and arrived at the resulting expression:

$$h = [0.725\ \kappa\ A_r/A_{bt} + 0.943\ \mathbf{M}\ \eta A_{ft}/A_{bt}](\pi-\psi)/\pi \qquad \text{(eqn 2.14)}$$

where

$\kappa = [k_f^3\rho_f^2 h_{fg} g/(D_o\mu_f\Delta T)]^{1/4}$

$\mathbf{M} = [k_f^3\rho_f h_{fg}\sigma(r_A + r_B)/(\mu_f e^2 r_A r_B \Delta T)]^{1/4}$

$A_{bt} = \pi D_o L$

$A_r = \pi D_r L$

A_{ft} = fin surface area,

D_o = fin-tip diameter,

D_r = root diameter of the finned tube,

L = length of the tube,

η = fin efficiency,

r_A = radius of curvature of condensate film at fin tip, and

r_B = radius of curvature of condensate film at fin base.

This expression provided an accuracy of better than 10% for condensation of R-11 on short, finely-spaced fins, but the accuracy dropped sharply with fins of increasing height and for larger fin spacing. This was due to the assumed linear pressure gradient on the fin surface as this model is not valid when gravity forces become dominant (i.e., as height of fin increases). According to the authors, as the pressure gradient decreases, the gravity force acting on the condensate begins to have more effect in pulling the condensate in the gravity direction. On the circumference of the tube, the gravity and radial directions are common only at the top of the tube. Therefore, equation (2.14) is valid for fin densities from 1200 to 1400 fins/m, and fin heights of less than 1 mm.

Honda and Nozu [Ref. 24] in 1984 reported on a complex and comprehensive approach to the problem. They divided the tube into flooded and unflooded regions. Account was taken of both gravitational and surface-tension forces. The condensate film profile on the fin flank was determined by incorporating the surface-tension-induced pressure gradient term in the momentum equation. Numerical solutions were obtained subject to prescribed boundary conditions and the results required additional integration to account for the difference in tube wall temperature in the flooded and unflooded parts of the tube. Their model predicted the vapor-side heat-transfer coefficient within ± 20% for most of the available data including 11 fluids and 22 tubes. However, the complexities associated with this model make it very difficult to use as a design tool.

In 1985 Webb, Rudy and Kedzierski [Refs. 25,26] developed a fairly simple model that shows some promise. When considering the unflooded region, they treated separately the interfin cylindrical surface and the fin flanks. For the latter, they used the heat-transfer coefficient proposed by Adamek [Ref. 27] who conducted theoretical work on surface-tension-driven condensation on a family of condensate surface profiles with curvatures given by:

$$r^{-1} = \theta_m(\xi + 1)[1-(s/S_m)^{\xi})/(S_m\,\xi)] \qquad \text{(eqn 2.15)}$$

where

s = coordinate along condensate film surface from fin tip,
S_m = length of convex surface of fin condensate film,
θ_m = rotation angle of normal to condensate film surface, and
ξ = parameter characterizing the aspect ratio of the fin cross section.

For the flooded region, Webb et al. developed a computer code which analyzed a two-dimensional conduction model to solve for the heat flux (q_{b2}) into the tube-side coolant which was compared to the heat flux (q_{b1}) assuming zero fin thickness. This ratio ($\Phi = q_{b2}/q_{b1}$) was used along with a linear temperature profile across the condensate film to establish a heat-transfer coefficient for this flooded region. Their model was shown to predict the heat-transfer coefficient within 20% for R-11 condensing on horizotal finned tubes with fin densities of 748, 1024, and 1378 fins/m. Also, Wanniarachchi et al. [Ref. 28] have shown this model to predict their

steam condensation data on five finned tubes within ± 20% at low (~85 mm Hg) and atmospheric pressures except for a sixth tube, which was fully flooded. For this tube, the model underpredicts the data by factors of 2.3 and 3.3 for atmospheric and low-pressure conditions, respectively. These tubes had rectangular-section fins with fin thickness and height of 1.0 mm and fin spacings of 0.5, 1.0, 1.5, 2.0, 4.0 and 9.0 mm on a root diameter of 19.0 mm.

3. **Effect of Drainage Strip**

Figure 2.1 shows schematic cross sections of a finned tube with and without a drainage strip. As can be seen, the presence of a drainage strip creates a smaller retention angle. If the strip is solid, the lower pressure at the bottom of the tube is pressumed to be caused by the small radius of curvature (concave shape) near the strip and the tube. For this reason, solid strip height may not play an important role in reducing the retention angle. On the other hand, with the use of a porous strip, it may be possible to achieve a further decrease in the retention angle owing to even smaller radii of curvature than can be achieved as a result of the porous structure.

In 1985, Honda and Nozu developed a model [Ref. 3] to predict the heat-transfer performance with a porous drainage strip attached at the lower part of a finned tube. They assumed that the mechanisms of condensate flow and heat transfer in the unflooded and flooded regions of the tube are basically the same as for the case of a finned tube without the drainage strip; but the retention angle is reduced in magnitude. Consequently, following the theory developed in [Ref. 24], they expressed the average Nusselt number as:

$$Nu = \frac{Nu_u \eta_u (1-T_{wu})\Phi_f + Nu_f \eta_f (1-T_{wf})(1-\Phi_f)}{(1-T_{wu})\Phi_f + (1-T_{wf})(1-\Phi_f)} \qquad \text{(eqn 2.16)}$$

where Nu_i, η_i and T_{wi} are the Nusselt number, the fin efficiency and the dimensionless average wall temperature at the fin root for region i (i = unflooded region, flooded region), respectively. They give the expressions for Nu_i, η_i and T_{wi} in [Ref. 24] and Φ_f is given by equation (2.17). Their model agreed within ± 10% with most of the experimental data [Ref. 1] for methanol and R-113.

In 1985, Honda and Nozu [Ref. 3] studied experimentally and analytically the effects of solid and porous drainage strips with various heights. For porous drainage strips, they derived the following expressions:

$$\Phi_f = \cos^{-1}(G/\pi) \qquad \text{(eqn 2.17)}$$

where

$G = (4\sigma\cos\theta/s_t - 2\Delta P_2)\rho g\, d_o - 1$,

$\Delta P_2 = \rho g(1 - F/K)\, x_1$, and

$F = \pi d_o q \nu/(\rho g\, h_{fg} t)$.

where

Φ_f = angle measured from the top of the tube to the point where condensate flooding between fins occurs,

θ = half tip angle of fin,

s_t = fin spacing at fin tip,

q = average heat flux based on nominal surface area,

t = thickness of drainage strip,

ν = kinematic viscosity of condensate ,

K = permeability of strip material, and

x_1 = overflow point on porous drainage strip (see Figure 2.1).

It is quite clear that any means of reducing the condensate retention angle has a beneficial effect on the vapor-side heat-transfer enhancement. As discussed earlier, the retention angle decreases with decreasing pressure within the condensate at the bottom of the tube where it is in contact with the drainage strip. To understand the mechanisms involved in this problem, Honda and Nozu [Ref. 3] used the following approach. First, the pressure difference between the surrounding vapor and the retained condensate at $\Phi = \Phi_f$ (i.e., the angle measured from tube top equals to the flooding angle below which the inter-fin space is almost filled with the retained condansate) is given by:

$$\Delta P = (2\sigma\cos\theta)/s_t \qquad \text{(eqn 2.18)}$$

where

σ = surface tension,

θ = half tip angle of fin, and

s_t = fin spacing at fin tip.

As discussed in [Ref. 3], since the pressures of both phases at the overflow point on the porous drainage strip are the same, ΔP should be equal to the sum of the static pressure difference of the retained condensate between $\Phi = \pi$ and $\Phi = \Phi_f$, ΔP_1, and the pressure change of the condensate flow in the porous strip, ΔP_2. Notice that ΔP_2 consists of two components: hydrostatic pressure rise from top to bottom of the strip and the frictional pressure drop associated with the flow through the porous medium.

$$\Delta P = \Delta P_1 + \Delta P_2 \qquad \text{(eqn 2.19)}$$

where

$$\Delta P_1 = \rho g\, d_o(1 + \cos\theta)/2 ,$$

$$\Delta P_2 = \rho g(1 - F/K)\, x_1 , \text{ and}$$

$$F = \pi d_o q \nu/(\rho g\, h_{fg} t) .$$

Figure 2.2 shows the variation of pressure within the condensate from the uppermost point on the tube to the overflow point on the porous drainage strip. The line A-A′ on this figure represents the pressure variation for a fully flooded finned tube without a drainage strip. The composite B-B′-B″ represents the pressure variation if a porous drainage strip is attached at the bottom of the tube. Notice that now the pressure at the overflow point of the strip must equal the vapor pressure (P_v), and this line has two distinct slopes representing the strip and the bottom portion of the tube. The presence of the strip lowers the pressure within the liquid at $\Phi = \pi$ from P_v for the case without the strip by a magnitude equal to ΔP_2. As can be seen, the slope of the line for $\Phi < \pi$ equals the slope of line A-A′. Since the minimum pressure possible within the condensate is P_l, condensate flooding decreases to $\Phi = \Phi_f$. In this manner, the presence of a drainage strip reduces the condensate retention angle. When this model is studied to get the minimum retention angle, (i.e., Φ_f equals to 180° for $G \leq -1$ in equation (2.17)), it results in:

$$\frac{2\,\sigma\cos\theta}{s_t} \leq \Delta P_2 \ . \qquad \text{(eqn 2.20)}$$

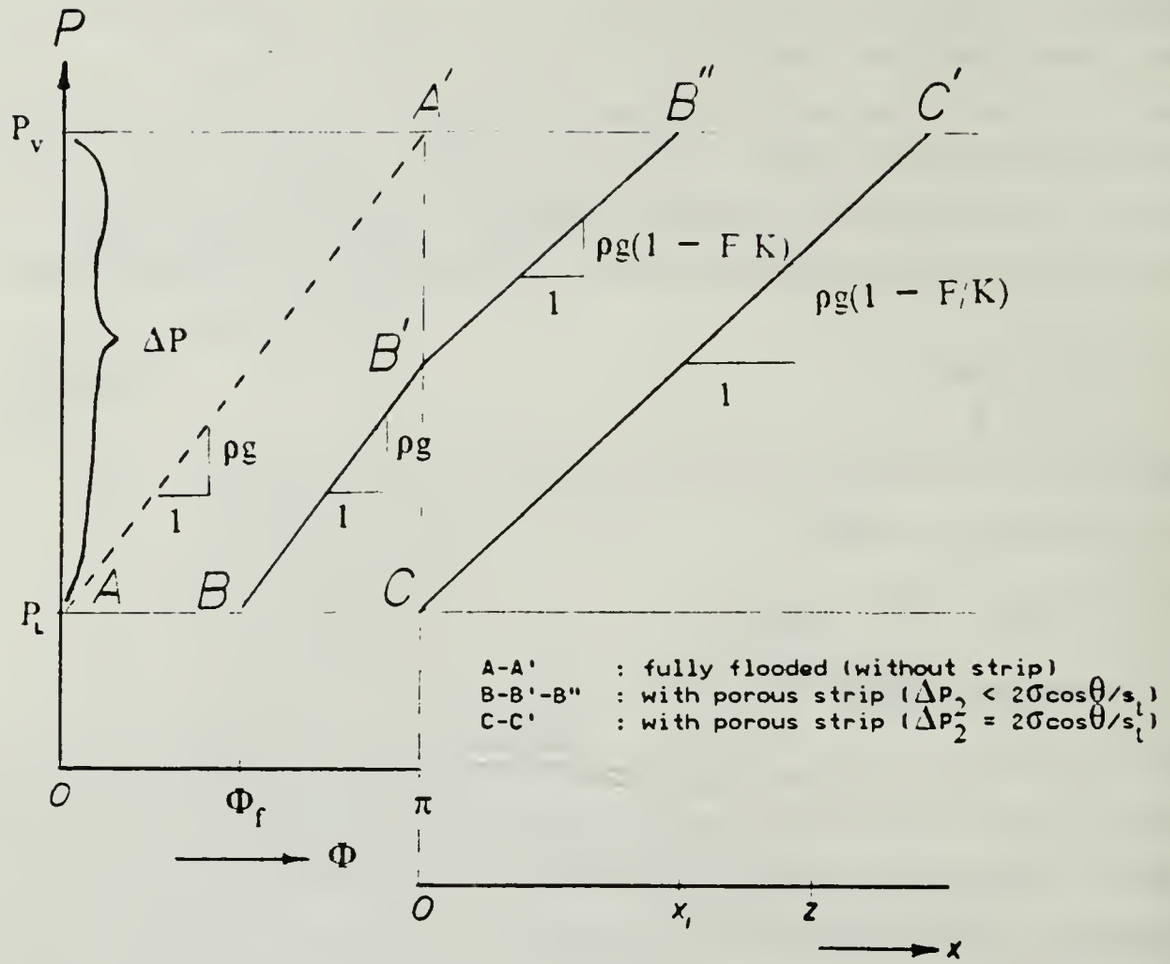

Figure 2.2 Schematic Representation of Pressure within Condensate with and without a Porous Drainage Strip.

Therefore, the higher the pressure drop within condensate from bottom to the top of the porous drainage strip, the better the enhancement. In order to increase ΔP_2, one or more of the following requirements could be achieved:

decrease tube diameter (d_o),
decrease heat flux (q),
increase porous strip thickness (t),
increase permeability (K), or
increase overflow distance on porous strip (x_1) by increasing strip height (z).

The line C-C′ represents the equality case of equation (2.20). For this situation, the strip could completely remove condensate flooding from the fin tube. However, the frictional pressure drop within the strip increases with increasing strip height, thus impeding the condensate flow process. In other words, the need for higher overflow

distance (x_1) is inversely proportional to permeability (K). Therefore, an optimum must exist between permeability and strip height for a given heat flux.

III. DESCRIPTION OF APPARATUS

A. TEST APPARATUS

The test apparatus used for this investigation was the same as used by Mitrou [Ref. 7] and other thesis students [Refs. 5,6]. A schematic of this apparatus is shown in Figure 3.1. Steam was generated using distilled water in a 304.8 mm (12 in.) diameter Pyrex glass section which was fitted with ten 4000-W, 440-V, Watlow immersion heaters. The steam from the boiler flowed upward and passed through a 304.8 mm (12 in.) to 152.4 mm (6 in.) reducing section to a 2.44 m (8 ft.) long section of Pyrex glass piping. The steam flowed through a 180-degree bend and entered a 1.52-m-long section before finally entering the stainless-steel test section, which is shown in Figure 3.2. The test tube was mounted horizontally in the test section. A portion of the steam condensed on the test tube, while the excess steam travelled downward and condensed in the auxiliary condenser. The condensate drained back to the boiler by gravity, completing the closed-loop operation of the system.

A viewport was provided to allow visual observation of the condensation mode to ensure filmwise condensation during data collection. The auxiliary condenser consisted of two 9.5 mm (3/8 in.) diameter water-cooled copper tubes helically coiled to a height of 457 mm (18 in.). The auxiliary condenser was cooled by a continuous supply of tap water through a flow meter. A throttle valve was provided to control the flow rate through the auxiliary condenser and to keep the system at the desired internal pressure. Tap water was collected in a large sump with a capacity of about 0.4 cubic meters (Figure 3.3), and was used to cool the test tube. Two centrifugal pumps connected in series, took the water from the sump and pumped it through a flow meter into the test tube. A valve on the discharge side of the second pump and before the flow meter, allowed the velocity of water flowing through the test tube to be varied from 0 to 4.4 m/s (14.4 ft/sec). The exit side of the test tube was provided with a mixing chamber for accurate measurement of the water outlet temperature.

A vacuum pump was operated continuously during the experiment to remove non-condensing gases from the test section. The system used to remove non-condensing gases is shown in Figure 3.3. It was unavoidable that the vacuum pump removed steam with trace amounts of air. To minimize the contamination of the pump

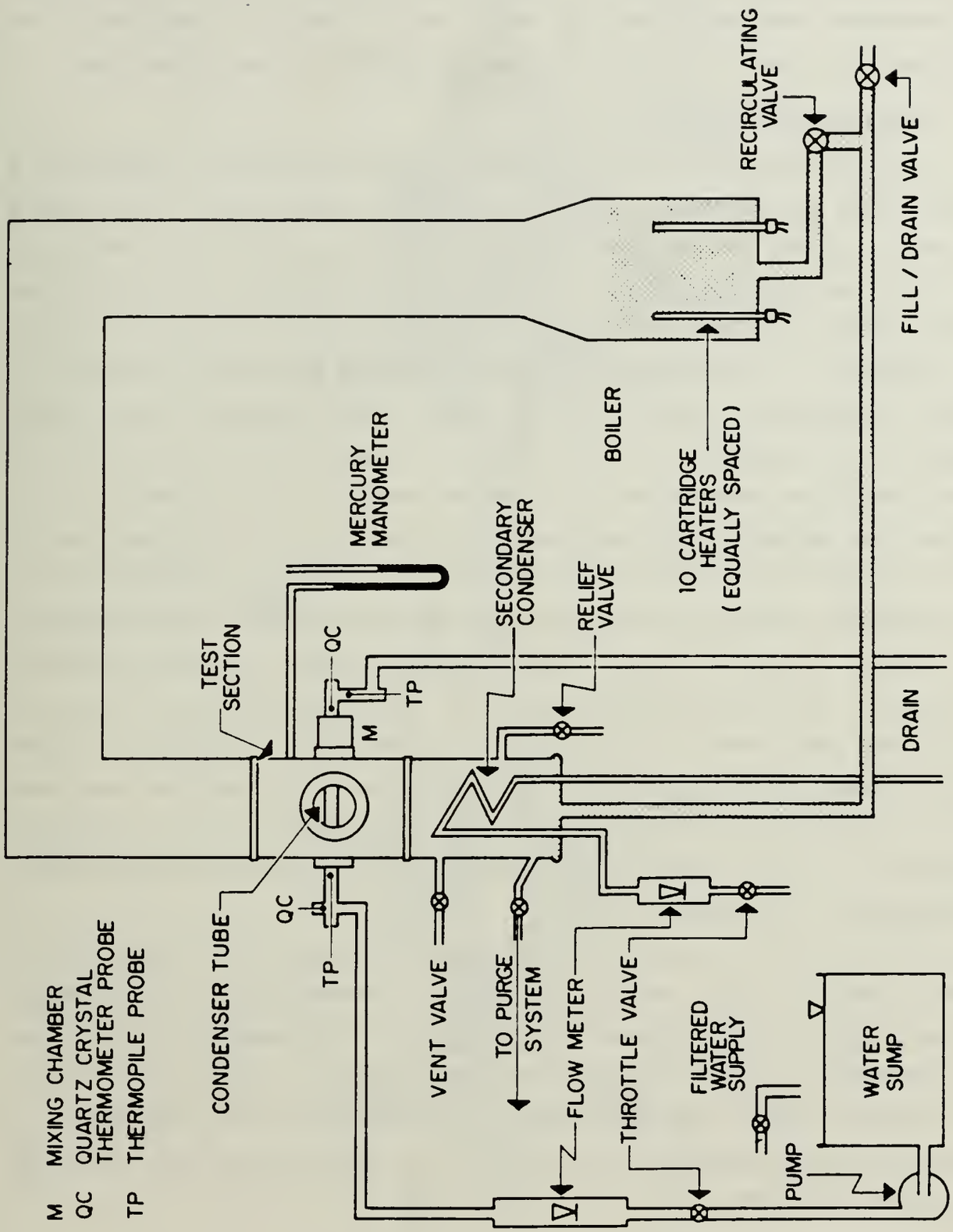

Figure 3.1 Schematic of Test Apparatus.

by the steam, another condenser was provided to condense as much steam possible. This condenser was cooled with tap water before entering the large sump. The condensate from this steam collected in a Plexiglas cylinder and was drained later.

B. INSTRUMENTATION

The electrical power input to the boiler, immersion heaters was controlled by a panel-mounted potentiometer. In order to compute the input power to the boiler a root-mean converter with an input voltage of 440 VAC generated a signal which was fed to the data-acquisition system. A more detailed description of the boiler power supply is provided by Poole [Ref. 15]. A pressure tap above the test tube was provided was connected to a U-tube, mercury-in-glass manometer graduated in millimeters to measure the absolute pressure of the system. The steam temperature, the saturation temperature corresponding to the manually-read pressure was used to calculate the non-condensing gas concentration. The temperature of the steam, condensate and the ambient were measured using calibrated copper-constantan thermocouples made of 0.25-mm-diameter wires. Two of them were used for the steam temperature, one for the condensate return and one for the ambient temperature. These thermocouples had an accuracy within $\pm$ 0.1 K when compared against a platinum-resistance thermometer. Since the temperature rise of the coolant through the test tube is the most critical measurement, considerable attention was paid to obtaining the highest possible accuracy of this measurement. For this purpose, two independent means were used: a Hewlett-Packard (HP) 2804A quartz thermometer with two probes having an accuracy of $\pm$ 0.02 K, along with a 10-junction, series-connected copper-constantan thermopile with a resolution of 0.003 K.

For most of the data collected, the quartz thermometers and the thermopile agreed to within $\pm$ 0.03 K and when the difference between these two measurements was more than $\pm$ 0.05 K, the data set was disregarded. For simplicity, all calculations were performed using quartz thermometer measurements. The cooling water flow rate was measured using a calibrated rotameter and the value was fed manually to the computer. Another rotameter was provided to set an adequate water flow rate through the auxiliary condenser.

C. VACUUM INTEGRITY

Vacuum tightness is very important for any condensation system, especially at low pressures similar to marine-vehicle condensers which operate at an absolute

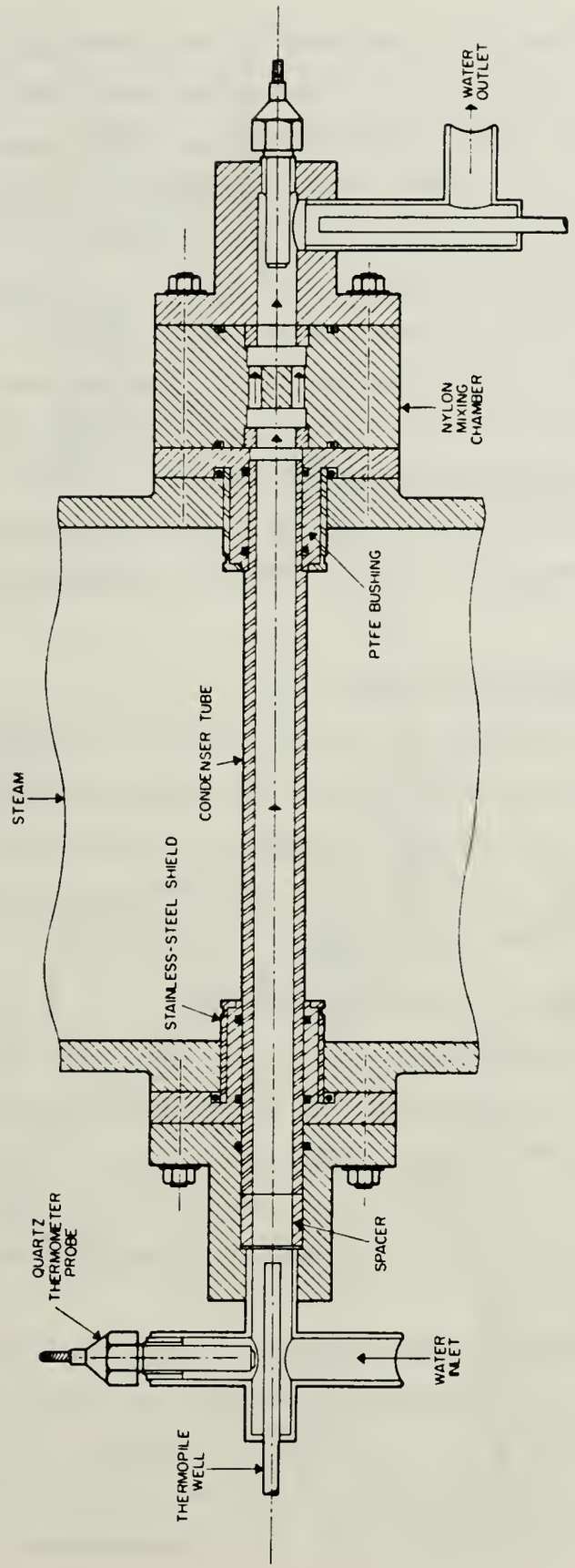

Figure 3.2 Schematic of Test Section (Insert Removed).

pressure of about 100 mm Hg. The reason for this is because even a small amount of non-condensing gas present with the condensing vapor tends to accumulate at the liquid-vapor interface. When this phenomenon takes place, an added thermal resistance occurs at the interface, which will degrade the heat-transfer performance considerably. A leak rate that corresponds to a pressure rise of about 10 mm Hg in 24 hours at the approximate operating low pressure ($\sim$ 85 mm Hg) in the auxiliary condenser side was found. As stated by the previous thesis students, in the past, the system allowed a leak rate corresponding to a pressure rise less than 2 mm Hg. However, at the begining of this investigation, a small leak was located close to the purge point in the secondary condenser (see Figure 3.1). Since continuous purging was carried out throughout all runs, and the leak occurred downstream to the test tube, the present leak rate is believed to have no detectable degradation on the condensation process.

D. DATA-ACQUISITION SYSTEM

An HP-9826A computer was used to control an HP-3497A Data-Acquisition System to monitor the system temperatures and boiler input power (using the converter signal). Raw data were processed immediately and also stored on a diskette for reprocessing at a later time. After all the data sets were completed, the data were reprocessed using a modified Wilson method.

E. TUBES AND DRAINAGE STRIPS TESTED

For this thesis effort, a total of sixteen drainage strips were manufactured and tested on two finned tubes each with a fin thickness and height of 1.0 mm but with a fin spacing of 0.5 mm and 1.0 mm. Figures 3.4, 3.5, 3.6, 3.7 show the geometry of the strips tested. Tables 1, 2 and 3 list all the strips tested and their dimensions. Each strip had a length of 133.4 mm, which is same as the length of the finned portion of the tube exposed to steam.

A total of five different strip heights were manufactured to investigate the effect of porous strip height on the heat-transfer performance of the two finned tubes. Table 2 lists the strips tested on the tube with a fin spacing of 0.5 mm. In order to investigate the effect of drainage points on the heat-transfer performance, one porous and one solid triangularly-shaped strip were manufactured. Table 3 lists their dimensions.

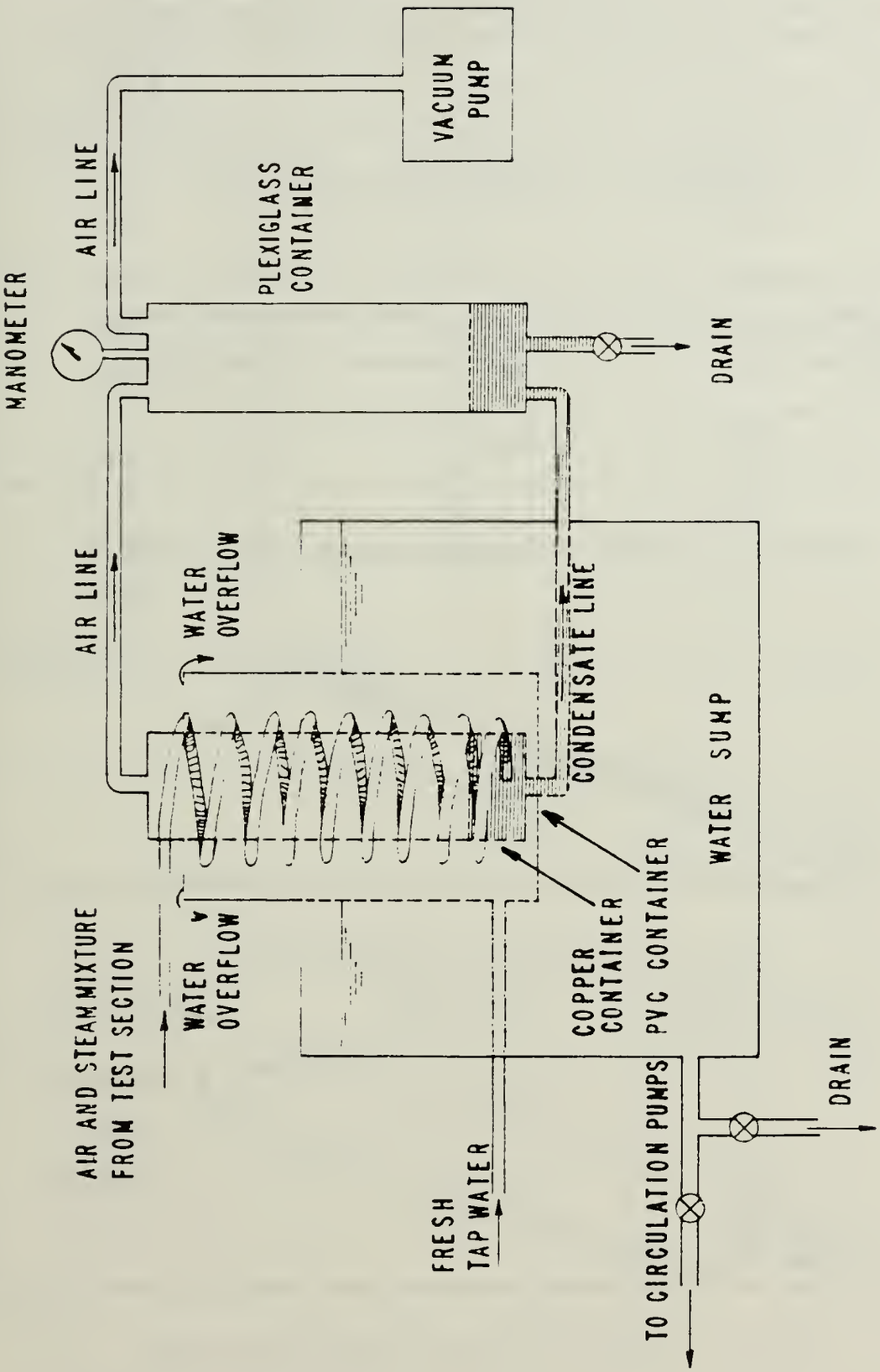

Figure 3.3 Schematic of Vacuum System and Cooling Water Sump.

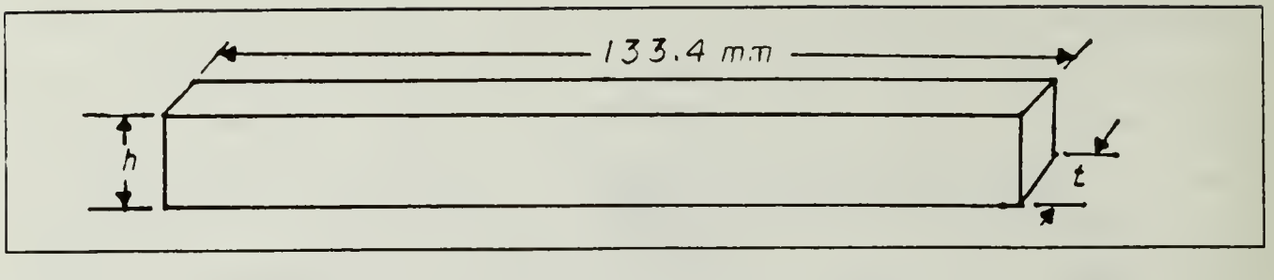

Figure 3.4 Geometry of Rectangular Strips.

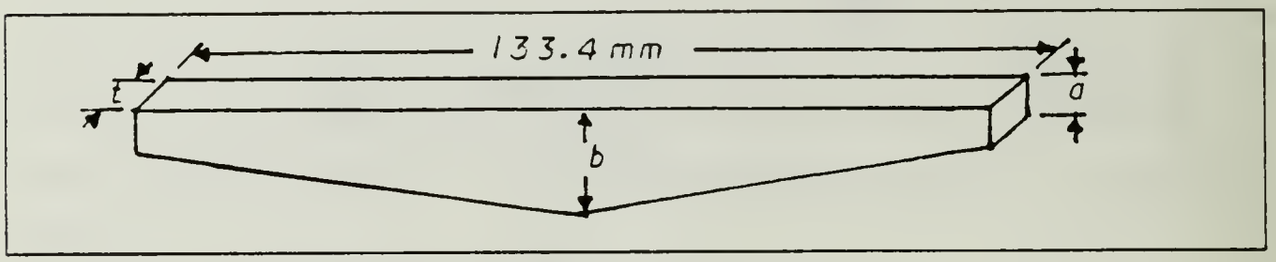

Figure 3.5 Geometry of Triangular-Shaped Drainage Strips.

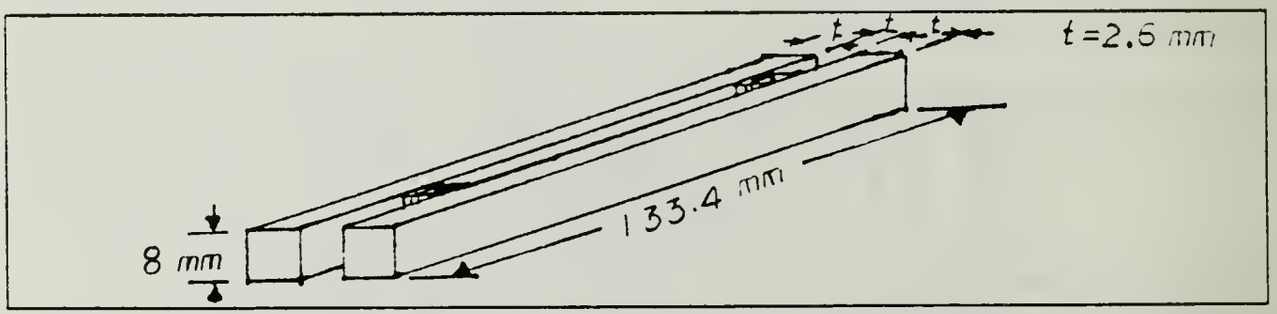

Figure 3.6 Geometry of Strip with Air Gap.

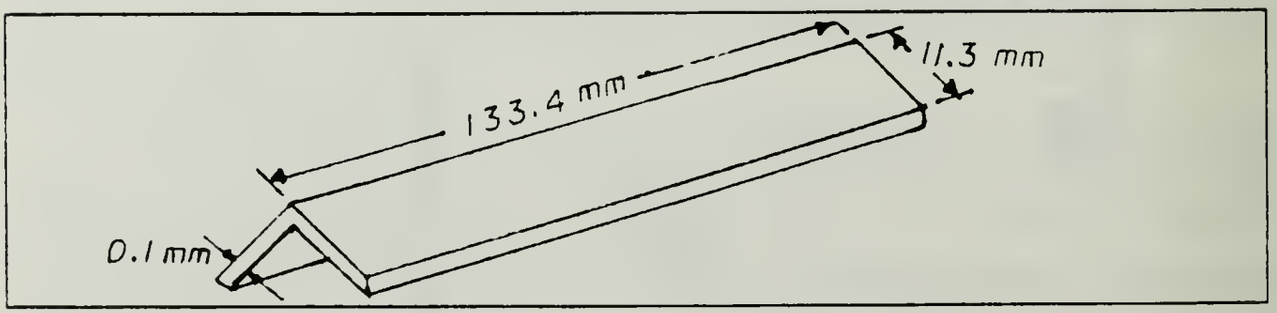

Figure 3.7 Geometry of Inverted V-Shaped Steel Strip.

TABLE 1

DIMENSIONS OF RECTANGULAR POROUS STRIPS

Pore diameter (mm)	Height (mm)	Thickness (mm)
0.05 - 0.13	3	3.2
0.05 - 0.13	7	3.2
0.05 - 0.13	8	3.2
0.05 - 0.13	11	3.2
0.05 - 0.13	15	3.2
0.05 - 0.13	8	2.6
0.05 - 0.13	8	5.2
0.025 - 0.05	8	7.8
0.0025 - 0.013	8	3.0

TABLE 2

DIMENSIONS OF RECTANGULAR SOLID STRIPS

Strip Material	Height (mm)	Thickness (mm)
Titanium	8	1.5
Titanium	8	3.0
Titanium	8	4.5
S. steel	8	0.1

TABLE 3

DIMENSIONS OF TRIANGULAR SHAPED DRAINAGE STRIPS

Strip Type	Minimum Height a (mm)	Maximum Height b (mm)	Thickness (mm)
Pore dia. 0.025-0.05 mm	4	8	2.6
Titanium	4	8	1.5

IV. SYSTEM OPERATION AND DATA REDUCTION

A. OPERATION

Since clean copper has poor wetting characteristics with water, steam will normally condense on copper under a partial dropwise mode, which is more effective than the filmwise mode. However, the purpose of this investigation was to take data with filmwise condensation and tested tubes were made from copper. Therefore, care had to be taken to ensure that the filmwise condensation mode prevailed throughout all the data runs reported in this thesis. In order to achieve this, the tubes had to be treated according to the following procedure:

1. The tube was rinsed by tap water to remove any contaminants that are soluble in water.
2. A mixture of equal parts of sodium-hydroxide and ethyl alcohol was prepared and heated to about 80 °C, while frequently being stirred until it became watery.
3. A coating of this mixture was applied uniformly around the tube.
4. The tube was placed in a steam bath and was heated by the steam for about an hour, while applying a new coating every 5 or 10 minutes.
5. The tube then was rinsed with water and put immediately into the test section to avoid any contaminants depositing on the tube leading to the dropwise problem.

This process resulted in the formation a of thin layer of dark oxide that has high wetting characteristics. Since this layer was very thin, its thermal resistance was negligible. This procedure was followed each time prior to the installation of a tube. When re-testing an already darkened tube, it was heated in the steam only for about 20 minutes, while applying the above-mentioned mixture.

The test apparatus was brought to operating pressure and temperature by adjusting the input power to the boiler heaters, the cooling water flow rate through the tube, and the cooling water flow rate to the auxiliary condenser. Steady-state conditions were assumed when the operating conditions were stabilized with fluctuations of less than $\pm$ 2 μV (i.e., $\pm$ 0.05 K) for the steam thermocouple and $\pm$ 0.005 K and $\pm$ 0.01 K for the cooling water temperature rise measurements for

atmospheric and at low pressures, respectively. Once steady-state operating conditions were reached, the cooling water flow rate through the test tube was fed to the computer manually while all temperature measurements, such as temperature rise of the cooling water through the test tube, vapor temperature, and the input power to the boiler were gathered by the data-aquisition system. For each cooling water flow rate of 80 percent (4.44 m/s), 70, 62, 54, 45, 35, 26, and 20 percent, and again at 80 percent, two sets of data were taken. These cooling water flow rates were selected to give approximately equally-spaced heat-flux values. After each change of the cooling water flow rate through the tube, the system pressure experienced a slow drift; so adjustment of the water flow rate through the auxiliary condenser was required to maintain the system pressure at the operating condition.

B. DATA REDUCTION

The program used for data reduction was the same as that used by Mitrou [Ref. 7], which included property functions, calibration curves for the cooling water flowmeter and for all thermocouples as well as the temperature rise due to frictional heating within the mixing chamber.

The separation of the individual thermal resistances (water-side, wall and vapor-side) from the overall heat-transfer resistance is very important to obtain the vapor-side heat-transfer coefficient. The vapor-side coefficient was based upon a smooth-tube area (i.e., the surface area of a smooth tube having an outside diameter equal to the fin root diameter). The overall heat-transfer resistance is given by equation (4.1), while the inside heat-transfer coefficient is given by a Sieder-Tate-type equation (4.2). In order to find the inside heat-transfer coefficient, three methods were considered by the previous investigators [Refs. 5,6,7,15], and are referred to as: direct method using wall thermocuples, modified Wilson plot method on smooth tube and modified Wilson plot method on finned tubes.

$$[1/(U_o A_o)] = [1/(h_i A_i)] + [1/(h_o A_o)] + R_w/A_o \qquad \text{(eqn 4.1)}$$

where

$R_w = D_o \ln(D_o/D_i)/2k_m$,

$A_i = \pi D_i(L + L_1\eta_1 + L_2\eta_2)$, and

η_1, η_2 = fin efficiencies at the inlet and outlet portions of the tube inside the Teflon bushings [Ref. 29].

$$Nu_i = h_i D_i/k = C_i Re^{0.8} Pr^{1/3}(\mu_c/\mu_w)^{0.14} + B \qquad \text{(eqn 4.2)}$$

As discussed by Wanniarachchi et al. [Ref. 28], the accuracy of the steam-side heat-transfer coefficient increases as the inside resistance becomes a smaller fraction of the overall resistance (see equation (4.1)). For this reason, all the tubes tested during this investigation were provided with a coiled insert. This insert boosted the inside coefficient for the following reasons: it provided a smaller cross sectional flow area, thus increasing the Reynolds number for a given mass flow rate; and it provided swirl flow within the tube resulting in improved mixing of the coolant.

1. **Direct Method Using Wall Thermocouples**

Direct measurements of wall temperature were made by Georgiadis [Ref. 5] using six thermocuples mounted in a thick-walled, smooth tube with the same bore diameter as that of the finned tubes. It was shown that the circumferential wall-temperature distribution followed a cosine curve given by equation (4.3) with a maximum drop of 18 K between the top and bottom of the tube

$$\Delta T/\overline{\Delta T} = 1-\alpha\cos(\theta/\pi)\,, \qquad \text{(eqn 4.3)}$$

where

ΔT = local temperature drop across condensate film,
$\overline{\Delta T}$ = average temperature drop across condensate film, and
θ = angle measured from top of the tube.

In the above equation, α was found to be from 0.135 to 0.202 and from 0.115 to 0.179 under low pressure and at atmospheric pressure, respectively. By using the average reading of all thermocouples for the wall temperature, and by applying the Fourier conduction law across the tube wall, the average inside wall temperature, $\overline{T}_{wi}$, was obtained. From this, the inside heat-transfer coefficient was computed using the following equation:

$$h_i = \frac{q}{T_s - \overline{T}_{wi}}\,. \qquad \text{(eqn 4.4)}$$

This h_i value was substituted into equation (4.2) and a least-squares tecnique was carried out to obtain the C_i and B values. Based on four independent runs, this method resulted in a coefficient C_i of 0.064 ± 0.001, together with a value for B of 26.4 ± 5.0. The value of C_i (0.064) is greater than the well-known Sieder-Tate constant of 0.027 for the plain tubes, mainly owing to the coiled insert. The constant B = 26.4 was used for improved fitting of the experimental data.

2. **Modified Wilson Plot on Smooth Tube**

This method was used by processing the data taken on a similar smooth, but uninstrumented tube. A Sieder-Tate-type equation was used for the inside heat-transfer coefficient, while a Nusselt-type equation was used for the outside heat-transfer coefficient as given by:

$$h_o = \beta[N/(\mu_f D_o q)]^{1/3} \qquad \text{(eqn 4.5)}$$

where

$N = k_f^3 \rho_f(\rho_f - \rho_v) h_{fg}$, and

q = radial heat flux .

In this method, both constants in equation (4.2) and (4.5) had to be determined iteratively. Substituting equation (4.2) (with B = 0.0) and equation (4.5) in the equation for the overall heat-transfer resistance given by equation (4.1), results in:

$$(1/U_o - R_w)\,\Gamma = D_o\Gamma/(C_i k_f \Omega) + (1/\beta) \qquad \text{(eqn 4.6)}$$

where

$$\Gamma = [N/(\mu_f D_o q)]^{1/3} \text{ , and} \qquad \text{(eqn 4.7)}$$

$$\Omega = (k/D_i)\, Re^{0.8} Pr^{1/3} (\mu_c/\mu_w)^{0.14} . \qquad \text{(eqn 4.8)}$$

Equation (4.8) is a linear equation of the form:

$$Y = mX + b \qquad \text{(eqn 4.9)}$$

where

$$Y = [(1/U_o) - R_w]\,\Gamma\,, \qquad \text{(eqn 4.10)}$$

$$X = D_o\Gamma/(k_f\Omega)\,, \qquad \text{(eqn 4.11)}$$

$$m = 1/C_i\,, \text{ and} \qquad \text{(eqn 4.12)}$$

$$b = 1/\beta\,. \qquad \text{(eqn 4.13)}$$

In order to begin the iteration, reasonable values were assumed for C_i and β. With these values, the Y and X values were calculated and a least-square technique was used to compute the slope and intercept values expressed in equations (4.12) and (4.13). This procedure was repeated until the assumed and computed values for C_i and β agreed to within 0.1 percent. Using this technique, Georgiadis [Ref. 5] found a C_i value of 0.071 $\pm$ 0.001 (average of four runs) with the B value set equal to zero.

3. **Modified Wilson Plot on Finned Tubes**

As discussed by Flook and Mitrou [Refs. 6,7], this third method is very similar to the second method outlined above, but no data were taken on a smooth tube. Instead, the data were taken directly on finned tubes by assuming a reasonable value for C_i, and at the end of the test run, the data were reprocessed using the modified Wilson plot analysis to yield a new value of C_i. During the present investigation, all of the data were processed using this third method. It is important to note that the C_i values found during this study were from 0.063 to 0.071, and these values give Nusselt numbers very close to the average of the values found from the two methods discussed above. Further, the C_i values were repeatable within $\pm$ 0.001 for any given tube. This third method appears to be superior to the other methods mainly because of its simplicity. For example, this method requires no new smooth tube (instrumented or uninstrumented) to be manufactured. Note that the manufacturing of instrumented tubes is a very difficult and time-consuming task [Ref. 4].

V. RESULTS AND DISCUSSION

A. INTRODUCTION

A number of data runs were made using the procedures described in Chapter IV. Each tube was tested at least three times, both at low and atmospheric pressures on different days, to ensure repeatability of the data. Complete filmwise condensation was maintained during all data runs reported in this thesis. As mention in Chapter III, a viewport was provided for visual observation to ensure filmwise condensation. Before collecting each data set, the appearance of the condensate film was checked. If the film appeared to be patchy or there was an indication of dropwise condensation, the run was discontinued and the data were discarded. However, there were cases where the film appeared filmwise but the data collected at the end of the run (cooling water flow rate of 80%) were different from that collected at the beginning for the same flow rate. For example, the heat-transfer coefficient was as much as 10% greater for the last data point and the cooling water temperature rise was also greater than that measured at the beginning. As discussed by Georgiadis [Ref. 5], this increased heat-transfer coefficient appears to be a result of the tube undergoing partial dropwise condensation with exposure to the steam. Since this trend was observed even though no droplets were visible, it is possible that the dropwise condensation was taking place at a microscopic level, especially near fin edges with a very thin condensate film. All data presented in this thesis displayed less than 5% disagreement in the steam-side heat-transfer coefficient between initial and final data sets.

During the runs that were made to check the repeatability, the tubes were taken out each time and were treated with the sodium hyroxide-ethyl alcohol solution as described in Chapter IV. Since the drainage strips were attached to the tube with three constantan wires (0.25 mm-diameter), it is possible that a small change of the position of the strip in relation to the tube may have occurred. This may be responsible for the maximum disagreement of 13% in the steam-side heat-transfer coefficient observed for different runs taken on a given tube.

The variation of the heat-transfer coefficient with heat flux is presented in this chapter. As discused earlier (Chapter IV, Section B), the steam-side coefficients were inferred by substracting the water-side and wall resistances from the overall resistance.

TABLE 4
THE TUBES USED FOR CHECKING THE REPEATABILITY

Tube No #	Fin Spacing, s (mm)	Fin Thickness, t (mm)	Fin Height, e (mm)
4	0.5	1.0	1.0
5	1.0	1.0	1.0
6	1.5	1.0	1.0

Further, the steam-side coefficient is based on the area of a smooth tube having a diameter equal to the root diameter of the finned tubes.

B. COMPARISON OF DATA REDUCTION METHODS AND REPEATABILITY

Data runs were performed on three finned tubes under similar conditions to verify the repeatability with data taken by Georgiadis [Ref. 5], Flook [Ref. 6] and Mitrou [Ref. 7], and the results are shown in Figures 5.1 through 5.6. In order to perform a fair comparison, all of the data were processed by using the third method to compute the inside coefficient (see Chapter IV, Section B).

The smooth-tube data and a curve representing Nusselt theory are also included for comparison. In addition, Figures 5.1 and 5.2 provide typical experimental uncertainties for all measurements. As can be seen, the uncertainty increases with decreasing heat flux and with increasing heat-transfer coefficient. For example, the uncertainties (see Figure 5.1) are about 5% at $q = 0.33$ MW/m^2 and about 20% at $q = 0.19$ MW/m^2. The reason for increased uncertainty with decreasing heat flux appears to be a result of increased water-side resistance. Notice that the decreasing heat flux is associated with a decreasing cooling water velocity, thus increasing the water-side resistance.

Data were taken at least on three different days for a given experimental condition, and repeatability was observed to within than 5% for most of the data. Thus, the data were repeatable to within better than that shown by the experimental uncertainties, which were computed thoretically based on maximum observed uncertainties for each measured variable.

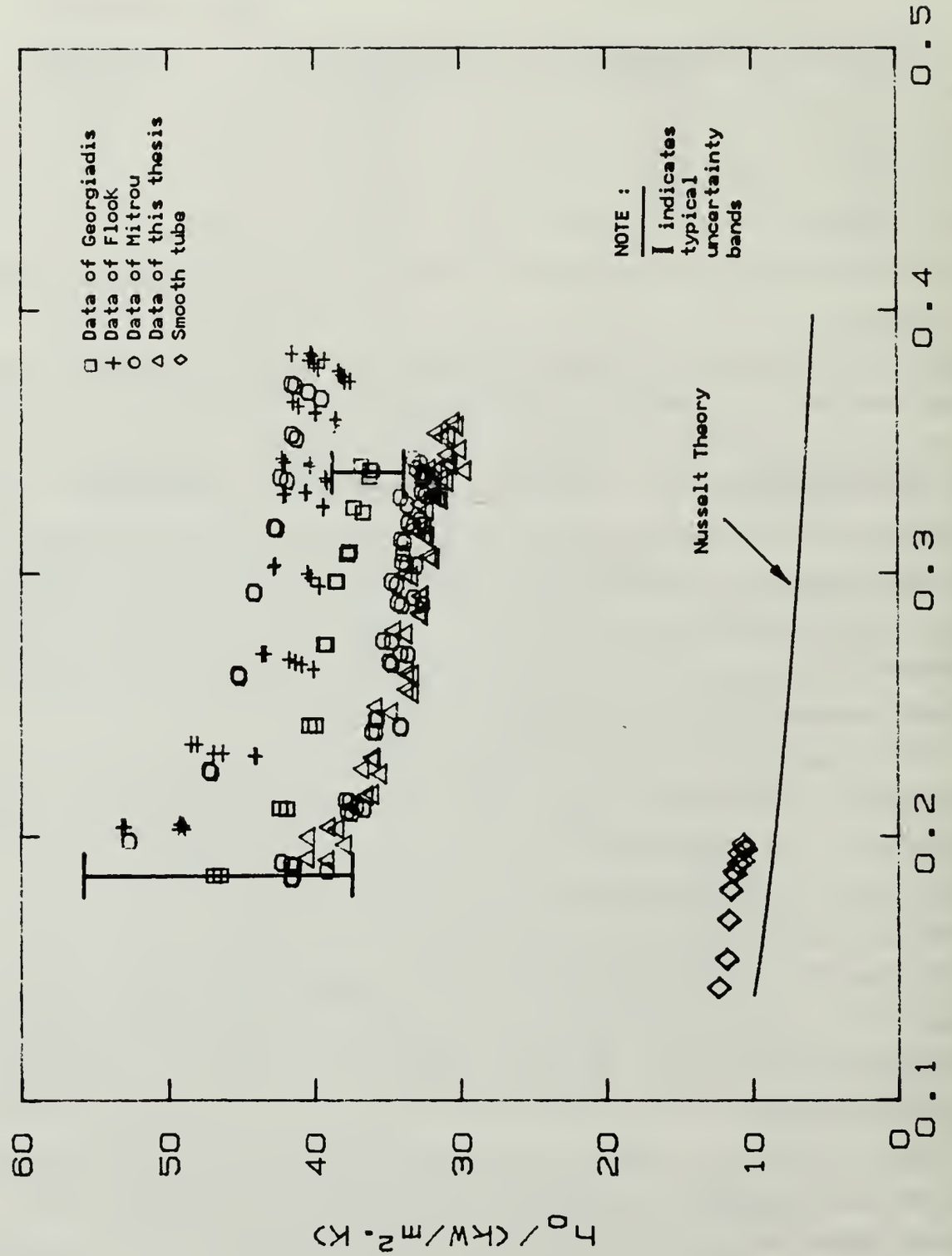

Figure 5.1 Comparison of Finned-Tube Data using Modified Wilson Plot on Finned Tubes ($V = 2.0$ m/s, $P_s = 85$ mm Hg, Tube # 6).

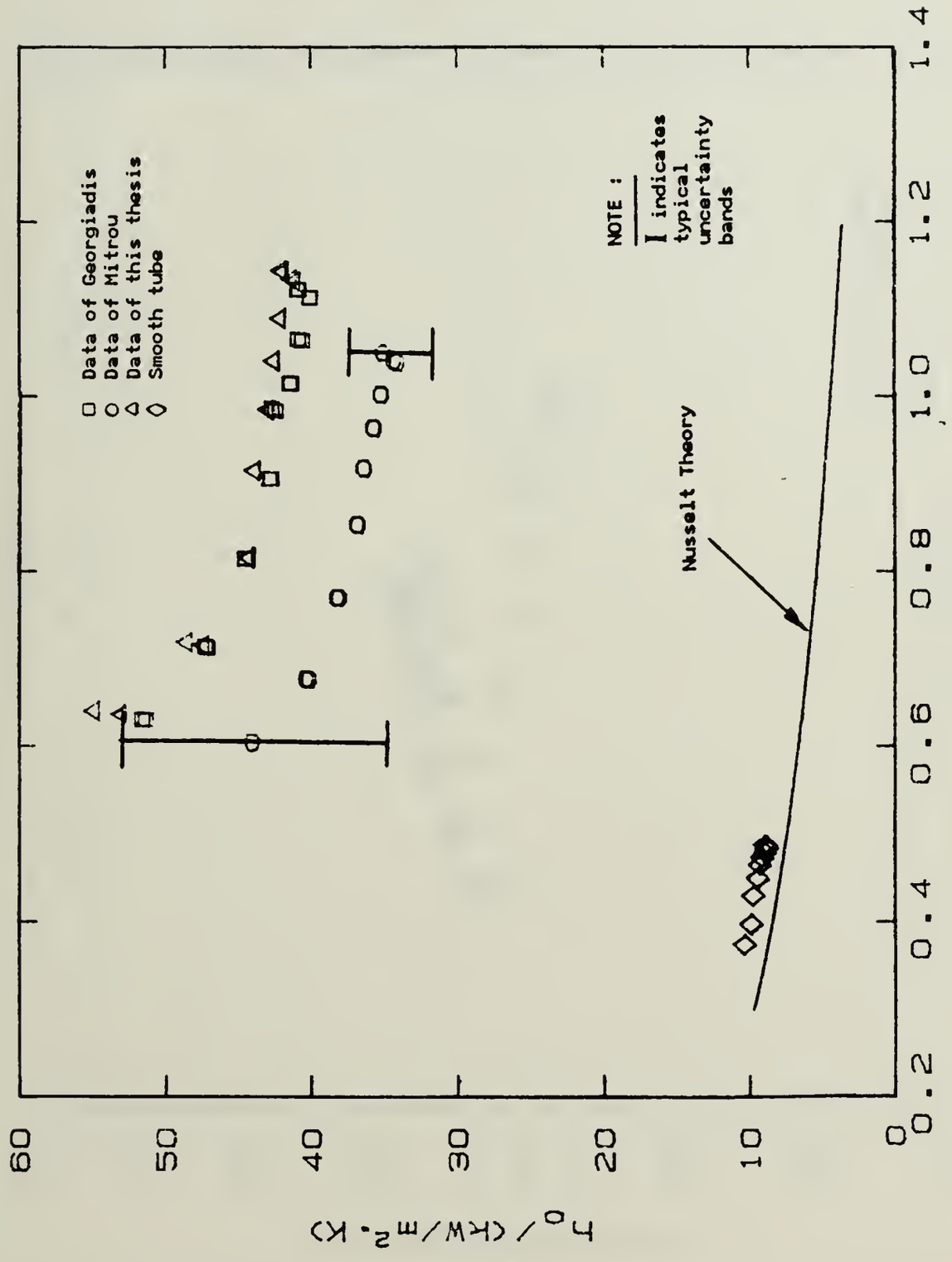

Figure 5.2 Comparison of Finned-Tube Data using Modified Wilson Plot on Finned Tubes (V = 1.0 m/s, Atm. runs, Tube # 6).

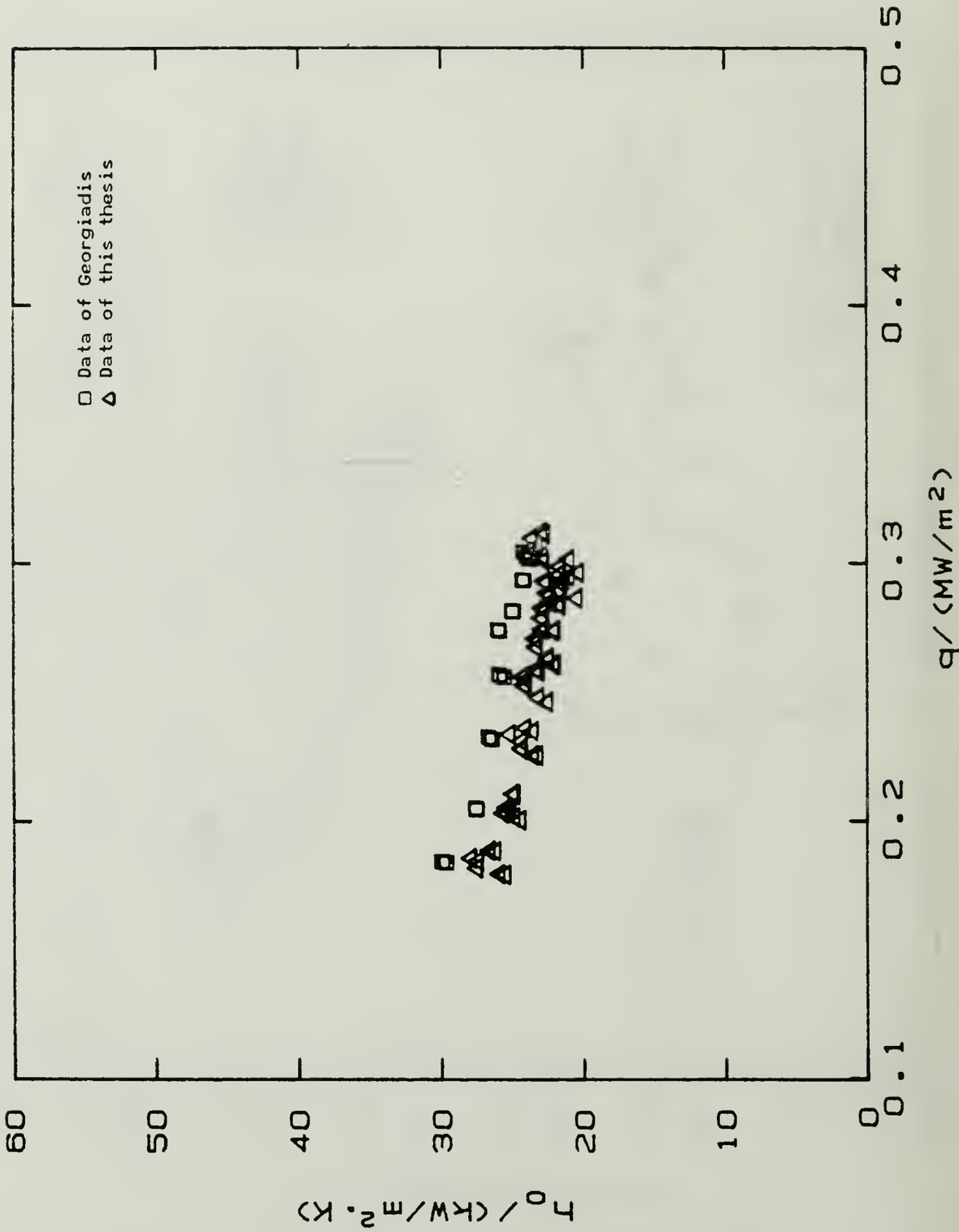

Figure 5.3 Comparison of Finned-Tube Data using Modified Wilson Plot on Finned Tubes ($V = 2.0$ m/s, $P_s = 85$ mm Hg, Tube # 4).

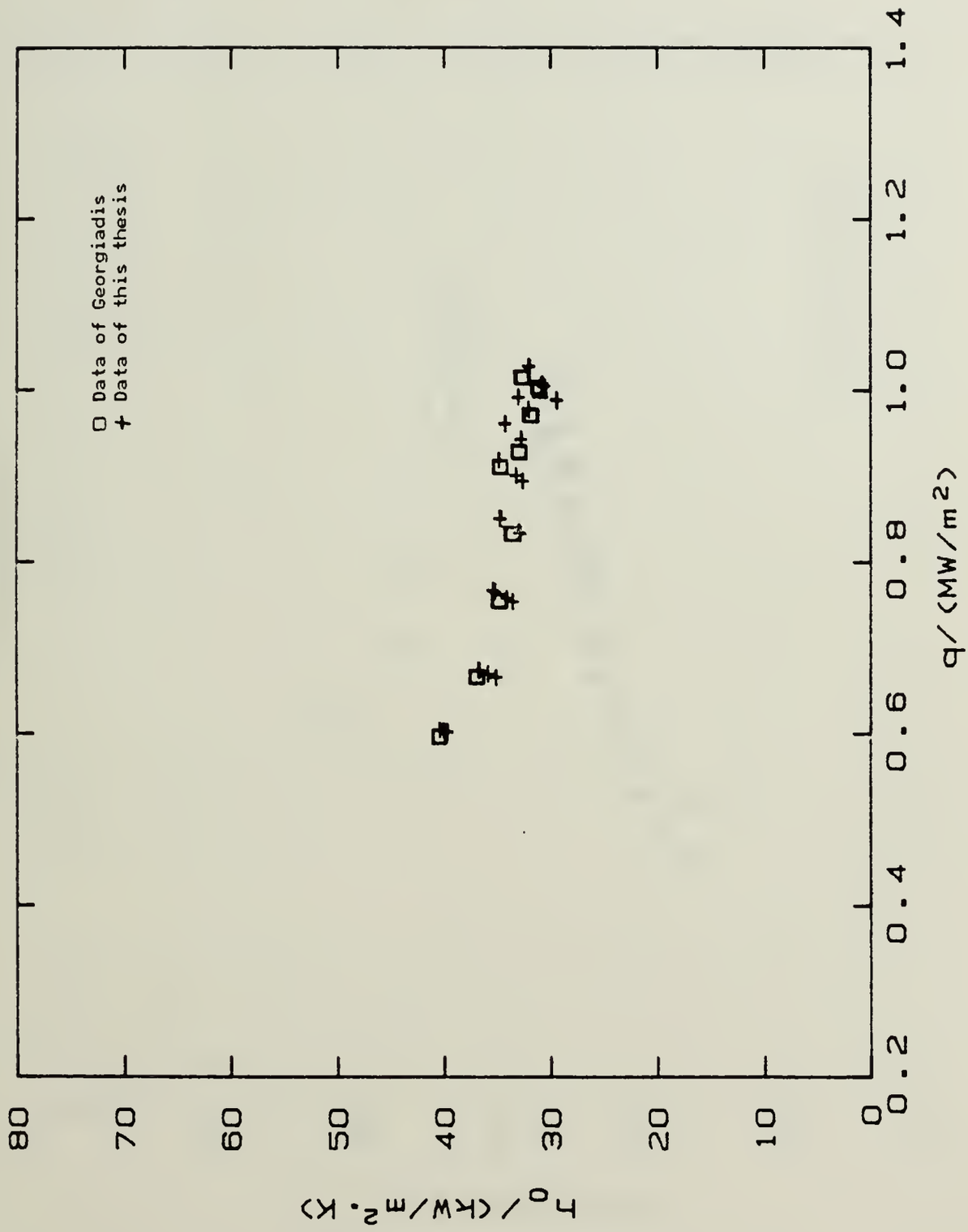

Figure 5.4 Comparison of Finned-Tube Data using Modified Wilson Plot on Finned Tubes (V = 1.0 m/s, Atm. runs, Tube # 4).

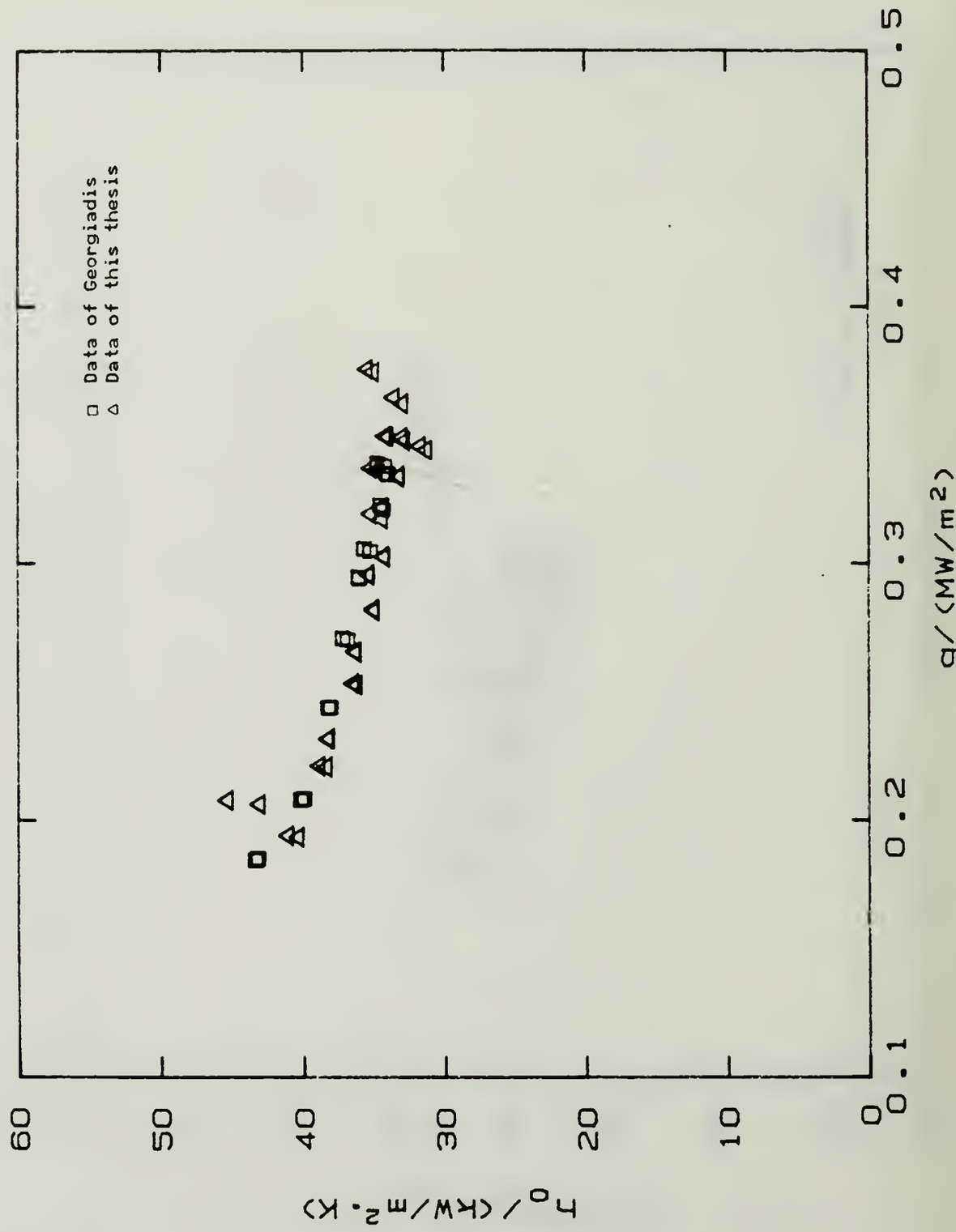

Figure 5.5 Comparison of Finned-Tube Data using Modified Wilson Plot on Finned Tubes ($V = 2.0$ m s, $P_s = 85$ mm Hg, Tube # 5).

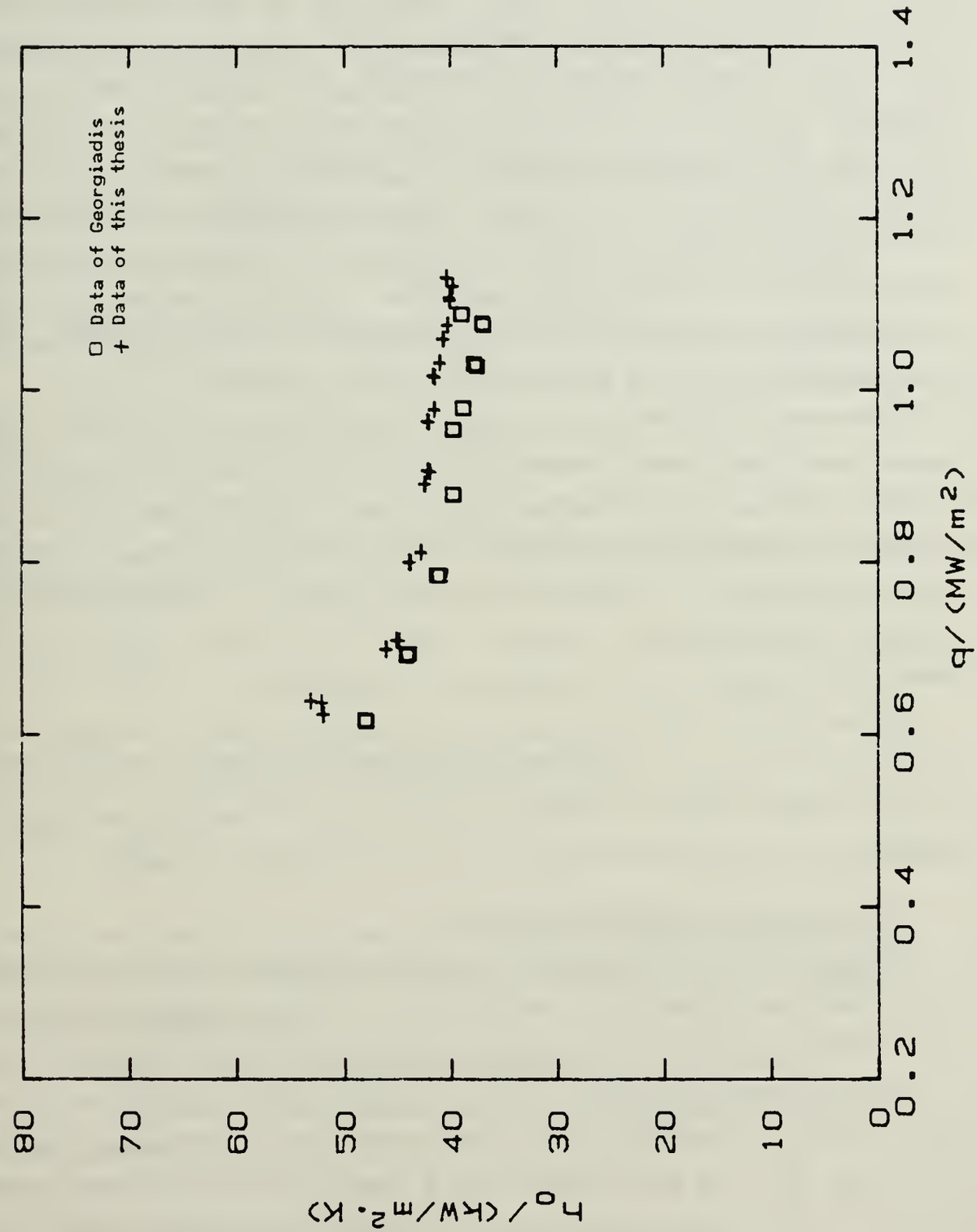

Figure 5.6 Comparison of Finned-Tube Data using Modified Wilson Plot on Finned Tubes (V = 1.0 m s, Atm. runs, Tube # 5).

Figures 5.1 and 5.2 represent the data for a finned tube with a fin spacing of 1.5 mm and fin height and fin thickness of 1.0 mm. As can be seen from Figure 5.1, the data of Georgiadis [Ref. 5], Flook [Ref. 6] and one of the four data runs of Mitrou [Ref. 7] show higher performance, while three of the four data runs of Mitrou and the present data are in good agreement. In other words, for a given heat flux (q) the data of Georgiadis, Flook and one data run of Mitrou show larger steam-side heat-transfer performance. The maximum disagreement in h_o between the present data and that of the previous data is about 20 to 25 percent. Figure 5.2 shows the repeatability of data for the same finned tube at atmospheric condition. On this figure, the present data are compared with the data of Georgiadis and Mitrou. Unlike the low pressure condition, the present data for this tube are in very good agreement with the data of Georgiadis, but the disagreement with the data of Mitrou is about 16 percent.

The reason for the above-mentioned discrepancies may be due to slightly dropwise conditions in some of the runs. However, attention must be drawn to the fact that every investigator showed repeatability, using at least two or three independent runs made on different days. It is possible that the different runs made by the same investigator on a given tube were slightly affected by microscopic dropwise condensation approximately to the same extent, thus showing good repeatability. However, this argument is only a conjecture at the present time.

Figures 5.3, 5.4, 5.5 and 5.6 show the repeatability of data for the tubes with fin spacings of 0.5 mm and 1.0 mm. These tubes had fin heights of 1.0 mm. In these figures, the present data are compared with the data of Georgiadis and maximum disagreement in h_o was found to be 8% at low and atmospheric pressures.

C. CONDENSATE RETENTION ANGLE

Attempts were made to measure the condensate retention angle on finned tubes # 4 and # 5 with and without porous drainage strips. The measurements without a strip were in excellent agreement with the theory (equation (2.4)), which has been validated by a number of previous investigators [Refs. 1,19,20,21]. Since it would not add much to the literature, the measurements without the strips are not presented in this thesis. On the other hand, the measurements with a porous drainage strip were somewhat impractical as truly static conditions were not possible. For example, when a porous drainage strip having a height of 7 mm or more was placed on the underside of either

tube # 4 or # 5, the condensate retained between the fins was pulled down into the porous strip during a short interval of time (about 1 second or less). A strip height of only 3 mm had a negligible effect on retention angle. Therefore, it was necessary to simulate a dynamic condition (i.e., with condensation) by allowing water to flow onto the top of the tube. In this manner, it was possible to establish a quasi-steady condensate retention angle. Unfortunately, this angle depended on the rate of water flow allowed at the top of the tube. Even though it would have been possible to measure the condensate retention angle simulating a given heat flux (by allowing the corresponding water flow rate to occur), such measurement was assumed to be beyond the scope of the present investigation. Therefore, the data for condensate retention angle with or without porous drainage strips are not presented in this thesis.

D. PERFORMANCE OF FINNED TUBES WITH DRAINAGE STRIPS

As discussed earlier in Chapter IV, Section B, all of the data presented in this section were processed using the third method for evaluating the water-side coefficient. Thus, the method titled "Modified Wilson Plot on Finned Tubes" was carried out for each of the data runs. Further, the figures presented in this section include least-squares fits to the experimental data. These fits were generated according to the following expression:

$$q = a\,\overline{\Delta T}^{b} \qquad \text{(eqn 5.1)}$$

where $\overline{\Delta T}$ was computed using the following equation:

$$\overline{\Delta T} = q / h_o\,, \qquad \text{(eqn 5.2)}$$

where q was measured experimentally. The experimentally determined values for the constants a and b in equation (5.1) both at low pressure and atmospheric conditions are given in Tables 5, 6 and 7.

1. Effect of Porous Strip Height on Heat-Transfer Performance

This section presents results showing the variations of the steam-side heat-transfer coefficient with heat flux with porous drainage strip height as a parameter. Data were taken on two copper tubes, each with the same fin height and fin thickness of 1.0 mm but with different fin spacing of 0.5 and 1.0 mm. Figures 5.7, 5.8, 5.9 and 5.10 present data for these tubes at low and atmospheric pressures, respectively.

TABLE 5

CONSTANTS OF EQUATION (5.1)
FOR PORE DIA. 0.05-0.13 MM

		Low Pressure		Atmospheric	
s (mm)	strip (mm)	a	b	a	b
0.5	3	48228	0.7136	96875	0.7155
0.5	7	52375	0.7148	97386	0.7083
0.5	8	55662	0.7158	95592	0.7123
0.5	11	57459	0.7148	106630	0.7115
0.5	15	56975	0.7143	103690	0.7111
1.0	3	63418	0.7212	113320	0.7162
1.0	7	72286	0.7203	118740	0.7240
1.0	11	71797	0.7183	115920	0.7198
1.0	15	78527	0.7160	117670	0.7173

TABLE 6

CONSTANTS OF EQUATION (5.1)
FOR PORE DIA. 0.025-0.05, S = 0.5 MM, Z = 8 MM

	Low Pressure		Atmospheric	
Strip	a	b	a	b
Single	57567	0.7149	101630	0.7161
Double	64465	0.7192	117200	0.7192
Triple	65249	0.7175	117610	0.7195
Tri. drainage	57245	0.7167	112050	0.7204

TABLE 7

CONSTANTS OF EQUATION (5.1)
FOR SOLID STRIPS, S = 0.5 MM, Z = 8 MM

	Low Pressure		Atmospheric	
Strip	a	b	a	b
Single	61109	0.7134	107290	0.7110
Double	57346	0.7125	100630	0.7119
Triple	60046	0.7158	104190	0.7150
Tri. drainage	60001	0.7109	111030	0.7052

As can be seen, the strip with a height of 3 mm did not give significant enhancement over the finned tube but the strip with a height of 7 mm provides 17% and 20% enhancement on the heat-transfer coefficient for low and and atmospheric pressures, respectively, compared to the case without a drainage strip. When the strip height was increased to 11 and 15 mm, further enhancements were observed. Unfortunately, it was not possible to test even larger strip heights to obtain the optimum value because of the limitation of the test section. Under low (85 mm Hg) and atmospheric pressures, 11 and 15 mm strips (pore diameter 0.05-0.13 mm) showed the best performance for the tube with a fin spacing of 0.5 mm. Thus, an optimum porous strip height of 11 to 15 mm appears to exist. The increase in performance with increasing strip height (up to the "optimum" value) agrees quite well with the Honda and Nozu [Ref. 3] theory as expressed by equation (2.20) and the discussion provided in Chapter II. Notice that ΔP_2 increases with increasing strip height and thereby decreases the retention angle. On the other hand, any decrease of performance with porous strip height beyond the "optimum" value can only be explained if this height exceeds the capillary height of the strip material. However, the computed theoretical capillary height was 20 cm for the strip having an average pore diameter of 0.05-0.13 mm, which is much larger than the "optimum" value observed. Therefore, there appears to be a contradiction between the observed data and the present theoretical understanding of this phenomenon.

For the tube with a spacing of 1.0 mm, the 15 mm strip showed the best performance at low pressure. On the other hand, at atmospheric pressure, 7, 15 and 11 mm strips resulted in performances that were about the same in view of the experimental repeatability. As mentioned in Section A, strips were attached to the tube with three constantan wires. Even though great care was taken when attaching strips at the same position at the bottom of the tube, a small change in the position of the strip may have occurred. Such a change in position could alter the pressure distribution in the axial direction at the bottom of the tube, and thus result in a small change in the heat-transfer performance. Of course, any dropwise condensation in microscopic level could also be responsible for changes in the steam-side heat-transfer coefficient. Unfortunately, it is not possible to determine which of the two causes just mentioned is truly responsible for the observed changes in the steam-side coefficient.

2. **Effect of Porous Strip Type and Thickness on Heat-Transfer Performance**

This section presents results showing the variation of the steam-side heat-transfer coefficient with heat flux having porous strip type and thickness as parameters. Data were taken on the tube with a fin spacing of 0.5 mm, which is fully flooded without a strip.

Three porosities (A, B and C had average pore diameters of 0.05-0.13 mm, 0.025-0.05 mm, 0.0025-0.013 mm, as stated by the manufacturer, and thicknesses of 3.2 mm, 2.6 mm, 3.0 mm, respectively) were investigated using a strip height of 8 mm. As seen from Figures 5.11 and 5.12, strip type B showed the best performance. As discussed in Chapter II, there exists an optimum pore size. If the pore size is too large, the strip would not provide enough suction at the bottom of the tube (i.e., the capillary height may be smaller than the strip height, thus resulting in poorer performance), while the flow resistance would be large (i.e., ΔP_2 in equation (2.19) will be smaller owing to larger F) if the pore size is very small.

Figures 5.13 and 5.14 show the data for low pressure and atmospheric pressure, respectively, with the strip thickness as a parameter using type B porous strips. These figures show that the heat-transfer performance increased by about 25% and 30% for low and atmospheric pressures, respectively, when the porous strip thickness was increased from 2.6 mm to 5.2 mm. When the thickness was further increased to 7.8 mm, no subsequent increase in the heat-transfer performance was observed. Therefore, the strip thickness appears to have an optimum value for the following reasons. First, the flow velocity of condensate decreases with increasing

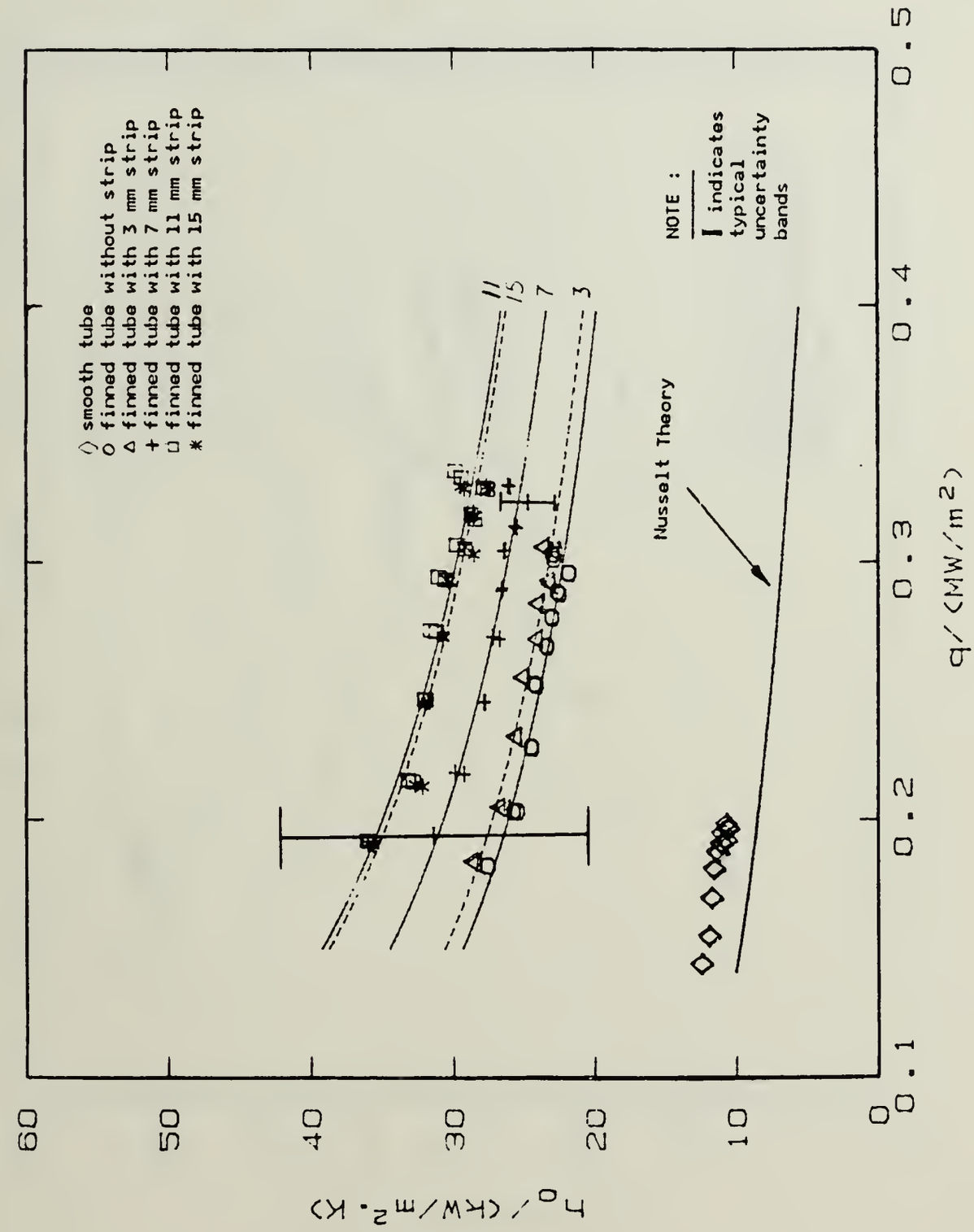

Figure 5.7 Effect of Strip Height on Heat-Transfer Coefficient (P_s = 85 mm Hg, Tube = 4, pore dia. = 0.05-0.13 mm).

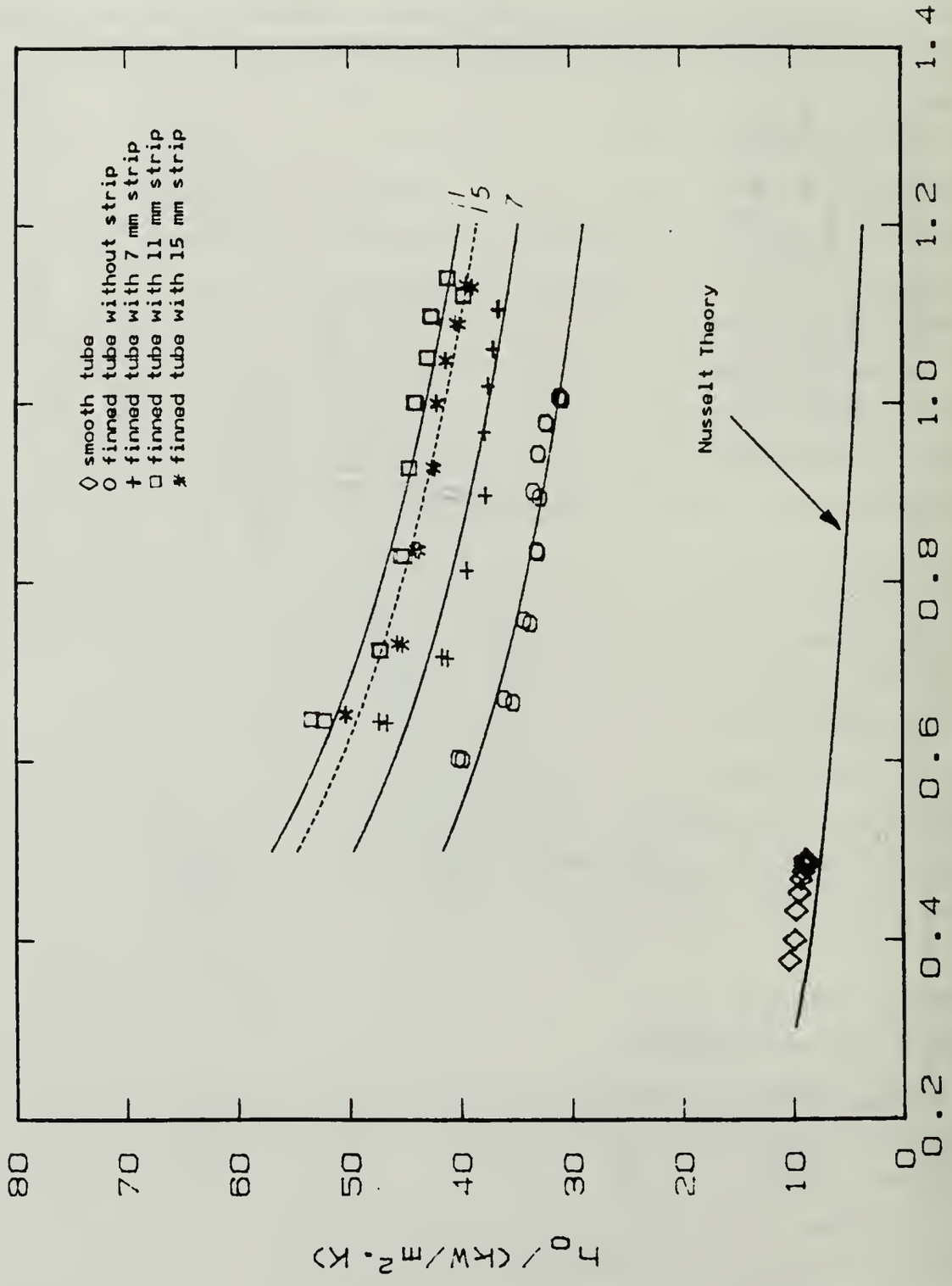

Figure 5.8 Effect of Strip Height on Heat-Transfer Coefficient (Atmospheric, Tube # 4, pore dia. = 0.05-0.13 mm).

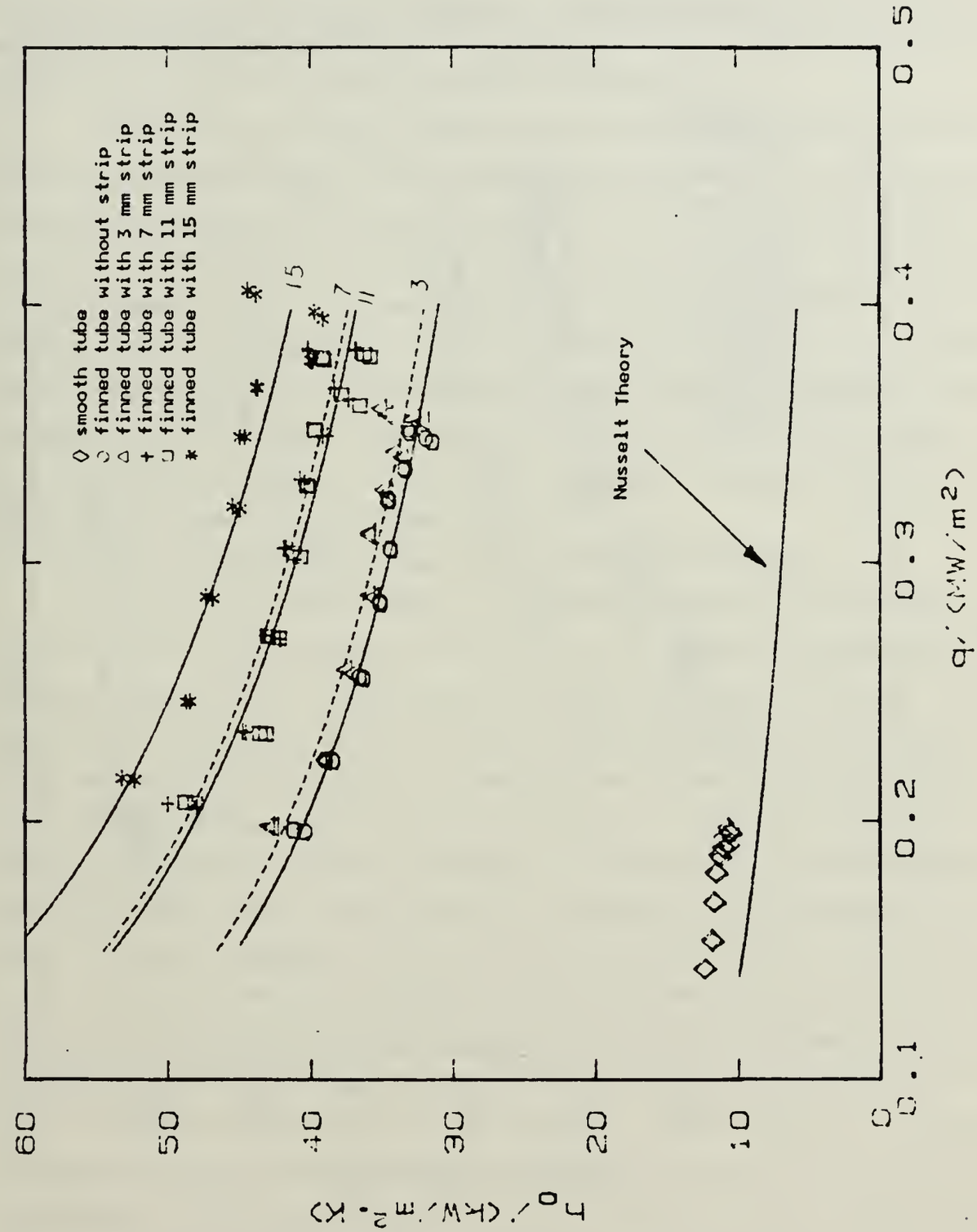

Figure 5.9 Effect of Strip Height on Heat-Transfer Coefficient (P_s = 85 mm Hg, Tube # 5, pore dia. = 0.05-0.13 mm).

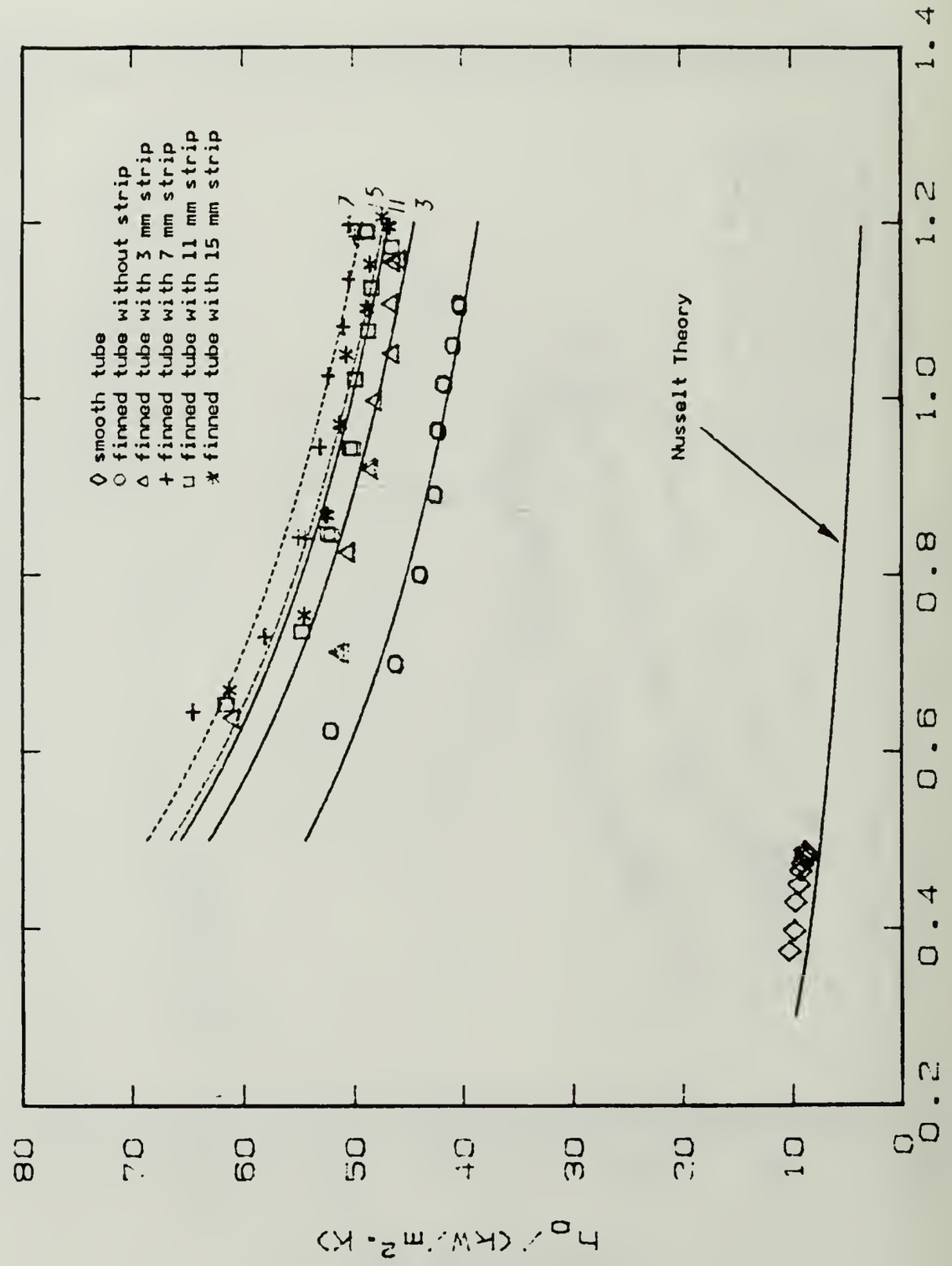

Figure 5.10 Effect of Strip Height on Heat-Transfer Coefficient (Atmospheric, Tube # 5, pore dia. = 0.05-0.13 mm).

thickness, thus, decreasing the flow resistance, which is a beneficial effect. Notice that, as explained by the discussion on Honda and Nozu [Ref. 3] theory in Chapter II, the retention angle decreases with decreasing condensate flow velocity or decreasing heat flux. Second, as seen in Figure 2.1, the area covered by the strip and the radius of the curvature of condensate surface at the corner of the strip and the tube increases with increasing strip thickness, resulting in a higher pressure in the condensate. This gives a larger retention angle and poorer heat-transfer performance.

Figures 5.13 and 5.14 also show the data with two type B strips having an air gap between them (see Figure 3.6 for strip with air gap geometry). As can be seen, the heat-transfer coefficient for the strip with an air gap was essentially the same as the case of the 7.8 mm strip where the air gap was replaced with another strip, which had the same thickness. The air gap between the two strips was expected to be filled with condensate, thus providing a path with low flow resistance. However, it was observed that this gap was not entirely filled with condensate during the condensation process. Therefore, it is possible that the expected effect was achieved only partially, thus observing almost no difference in heat-transfer performance compared to the case with this air gap replaced with another porous strip.

3. **Effect of Solid Strip Thickness on Heat-Transfer Performance**

In order to study the effect of solid strip thickness, data were taken with finned tube # 4 with a fin spacing of 0.5 mm. All the strips were manufactured with the same height of 8 mm. Dimensions for these strips are given in Table 2. As seen from Figures 5.15 and 5.16, the 1.5 mm solid strip thickness gave the best performance among the four thicknesses tested. For example, the 1.5 mm-thickness strip resulted in heat-transfer coefficients about 40% and 45% greater than the case without any strip for low and atmospheric pressure, respectively. The observed results are as expected as one would expect increased performance with decreasing solid strip thickness. This is because the radius of curvature of the condensate film at the bottom of the tube (see Figure 2.1) decreases with decreasing strip thickness. However, when the 0.1 mm-thick strip was tested, the performance was worse than the 1.5 mm thick strip. For the 0.1 mm-thick strip, five constantan wires were used to attach the strip at the bottom of the tube. Since this strip was very thin and flexible, a slight warpage in the strip was impossible to avoid. This problem may have caused the decrease in the heat-transfer performance. Data were also taken for a 90°, inverted V-shaped drainage strip, as shown in Figures 5.15 and 5.16. This strip had a thickness of 0.1 mm. As seen from

these figures, the performance with this strip is less than that of 1.5 mm-thick strip. As mentioned in Chapter II, Section C, the lower pressure at the bottom of the tube is caused by the small radius of curvature near the strip at the bottom of the tube. However, while the data for the inverted V-shaped strip was being taken, it was observed that condensate drainage did not occur from the sides, but instead, condensate accumulated at the corner of the V-shaped strip, and drained at one end of the tube. Apparently, the 90° inverted angle of this inverted V-shaped strip was too large to allow adequate drainage by gravity. A slight inclination of the test tube in the apparatus was responsible for this observation. Unfortunately, it was not possible to modify the apparatus to correct this problem, and this probably influenced the data for this strip.

4. **Effect of Triangular-Shaped Drainage Strip on Heat-Transfer Performance**

One porous and one solid triangular-shaped strip were manufactured to study the effect of single-point drainage on the heat-transfer performance. Dimensions of these strips are given in Figure 3.5 and Table 3. It was observed that the drainage of condensate occurred at the mid point of the strip both at low and atmospheric pressures. Figures 5.17 and 5.18 show a comparison of data for tube # 4 fitted with and without porous drainage strips. One run represents a porous drainage strip having a triangular shape resulting in single-point drainage. The second strip had a uniform height resulting in multiple, random drainage points. As seen in Figure 5.17 for low pressure condition, these drainage strips gave approximately equal enhancement. However, Figure 5.18 for the atmospheric condition, shows about 10% improvement in the steam-side coefficient for the triangular-shaped strip compared to the strip with uniform height. Based on this argument, the difference in performances for the two cases would be greater at atmospheric pressure due to the larger condensate flow rate.

Figures 5.19 and 5.20 show data similar to those presented in Figures 5.17 and 5.18, but for solid drainage strips. Unlike for the previous case, the solid drainage strips at low and atmospheric pressures provided heat-transfer performance approximately the same as the case with a strip of uniform height. The reason for this is not clear at this time.

5. **Summary**

Finally, Figures 5.21 and 5.22 show a direct comparison of performance for Tube # 4 with a solid drainage strip and two type B porous drainage strips. All of these strips had a height of 8 mm. As can be seen, the 5.2 mm and 2.6 mm-thick

porous strips and the 1.5 mm-thick solid strip resulted in steam-side enhancements (compared to smooth tube for constant heat flux) of 3.7, 3.1 and 3.4 for low pressure and 7.5, 6.0 and 6.4 for atmospheric pressure, respectively.

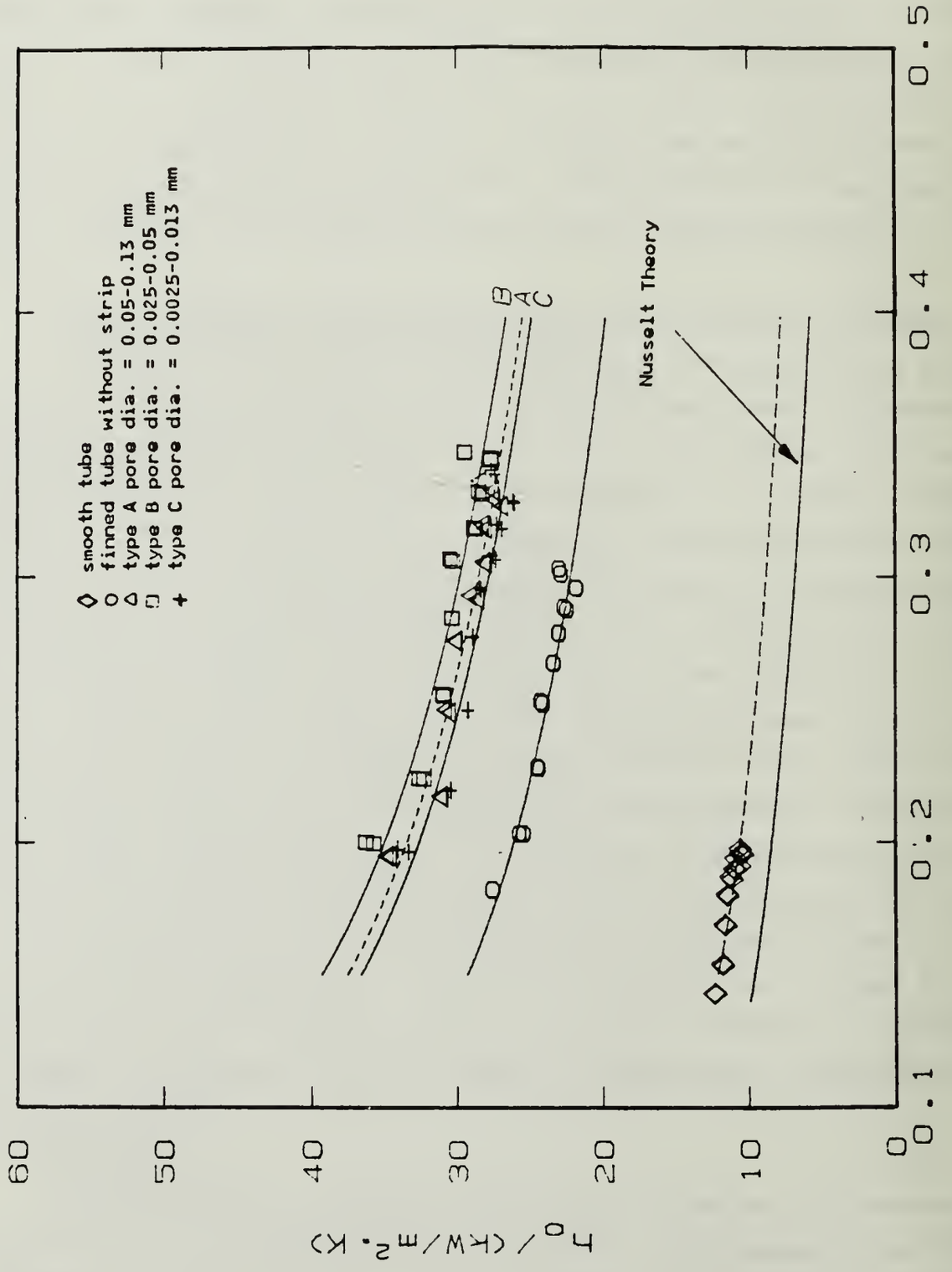

Figure 5.11 Effect of Porous Strip Type on Heat-Transfer Coefficient (P_s = 85 mm Hg, Strip Thickness ≃ 3 mm, Strip Height = 8 mm, Tube # 4).

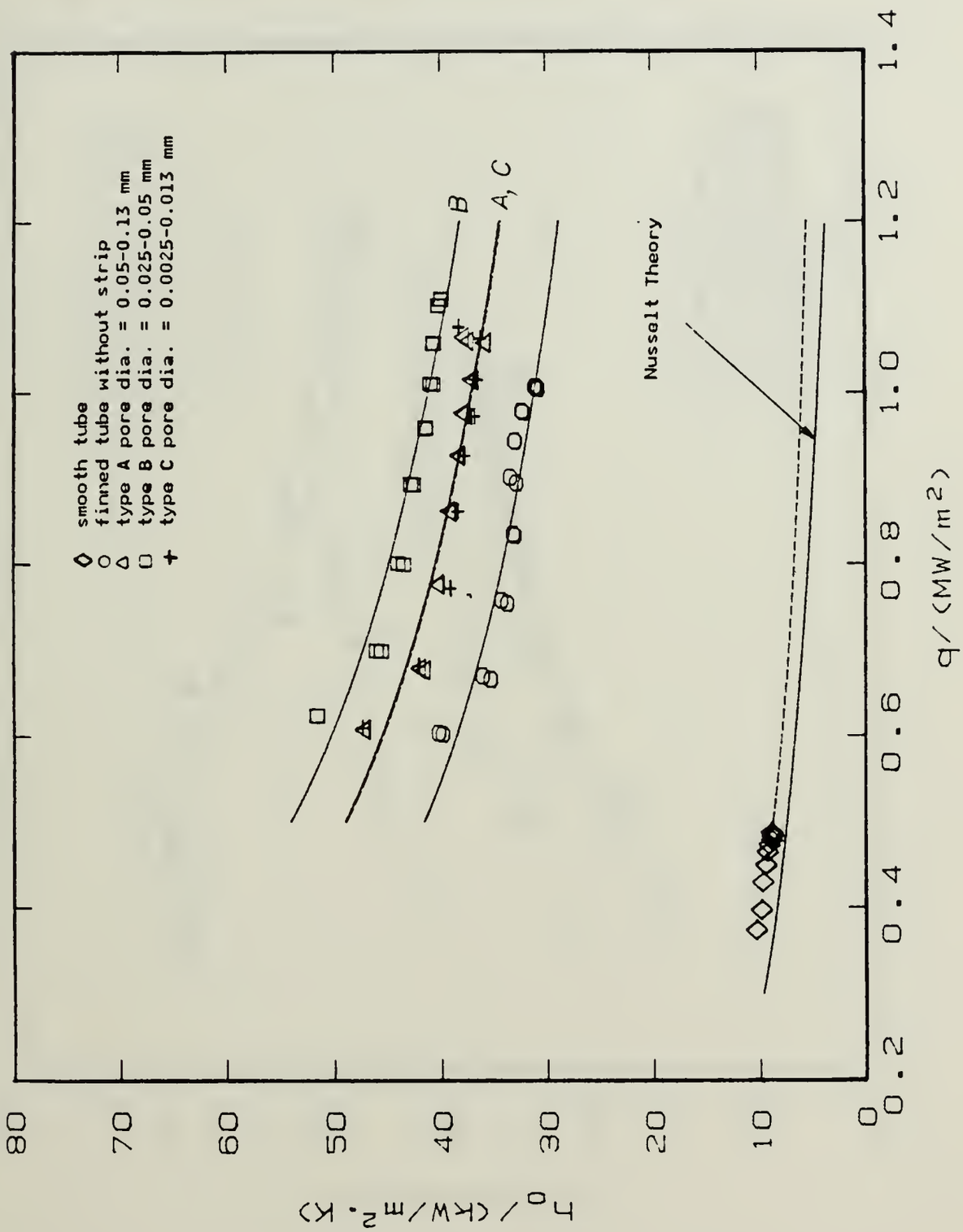

Figure 5.12 Effect of Porous Strip Type on Heat-Transfer Coefficient (Atmospheric runs, Strip Thickness $\simeq$ 3 mm, Strip Height = 8 mm, Tube # 4).

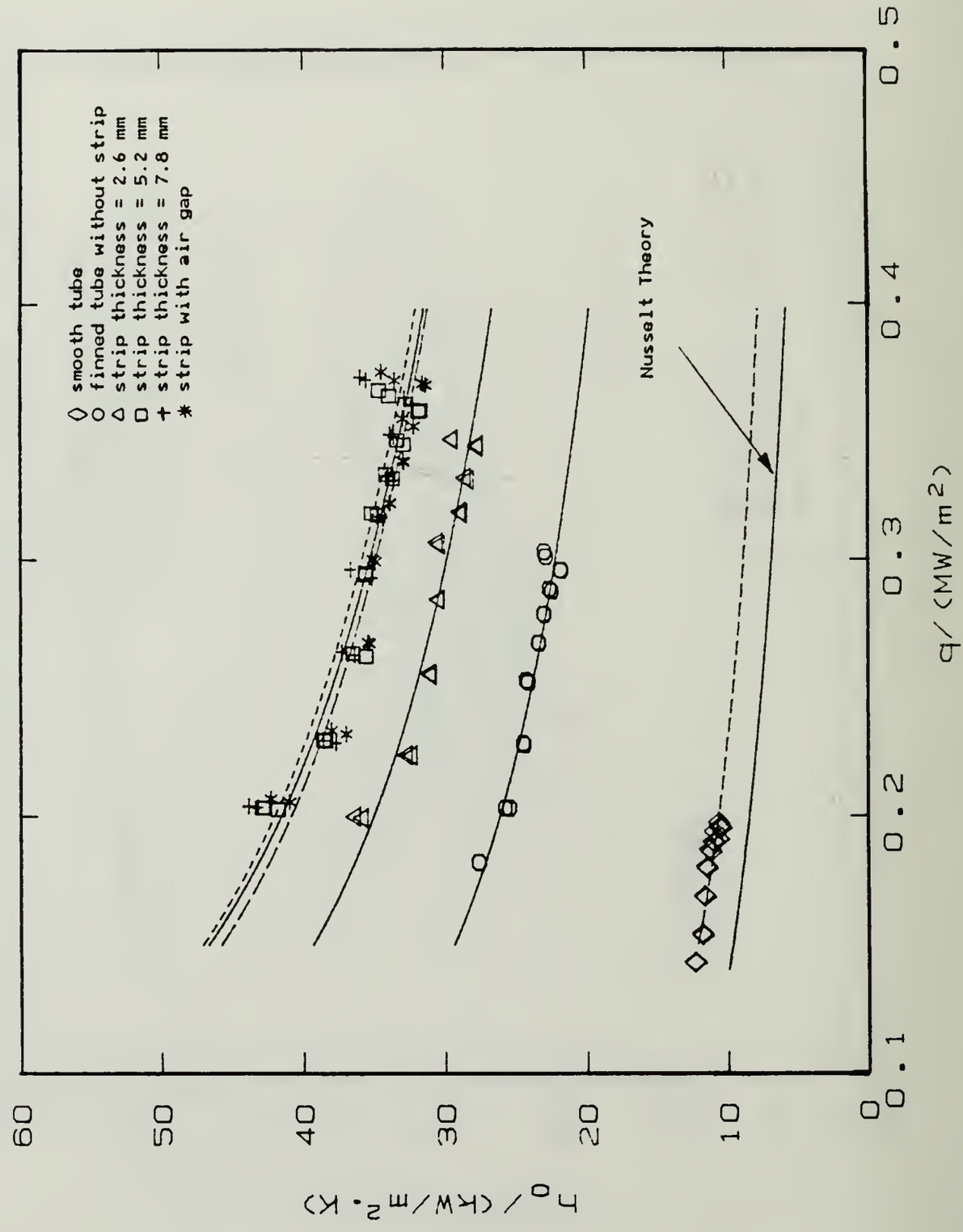

Figure 5.13 Effect of Porous Strip Thickness on Heat-Transfer Coefficient (P_s = 85 mm Hg. Strip Height = 8 mm. Tube = 4).

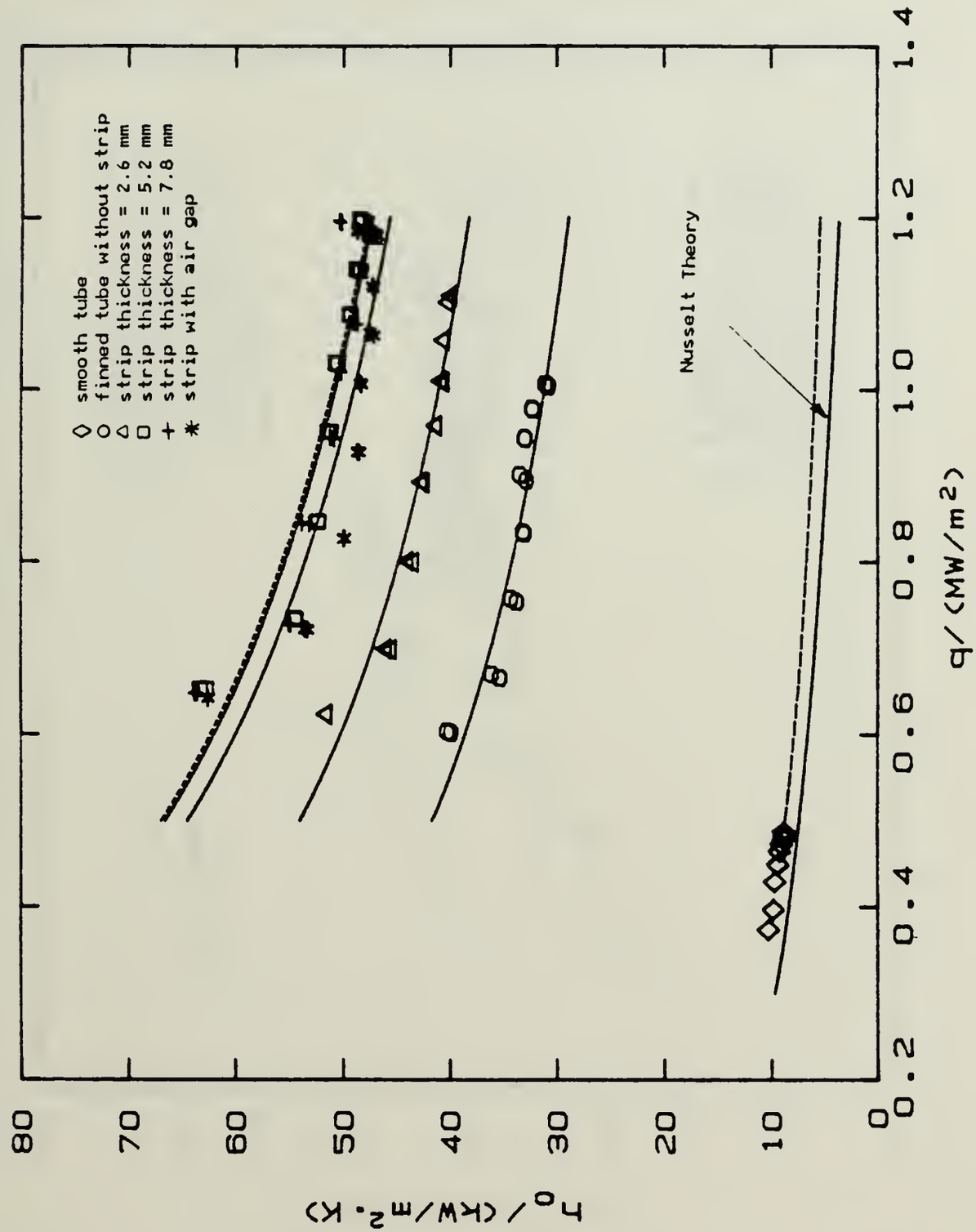

Figure 5.14 Effect of Porous Strip Thickness on Heat-Transfer Coefficient (Atmospheric runs, Strip Height = 8 mm, Tube # 4).

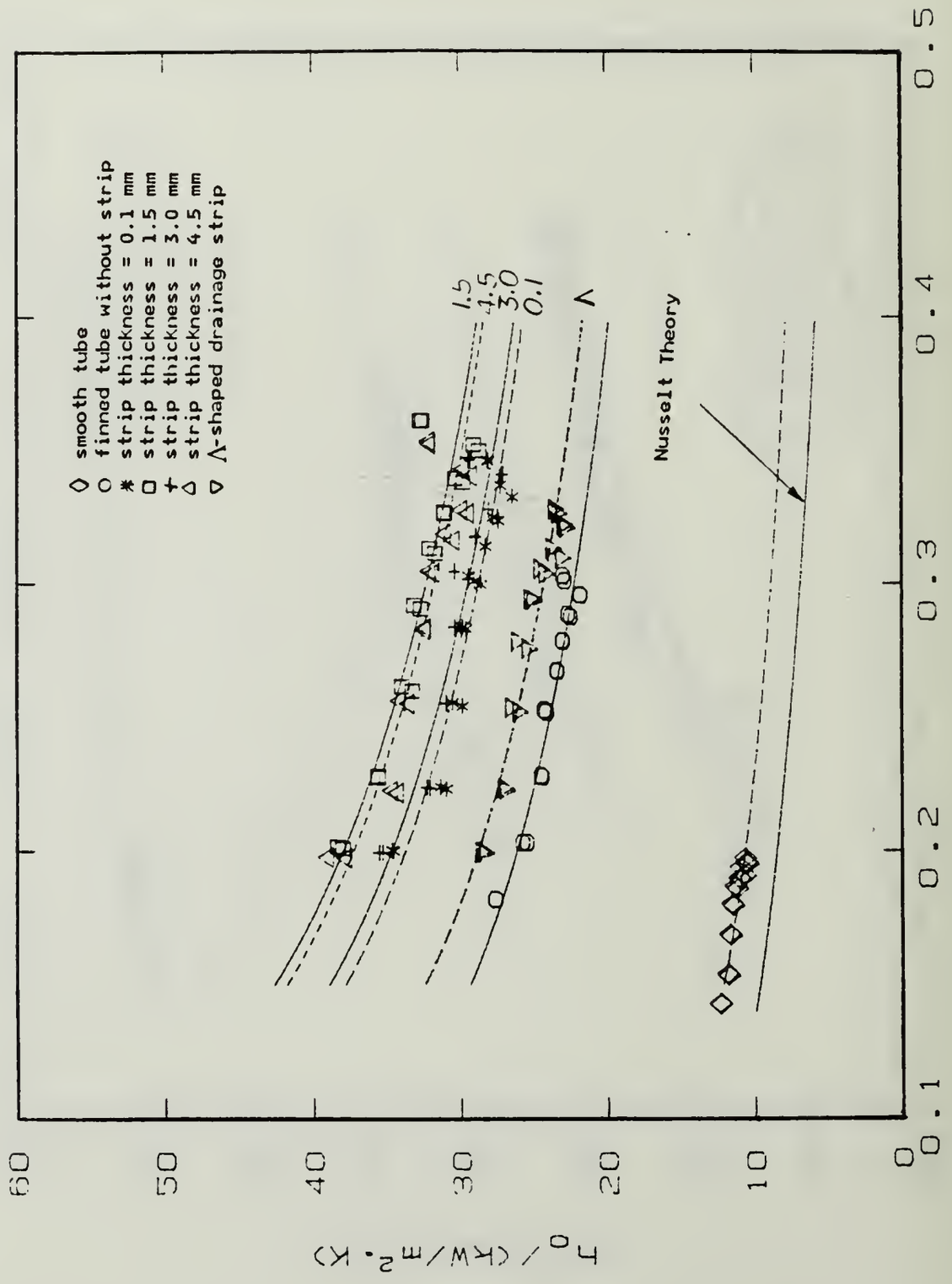

Figure 5.15 Effect of Solid Strip Thickness on Heat-Transfer Coefficient (P_s = 85 mm Hg, Strip Height = 8 mm, Tube # 4).

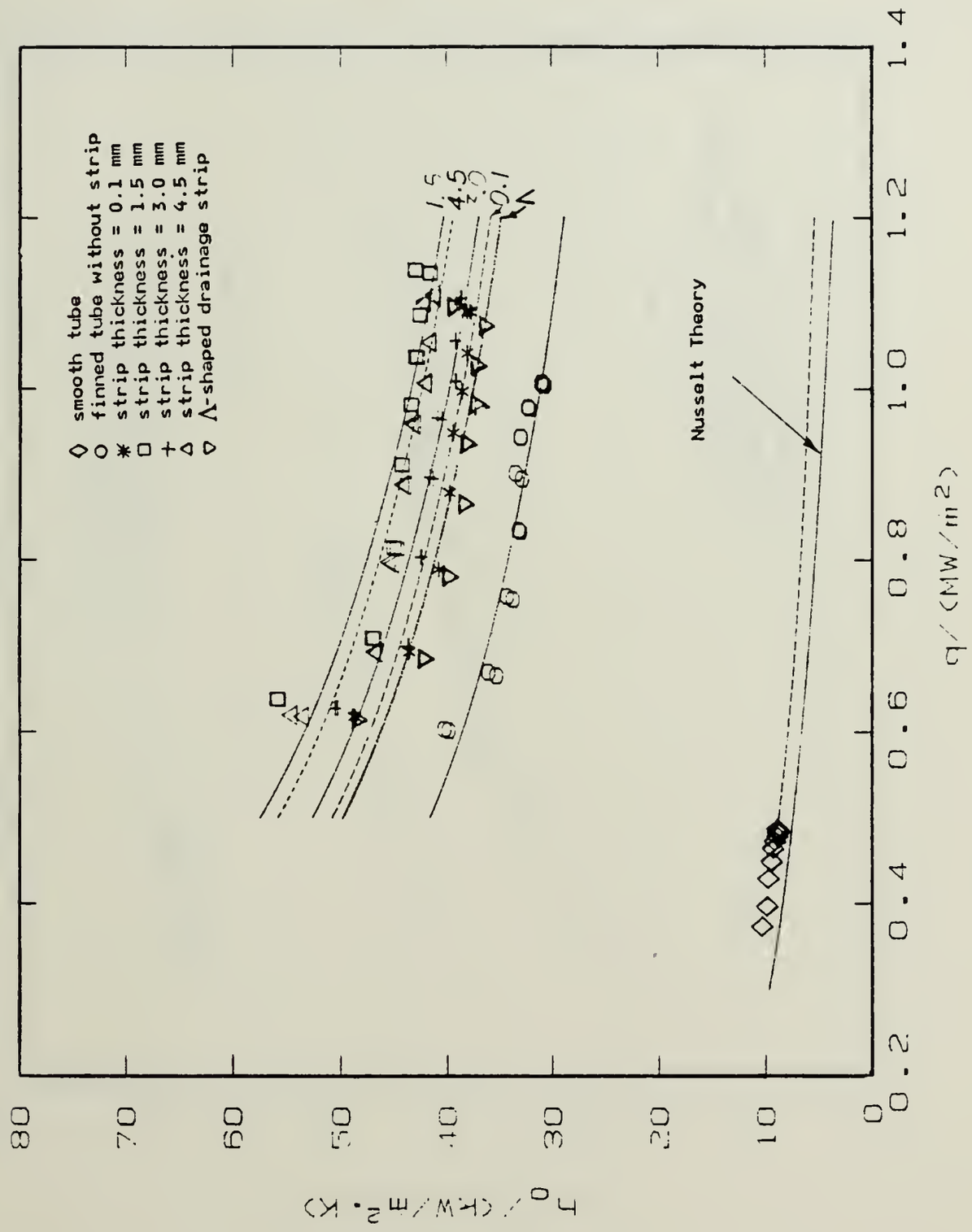

Figure 5.16 Effect of Solid Strip Thickness on Heat-Transfer Coefficient (Atmospheric runs, Strip Height = 8 mm, Tube = 4).

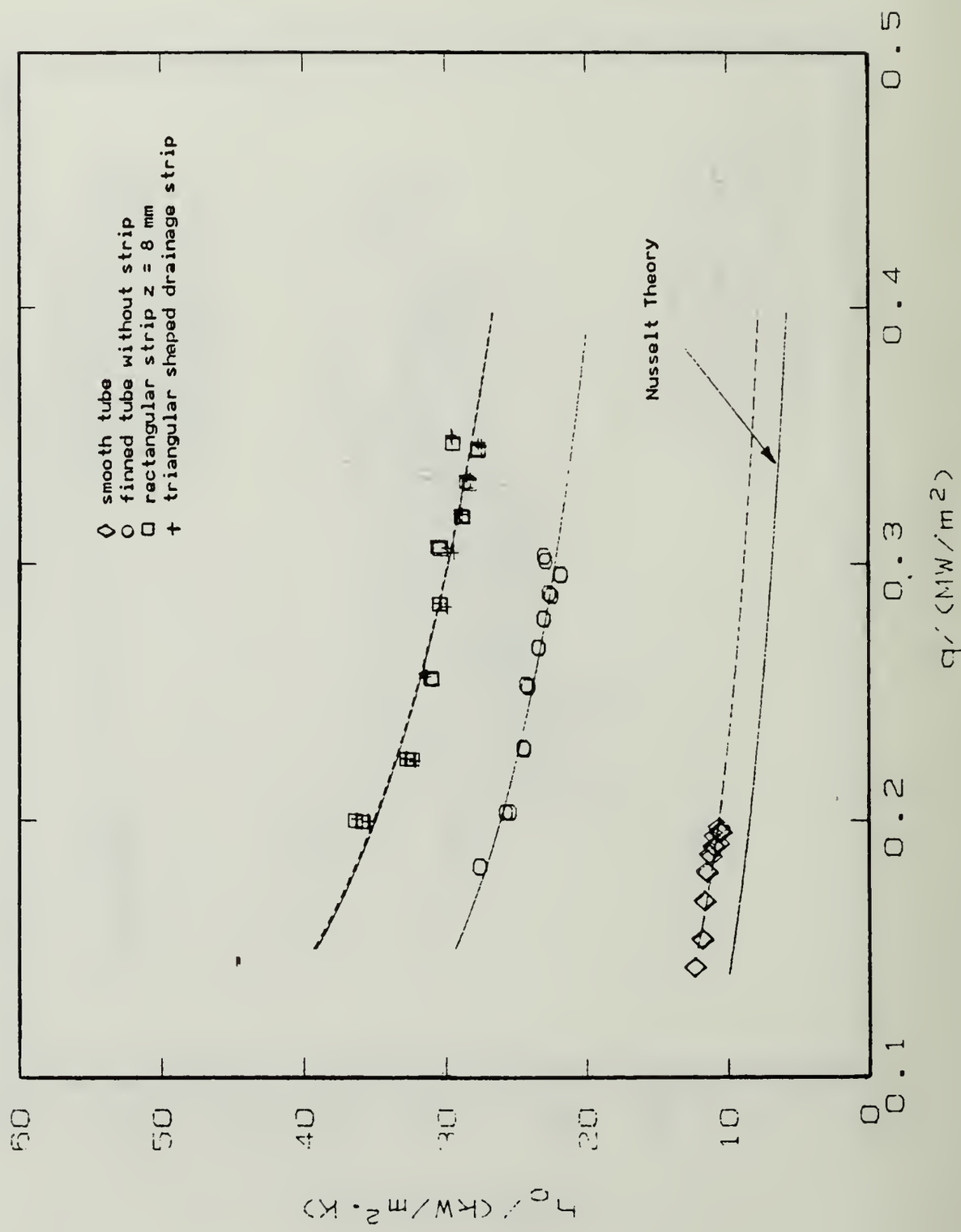

Figure 5.17 Effect of Porous Triangular Shaped Drainage Strip (Pore diameter 0.025-0.05 mm. P_s = 85 mm Hg. Tube # 4).

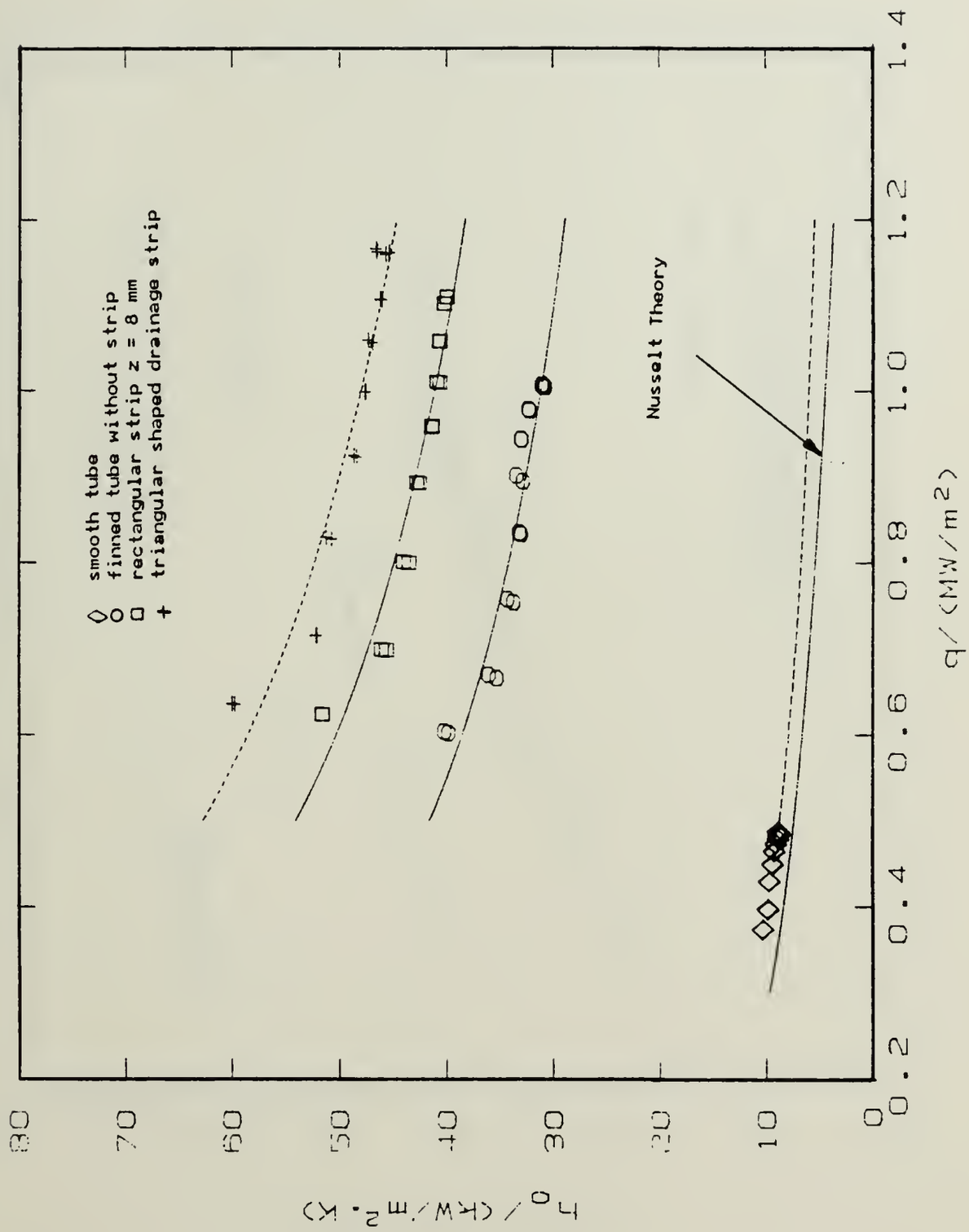

Figure 5.18 Effect of Porous Triangular Shaped Drainage Strip (Pore diameter 0.025-0.05 mm. Atmospheric runs. Tube # 4).

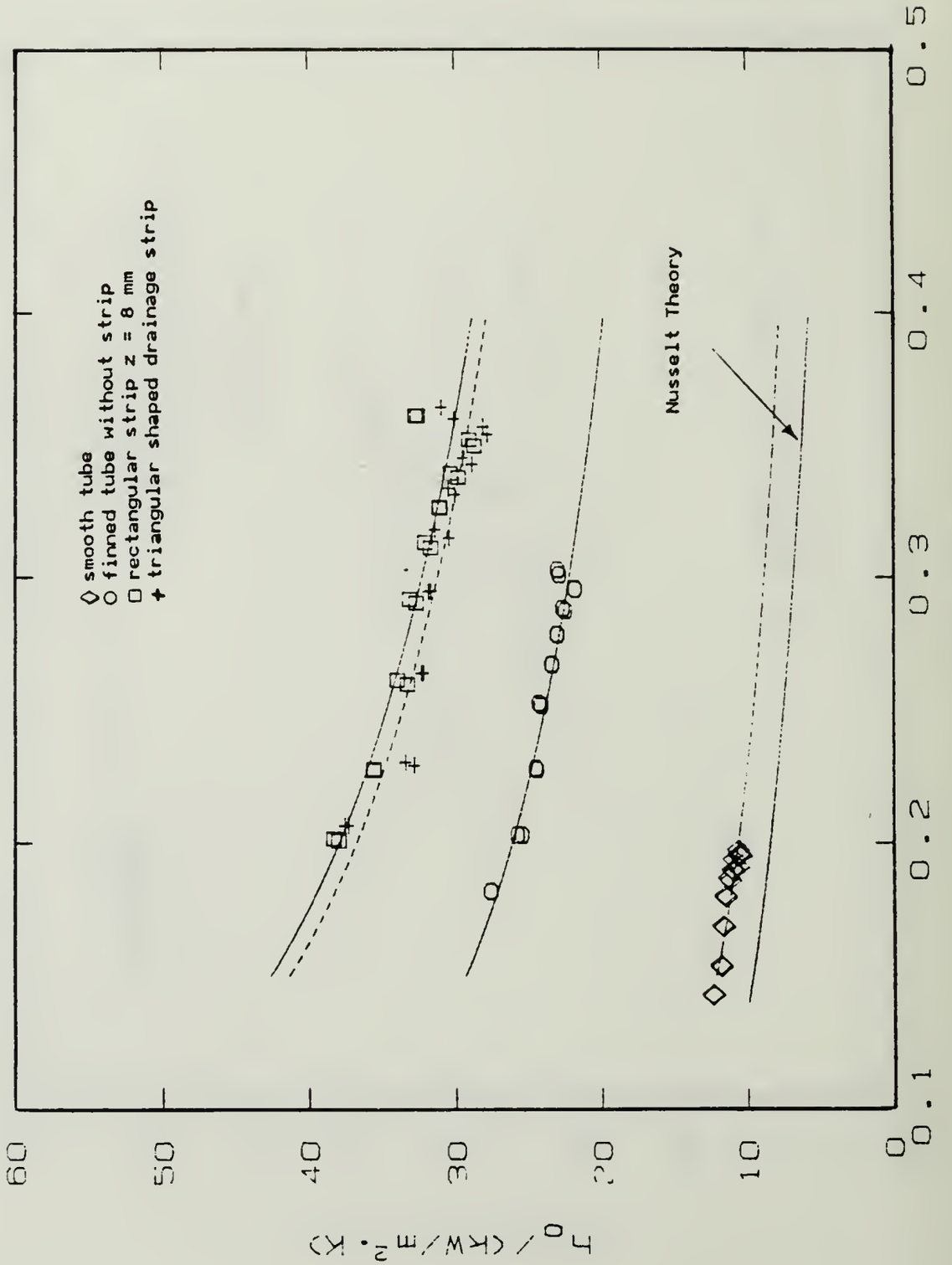

Figure 5.19 Effect of Solid Triangular Shaped Drainage Strip (Strip thickness = 1.5 mm, P_s = 85 mm Hg, Tube # 4).

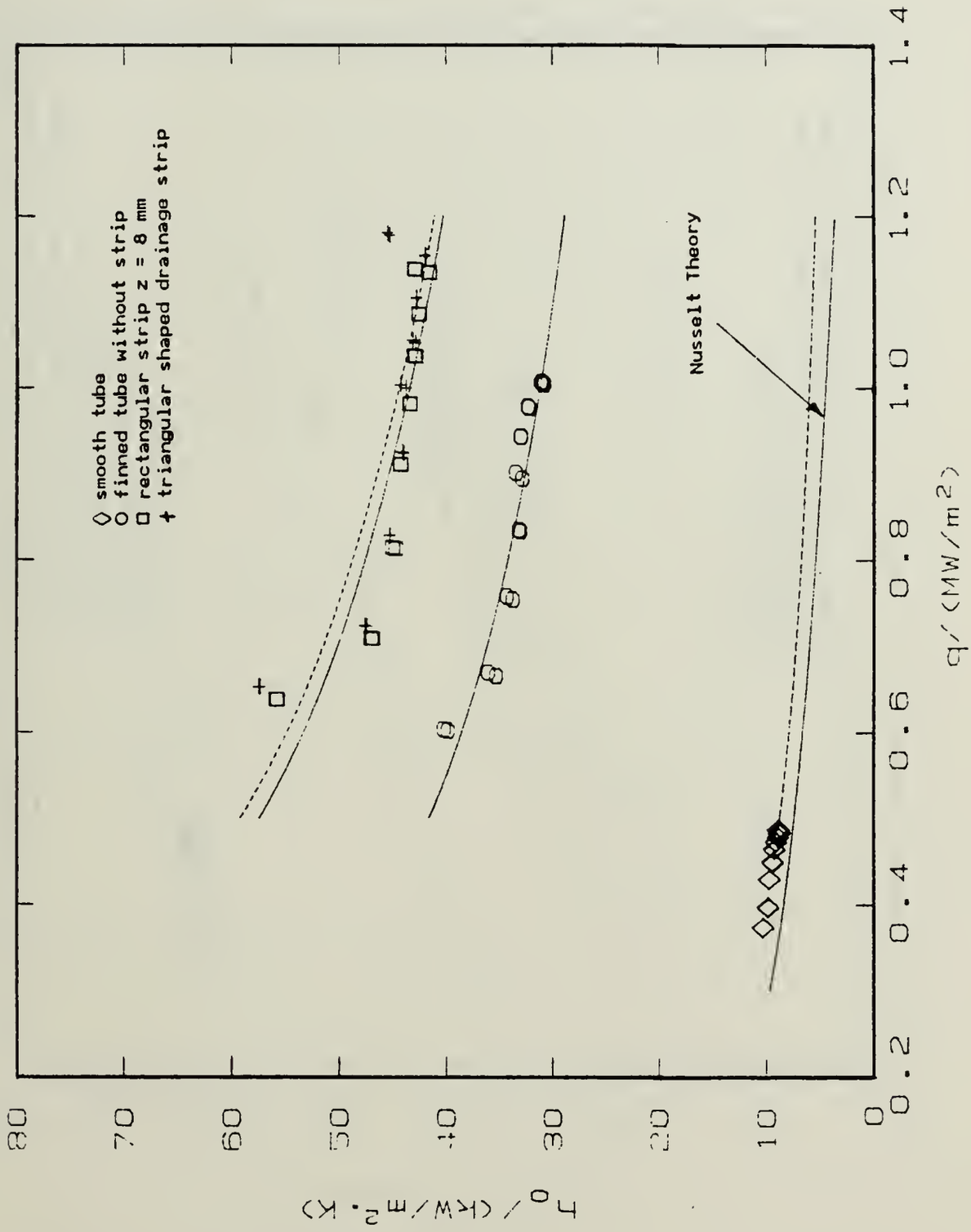

Figure 5.20 Effect of Solid Triangular Shaped Drainage Strip (Strip thickness = 1.5 mm, Atmospheric runs, Tube # 4).

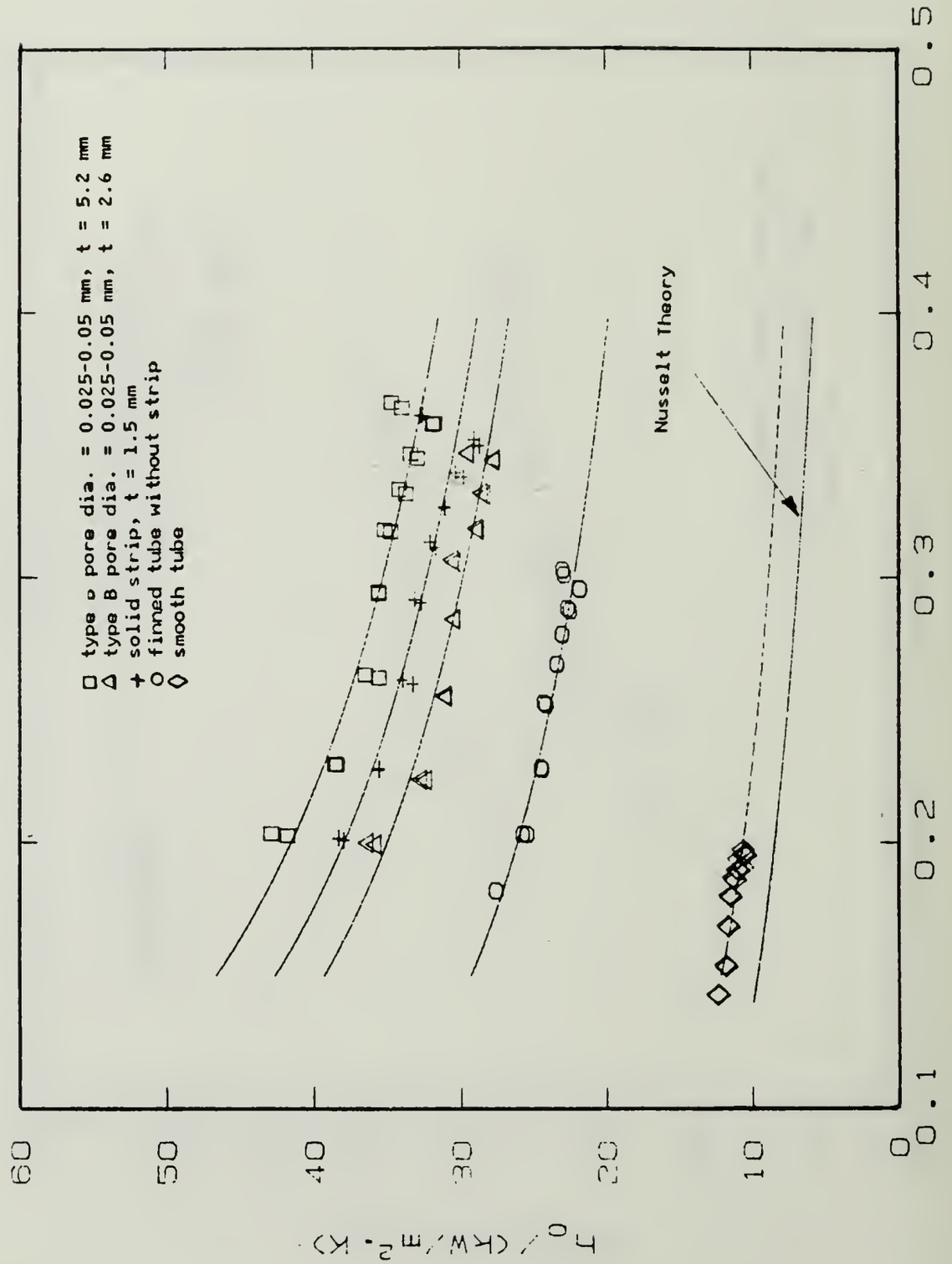

Figure 5.21 Effect of Strip Type and Thickness on Heat-Transfer Performance (P_s = 85 mm Hg. Strip Height = 8 mm. Tube # 4).

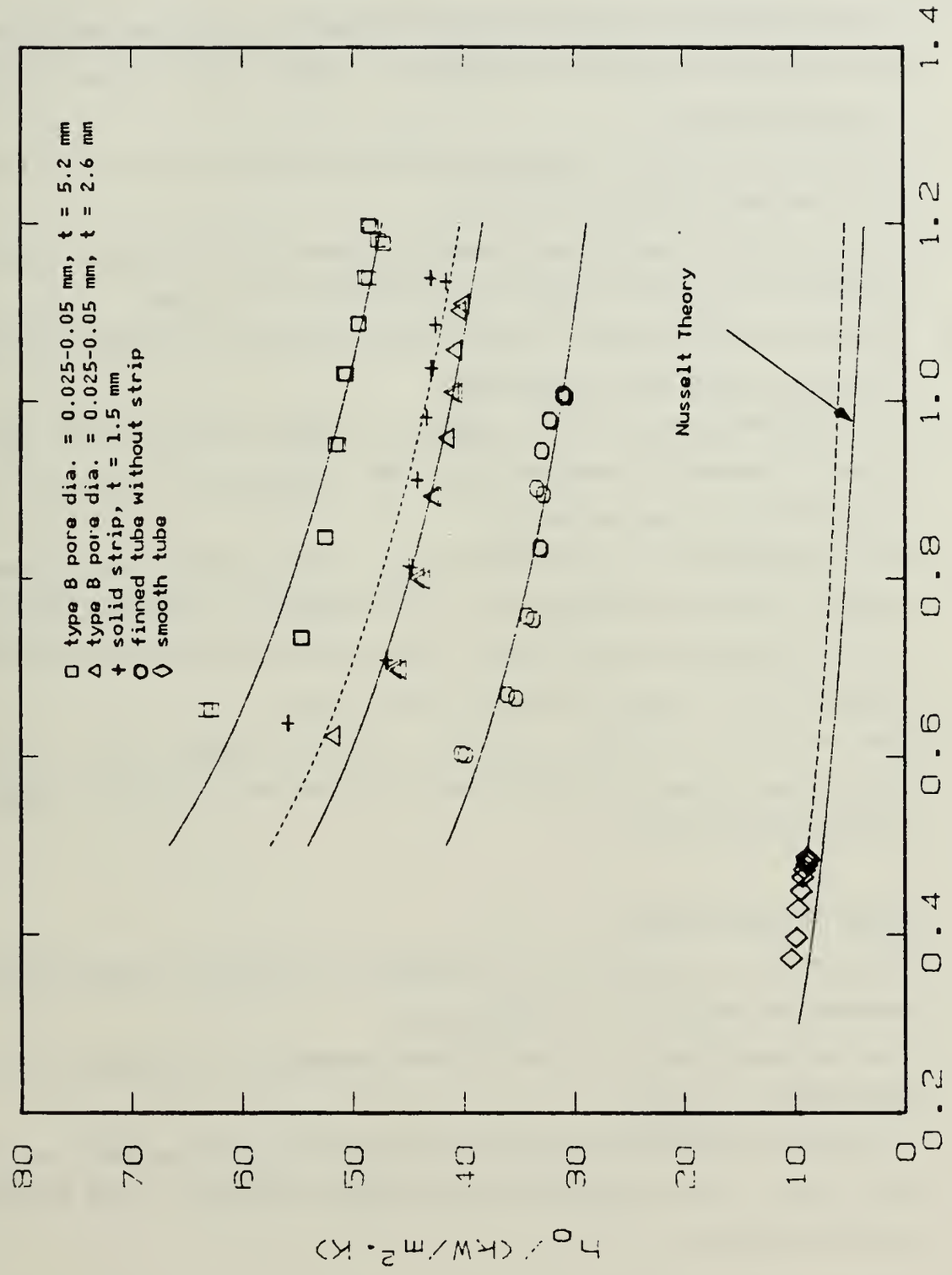

Figure 5.22 Effect of Strip Type and Thickness on Heat-Transfer Performance (Atmospheric runs, Strip Height = 8 mm, Tube # 4).

VI. CONCLUSIONS AND RECOMMENDATIONS

A. CONCLUSIONS

1. The use of porous and solid drainage strips leads to significant enhancement of the steam-side heat-transfer coefficient on finned tubes because condensate retention is reduced.
2. Porous strips having an average pore diameter 0.025-0.05 mm (type B) resulted in the best heat-transfer performance.
3. The heat-transfer performance generally increased with increasing porous strip height up to a possible optimum value between 11 to 15 mm.
4. The porous and solid strips of equal height of 8 mm gave optimum thicknesses of 5.2 mm and 1.5 mm, respectively.
5. The optimum porous strip in conclusion 4 above gave up to 9% and 17% greater steam-side enhancement than the optimum solid strip for low and atmospheric pressures, respectively.
6. The enhancement obtained with drainage strips increased with decreasing fin spacing. A maximum enhancement over the finned tube was found to be about 1.6 at low and atmospheric pressures for the tube with a fin spacing of 0.5 mm attached with a 5.2 mm-thick type B porous strip.
7. The use of a triangular strip with a single drainage point resulted in enhancement similar to or slightly better than the strip with uniform height with multiple drainage points.

B. RECOMMENDATIONS

1. Take data on the tube with a fin spacing of 1.0 mm with drainage strips and compare the trend with the existing data.
2. Take additional data on a finned tube to determine the optimum porous strip type-height combination.
3. Use plastic shields around the tube to allow heat transfer on only one portion of the tube, and investigate the heat-transfer coefficient in the flooded and unflooded regions.

4. Take data using different fluids to study the effect of fluid properties on the observed heat-tranfer performance.

APPENDIX A
LISTING OF RAW DATA

The following pages contain raw data obtained for tubes # 4 and # 5 at low and atmospheric pressures.

TABLE 8

RAW DATA FOR FIN SPACING 0.5 MM TUBE WITH STRIP (HEIGHT = 7 MM AND PORE DIAMETER = 0.05-0.13 MM)

Tube Number: 04
File Name: S8F04V
Pressure Condition: Vacuum
Steam Velocity: 2.0 (m/s)

Data #	Vw (m/s)	Tin (C)	Tout (C)	Ts (C)
1	4.41	20.66	21.77	48.47
2	4.41	20.67	21.78	48.45
3	3.87	20.73	21.96	48.46
4	3.87	20.73	21.96	48.41
5	3.43	20.80	22.13	48.42
6	3.43	20.80	22.14	48.49
7	3.00	20.87	22.33	48.51
8	3.00	20.89	22.34	48.40
9	2.51	20.99	22.61	48.50
10	2.51	21.00	22.62	48.39
11	1.97	21.15	23.03	48.42
12	1.97	21.16	23.04	48.43
13	1.49	21.36	23.57	48.49
14	1.49	21.36	23.58	48.40
15	1.16	21.57	24.09	48.47
16	1.16	21.57	24.09	48.47
17	4.41	20.80	21.93	48.45
18	4.41	20.80	21.93	48.42

Tube Number: 04
File Name: S8F04AT
Pressure Condition: Atmospheric
Steam Velocity: 1.0 (m/s)

Data #	Vw (m/s)	Tin (C)	Tout (C)	Ts (C)
1	4.40	21.11	24.90	99.94
2	4.40	21.14	24.93	99.96
3	3.86	21.20	25.34	100.00
4	3.86	21.21	25.36	99.97
5	3.43	21.26	25.75	99.93
6	3.43	21.27	25.75	99.95
7	3.00	21.39	26.25	99.95
8	3.00	21.39	26.26	99.93
9	2.51	21.50	26.89	99.98
10	2.51	21.52	26.91	99.95
11	1.97	21.69	27.92	99.96
12	1.97	21.70	27.93	99.95
13	1.49	21.91	29.17	100.00
14	1.49	21.92	29.20	99.96
15	1.16	22.16	30.51	99.96
16	1.16	22.17	30.54	99.92
17	4.40	21.42	25.21	99.99
18	4.40	21.42	25.20	99.97

TABLE 9

RAW DATA FOR FIN SPACING 0.5 MM TUBE WITH STRIP
(HEIGHT = 8 MM AND PORE DIAMETER = 0.05-0.13 MM)

Tube Number: 04
File Name: 30P8F04V1
Pressure Condition: Vacuum
Steam Velocity: 2.0 (m/s)

Data #	Vw (m/s)	Tin (C)	Tout (C)	Ts (C)
1	4.40	21.47	22.60	48.39
2	4.40	21.46	22.58	48.43
3	3.86	21.48	22.73	48.50
4	3.86	21.48	22.72	48.44
5	3.43	21.51	22.85	48.48
6	3.43	21.50	22.84	48.48
7	3.00	21.53	23.00	48.41
8	3.00	21.52	22.99	48.46
9	2.51	21.58	23.24	48.44
10	2.51	21.56	23.22	48.44
11	1.97	21.67	23.58	48.44
12	1.97	21.67	23.58	48.49
13	1.49	21.82	24.03	48.42
14	1.49	21.82	24.03	48.44
15	1.16	22.00	24.54	48.37
16	1.16	22.00	24.53	48.39
17	4.40	21.23	22.38	48.34
18	4.40	21.23	22.37	48.42

Tube Number: 04
File Name: 30P8F04A1
Pressure Condition: Atmospheric
Steam Velocity: 1.0 (m/s)

Data #	Vw (m/s)	Tin (C)	Tout (C)	Ts (C)
1	4.39	22.65	26.29	99.99
2	4.39	22.72	26.36	99.96
3	3.85	23.28	27.25	99.94
4	3.85	23.29	27.27	99.92
5	3.42	23.42	27.73	99.96
6	3.42	23.44	27.75	99.99
7	2.99	23.74	28.41	99.91
8	2.99	23.77	28.46	100.05
9	2.50	24.06	29.25	99.87
10	2.50	24.10	29.30	99.90
11	1.96	24.34	30.30	99.98
12	1.96	24.36	30.33	100.03
13	1.48	24.65	31.55	99.86
14	1.48	24.67	31.58	99.89
15	1.16	24.91	32.84	99.90
16	1.16	24.95	32.86	99.88
17	4.38	24.29	27.96	99.97
18	4.38	24.30	27.95	99.95

TABLE 10

RAW DATA FOR FIN SPACING 0.5 MM TUBE WITH STRIP (HEIGHT = 11 MM AND PORE DIAMETER = 0.05-0.13 MM)

Tube Number: 94
File Name: S12F04V5
Pressure Condition: Vacuum
Steam Velocity: 2.0 (m/s)

Data #	Vw (m/s)	Tin (C)	Tout (C)	Ts (C)
1	4.40	21.82	22.95	48.45
2	4.40	21.84	22.97	48.40
3	3.86	21.97	23.21	48.44
4	3.86	21.99	23.24	48.51
5	3.43	22.13	23.47	48.48
6	3.43	22.14	23.49	48.39
7	2.99	22.28	23.76	48.39
8	2.99	22.30	23.78	48.46
9	2.51	22.43	24.08	48.44
10	2.51	22.44	24.08	48.39
11	1.97	22.58	24.47	48.45
12	1.97	22.58	24.47	48.46
13	1.48	22.78	24.96	48.41
14	1.48	22.78	24.97	48.41
15	1.16	23.01	25.50	48.44
16	1.16	23.01	25.50	48.42
17	4.40	22.27	23.42	48.49
18	4.40	22.27	23.41	48.45

Tube Number: 94
File Name: S12F04AT5
Pressure Condition: Atmospheric
Steam Velocity: 1.0 (m/s)

Data #	Vw (m/s)	Tin (C)	Tout (C)	Ts (C)
1	4.40	22.44	26.35	99.98
2	4.40	22.44	26.36	99.97
3	3.86	22.57	26.86	99.94
4	3.86	22.58	26.87	99.97
5	3.42	22.70	27.33	99.96
6	3.42	22.71	27.35	99.97
7	2.99	22.81	27.86	99.93
8	2.99	22.81	27.86	99.96
9	2.51	22.93	28.51	99.94
10	2.51	22.94	28.53	99.95
11	1.97	23.12	29.48	99.92
12	1.97	23.13	29.48	100.00
13	1.48	23.34	30.72	99.94
14	1.48	23.34	30.71	99.92
15	1.16	23.53	31.95	99.93
16	1.16	23.59	31.99	100.03
17	4.39	22.84	26.69	99.92
18	4.39	22.84	26.69	99.98

TABLE 11

RAW DATA FOR FIN SPACING 0.5 MM TUBE WITH STRIP (HEIGHT = 15 MM AND PORE DIAMETER = 0.05-0.13 MM)

Tube Number: 04
File Name: S16F04V1
Pressure Condition: Vacuum
Steam Velocity: 2.0 (m/s)

Data #	Vw (m/s)	Tin (C)	Tout (C)	Ts (C)
1	4.40	21.89	23.02	48.46
2	4.40	21.91	23.04	48.47
3	3.86	22.04	23.28	48.50
4	3.86	22.06	23.30	48.46
5	3.43	22.23	23.57	48.48
6	3.43	22.25	23.60	48.51
7	2.99	22.42	23.90	48.46
8	2.99	22.45	23.93	48.49
9	2.51	22.64	24.28	48.44
10	2.51	22.66	24.29	48.42
11	1.97	22.82	24.71	48.46
12	1.97	22.90	24.78	48.42
13	1.48	23.15	25.31	48.48
14	1.48	23.15	25.33	48.44
15	1.16	23.38	25.96	48.46
16	1.16	23.39	25.88	48.46
17	4.39	22.72	23.85	48.46
18	4.39	22.73	23.86	48.50

Tube Number: 04
File Name: S16F04A13
Pressure Condition: Atmospheric
Steam Velocity: 1.0 (m/s)

Data #	Vw (m/s)	Tin (C)	Tout (C)	Ts (C)
1	4.40	22.25	26.13	99.98
2	4.40	22.26	26.14	99.97
3	3.86	22.38	26.64	99.97
4	3.86	22.39	26.66	99.88
5	3.43	22.52	27.14	99.94
6	3.42	22.53	27.15	99.90
7	2.99	22.64	27.68	99.95
8	2.99	22.64	27.68	99.94
9	2.51	22.76	28.35	99.95
10	2.51	22.77	28.34	99.97
11	1.97	22.91	29.32	99.96
12	1.97	22.91	29.32	99.91
13	1.48	23.10	30.53	99.97
14	1.48	23.10	30.55	99.97
15	1.16	23.32	31.80	99.89
16	1.16	23.32	31.81	99.96
17	4.39	22.58	26.48	99.98
18	4.39	22.58	26.48	99.98

TABLE 12

RAW DATA FOR FIN SPACING 1.0 MM TUBE WITH STRIP (HEIGHT = 3 MM AND PORE DIAMETER = 0.05-0.13 MM)

Tube Number: 05
File Name: SS4F05V2
Pressure Condition: Vacuum
Steam Velocity: 2.0 (m/s)

Data #	Vw (m/s)	Tin (C)	Tout (C)	Ts (C)
1	4.40	21.23	22.43	48.45
2	4.40	21.24	22.45	48.47
3	3.86	21.40	22.71	48.44
4	3.86	21.41	22.74	48.43
5	3.43	21.51	22.94	48.48
6	3.43	21.53	22.96	48.47
7	3.00	21.63	23.18	48.42
8	3.00	21.65	23.20	48.43
9	2.51	21.77	23.48	48.49
10	2.51	21.78	23.49	48.39
11	1.97	21.95	23.92	48.44
12	1.97	21.95	23.92	48.42
13	1.48	22.15	24.43	48.39
14	1.48	22.16	24.43	48.42
15	1.16	22.40	24.96	48.47
16	1.16	22.40	24.97	48.43
17	4.40	21.67	22.89	48.50
18	4.40	21.67	22.90	48.48

Tube Number: 05
File Name: SS4F05AT2
Pressure Condition: Atmospheric
Steam Velocity: 1.0 (m/s)

Data #	Vw (m/s)	Tin (C)	Tout (C)	Ts (C)
1	4.39	22.54	26.53	99.94
2	4.39	22.62	26.60	99.87
3	3.85	22.73	27.07	100.00
4	3.85	22.73	27.07	100.01
5	3.42	22.99	27.62	100.01
6	3.42	23.00	27.64	99.98
7	2.99	23.31	28.34	99.93
8	2.99	23.33	28.36	99.97
9	2.51	23.46	29.00	99.89
10	2.51	23.47	29.02	99.95
11	1.97	23.65	29.99	99.96
12	1.97	23.67	30.00	100.01
13	1.48	23.86	31.10	99.92
14	1.48	23.86	31.12	99.91
15	1.16	24.10	32.41	99.95
16	1.16	24.10	32.41	99.94
17	4.39	23.36	27.33	99.93
18	4.39	23.39	27.36	99.98

TABLE 13

RAW DATA FOR FIN SPACING 1.0 MM TUBE WITH STRIP (HEIGHT = 7 MM AND PORE DIAMETER = 0.05-0.13 MM)

Tube Number: 05
File Name: S8F05V10
Pressure Condition: Vacuum
Steam Velocity: 2.0 (m/s)

Data #	Vw (m/s)	Tin (C)	Tout (C)	Ts (C)
1	4.41	20.60	21.91	48.45
2	4.41	20.62	21.93	48.43
3	3.87	20.80	22.22	48.45
4	3.86	20.84	22.27	48.51
5	3.43	21.11	22.65	48.44
6	3.43	21.11	22.65	48.53
7	3.00	21.29	22.96	48.48
8	3.00	21.31	22.97	48.44
9	2.51	21.58	23.42	48.47
10	2.51	21.59	23.43	48.44
11	1.97	21.75	23.82	48.43
12	1.97	21.77	23.85	48.41
13	1.49	22.00	24.38	48.43
14	1.49	22.01	24.39	48.44
15	1.16	22.28	24.96	48.49
16	1.16	22.29	24.98	48.46
17	4.40	21.57	22.88	48.39
18	4.40	21.59	22.90	48.45

Tube Number: 05
File Name: S8F05AT10
Pressure Condition: Atmospheric
Steam Velocity: 1.0 (m/s)

Data #	Vw (m/s)	Tin (C)	Tout (C)	Ts (C)
1	4.39	22.54	26.55	99.94
2	4.39	22.67	26.79	99.87
3	3.85	22.93	27.38	99.94
4	3.85	22.97	27.42	99.94
5	3.42	23.11	27.89	99.98
6	3.42	23.13	27.90	99.97
7	2.99	23.22	28.40	100.01
8	2.99	23.25	28.42	99.98
9	2.51	23.42	29.11	99.96
10	2.51	23.45	29.15	99.95
11	1.97	23.65	30.11	99.96
12	1.97	23.67	30.14	99.92
13	1.48	23.96	31.40	99.95
14	1.48	23.96	31.41	99.91
15	1.16	24.20	32.61	100.00
16	1.16	24.24	32.65	99.99
17	4.39	23.60	27.68	99.98
18	4.39	23.62	27.68	99.97

TABLE 14

RAW DATA FOR FIN SPACING 1.0 MM TUBE WITH STRIP (HEIGHT = 11 MM AND PORE DIAMETER = 0.05-0.13 MM)

Tube Number: 05
File Name: S12F05V5
Pressure Condition: Vacuum
Steam Velocity: 2.0 (m/s)

Data #	Vw (m/s)	Tin (C)	Tout (C)	Ts (C)
1	4.40	20.97	22.27	48.46
2	4.40	21.02	22.32	48.45
3	3.86	21.28	22.69	48.46
4	3.86	21.32	22.75	48.46
5	3.43	21.50	23.05	48.45
6	3.43	21.54	23.09	48.45
7	3.00	21.92	23.58	48.53
8	3.00	21.93	23.59	48.51
9	2.51	22.14	23.97	48.40
10	2.51	22.21	24.03	48.40
11	1.97	22.39	24.47	48.41
12	1.97	22.39	24.47	48.47
13	1.48	22.58	24.96	48.43
14	1.48	22.58	24.96	48.48
15	1.16	22.77	25.46	48.47
16	1.16	22.80	25.49	48.51
17	4.40	22.06	23.36	48.44
18	4.40	22.08	23.38	48.49

Tube Number: 05
File Name: S12F05AT5
Pressure Condition: Atmospheric
Steam Velocity: 1.0 (m/s)

Data #	Vw (m/s)	Tin (C)	Tout (C)	Ts (C)
1	4.39	24.01	28.05	100.02
2	4.39	24.04	28.07	99.95
3	3.85	24.15	28.57	99.92
4	3.85	24.14	28.56	99.93
5	3.42	24.20	28.95	99.94
6	3.42	24.20	28.96	100.00
7	2.99	24.27	29.44	99.96
8	2.99	24.28	29.45	99.93
9	2.50	24.36	30.05	99.96
10	2.50	24.35	30.04	99.91
11	1.96	24.48	30.98	99.92
12	1.96	24.49	30.99	99.98
13	1.48	24.68	32.19	99.99
14	1.48	24.69	32.19	99.97
15	1.16	24.89	33.41	100.00
16	1.16	24.89	33.41	99.97
17	4.38	24.15	28.26	99.97
18	4.38	24.15	28.25	99.98

TABLE 15

RAW DATA FOR FIN SPACING 1.0 MM TUBE WITH STRIP (HEIGHT = 15 MM AND PORE DIAMETER = 0.05-0.13 MM)

Tube Number: 05
File Name: S16F05V10
Pressure Condition: Vacuum
Steam Velocity: 2.0 (m/s)

Data #	Vw (m/s)	Tin (C)	Tout (C)	Ts (C)
1	4.40	21.20	22.56	48.47
2	4.40	21.20	22.55	48.43
3	3.86	21.27	22.74	48.51
4	3.86	21.27	22.75	48.49
5	3.43	21.48	23.10	48.41
6	3.43	21.49	23.11	48.42
7	3.00	21.66	23.42	48.48
8	3.00	21.68	23.44	48.44
9	2.51	21.80	23.73	48.48
10	2.51	21.81	23.74	48.49
11	1.97	22.02	24.21	48.49
12	1.97	22.03	24.22	48.49
13	1.48	22.24	24.74	48.46
14	1.48	22.25	24.75	48.42
15	1.16	22.47	25.29	48.48
16	1.16	22.52	25.33	48.50
17	4.40	21.80	23.19	48.50
18	4.40	21.81	23.20	48.48

Tube Number: 05
File Name: S16F05A10
Pressure Condition: Atmospheric
Steam Velocity: 1.0 (m/s)

Data #	Vw (m/s)	Tin (C)	Tout (C)	Ts (C)
1	4.39	23.10	27.25	99.98
2	4.39	23.10	27.25	100.00
3	3.85	23.23	27.75	99.95
4	3.85	23.26	27.78	99.97
5	3.42	23.34	28.20	99.97
6	3.42	23.34	28.21	99.93
7	2.99	23.54	28.84	99.93
8	2.99	23.55	28.87	99.94
9	2.50	23.67	29.52	99.90
10	2.50	23.67	29.52	99.94
11	1.97	23.84	30.50	99.99
12	1.97	23.83	30.50	99.96
13	1.48	24.04	31.73	100.01
14	1.48	24.05	31.74	100.02
15	1.16	24.25	32.98	99.97
16	1.16	24.26	32.99	99.95
17	4.39	23.54	27.66	99.94
18	4.39	23.55	27.67	99.99

TABLE 16

RAW DATA FOR FIN SPACING 0.5 MM TUBE WITH STRIP (HEIGHT = 8 MM, PORE DIAMETER = 0.025-0.05 MM AND THICKNESS = 2.6 MM)

Tube Number: 04
File Name: SS8F04V2
Pressure Condition: Vacuum
Steam Velocity: 2.0 (m/s)

Data #	Vw (m/s)	Tin (C)	Tout (C)	Ts (C)
1	4.41	20.46	21.64	48.48
2	4.41	20.48	21.66	48.43
3	3.87	20.60	21.90	48.44
4	3.87	20.63	21.92	48.48
5	3.43	20.77	22.17	48.50
6	3.43	20.79	22.19	48.51
7	3.00	20.93	22.46	48.41
8	3.00	20.95	22.49	48.47
9	2.51	21.10	22.81	48.49
10	2.51	21.11	22.82	48.50
11	1.97	21.30	23.25	48.49
12	1.97	21.33	23.28	48.47
13	1.49	21.54	23.81	48.47
14	1.49	21.55	23.83	48.42
15	1.16	21.78	24.36	48.38
16	1.16	21.79	24.39	48.38
17	4.40	21.11	22.30	48.48
18	4.40	21.14	22.33	48.48

Tube Number: 04
File Name: SS8F04A1
Pressure Condition: Atmospheric
Steam Velocity: 1.0 (m/s)

Data #	Vw (m/s)	Tin (C)	Tout (C)	Ts (C)
1	4.40	22.36	26.17	99.97
2	4.40	22.40	26.21	99.95
3	3.86	22.68	26.82	99.89
4	3.85	22.74	26.88	99.94
5	3.42	22.91	27.37	99.94
6	3.42	22.95	27.40	99.87
7	2.99	23.11	27.95	100.01
8	2.99	23.16	27.99	99.94
9	2.51	23.32	28.69	100.00
10	2.51	23.35	28.72	99.92
11	1.97	23.53	29.66	99.98
12	1.97	23.56	29.70	99.90
13	1.48	23.78	30.89	99.94
14	1.48	23.80	30.92	99.89
15	1.16	24.04	32.16	99.91
16	1.16	24.04	32.17	99.94
17	4.39	23.37	27.15	99.95
18	4.39	23.40	27.19	99.97

TABLE 17

RAW DATA FOR FIN SPACING 0.5 MM TUBE WITH STRIP (HEIGHT = 8 MM, PORE DIAMETER = 0.025-0.05 MM AND THICKNESS = 5.2 MM)

Tube Number: 04
File Name: DS8F04V1
Pressure Condition: Vacuum
Steam Velocity: 2.0 (m/s)

Data #	Vw (m/s)	Tin (F)	Tout (C)	Ts (C)
1	4.40	20.91	22.13	48.51
2	4.40	20.92	22.14	48.43
3	3.36	21.00	22.36	48.46
4	3.36	21.01	22.35	48.48
5	3.43	21.06	22.53	48.47
6	3.43	21.07	22.52	48.48
7	3.00	21.16	22.75	48.50
8	3.00	21.16	22.76	48.46
9	2.51	21.29	23.05	48.47
10	2.51	21.30	23.07	48.44
11	1.97	21.46	23.47	48.52
12	1.97	21.50	23.51	48.48
13	1.49	21.70	24.04	48.46
14	1.49	21.72	24.05	48.46
15	1.16	21.91	24.54	48.44
16	1.16	21.95	24.59	48.44
17	4.40	21.27	22.52	48.44
18	4.40	21.27	22.52	48.51

Tube Number: 04
File Name: DS8F04A1
Pressure Condition: Atmospheric
Steam Velocity: 1.0 (m/s)

Data #	Vw (m/s)	Tin (C)	Tout (F)	Ts (C)
1	4.40	22.22	26.33	99.97
2	4.40	22.24	26.35	99.97
3	3.86	22.29	26.83	99.98
4	3.86	22.42	26.88	99.95
5	3.42	22.60	27.39	100.02
6	3.42	22.62	27.41	99.93
7	2.99	22.76	27.95	99.99
8	2.99	22.77	27.97	100.00
9	2.51	22.94	28.66	99.99
10	2.51	22.96	28.68	99.92
11	1.97	23.19	29.68	99.99
12	1.97	23.20	29.69	99.94
13	1.48	23.41	30.89	99.97
14	1.48	23.44	30.90	99.90
15	1.16	23.74	32.24	100.00
16	1.16	23.75	32.24	99.88
17	4.39	23.15	27.21	99.97
18	4.39	23.15	27.19	99.97

TABLE 18

RAW DATA FOR FIN SPACING 0.5 MM TUBE WITH STRIP (HEIGHT = 8 MM, PORE DIAMETER = 0.025-0.05 MM AND THICKNESS = 7.8 MM)

Tube Number: 04
File Name: T8F04V3
Pressure Condition: Vacuum
Steam Velocity: 2.0 (m/s)

Data #	Vw (m/s)	Tin (C)	Tout (C)	Ts (C)
1	4.40	20.96	22.20	48.51
2	4.40	20.98	22.22	48.51
3	3.86	21.06	22.43	48.49
4	3.86	21.08	22.44	48.51
5	3.43	21.15	22.61	48.48
6	3.43	21.15	22.61	48.48
7	3.00	21.24	22.83	48.53
8	3.00	21.25	22.84	48.47
9	2.51	21.38	23.14	48.44
10	2.51	21.39	23.17	48.41
11	1.97	21.59	23.60	48.49
12	1.97	21.60	23.62	48.42
13	1.49	21.80	24.12	48.50
14	1.49	21.80	24.13	48.46
15	1.16	22.01	24.66	48.42
16	1.16	22.02	24.66	48.43
17	4.40	21.28	22.55	48.44
18	4.40	21.28	22.56	48.40

Tube Number: 04
File Name: T8F04A3
Pressure Condition: Atmospheric
Steam Velocity: 1.0 (m/s)

Data #	Vw (m/s)	Tin (C)	Tout (C)	Ts (C)
1	4.40	21.95	25.04	99.95
2	4.40	21.98	26.06	99.96
3	3.86	22.15	26.58	100.01
4	3.86	22.21	26.63	99.97
5	3.43	22.35	27.09	100.00
6	3.43	22.40	27.15	99.97
7	2.99	22.52	27.66	99.96
8	2.99	22.53	27.68	99.99
9	2.51	22.67	28.35	99.99
10	2.51	22.70	28.38	100.04
11	1.97	22.92	29.39	100.01
12	1.97	22.96	29.44	100.00
13	1.48	23.24	30.65	99.95
14	1.48	23.27	30.67	99.88
15	1.16	23.50	31.94	100.01
16	1.16	23.51	31.95	100.00
17	4.39	22.90	27.01	99.93
18	4.39	22.88	26.99	99.93

TABLE 19

RAW DATA FOR FIN SPACING 0.5 MM TUBE WITH
SOLID TRIANGULAR SHAPED STRIP (THICKNESS = 1.5 MM)

Tube Number:		04			Tube Number:		04		
File Name:		UM8F04V1			File Name:		UM8F04A1		
Pressure Condition:		Vacuum			Pressure Condition:		Atmospheric		
Steam Velocity:		2.0 (m/s)			Steam Velocity:		1.0 (m/s)		
Data #	Vw (m/s)	Tin (C)	Tout (C)	Ts (C)	Data #	Vw (m/s)	Tin (C)	Tout (C)	Ts (C)
1	4.41	19.54	20.76	48.49	1	4.40	21.05	25.01	99.98
2	4.41	19.58	20.80	48.44	2	4.40	21.10	25.06	99.9
3	3.87	19.73	21.07	48.47	3	3.86	21.33	25.65	99.96
4	3.87	19.75	21.09	48.42	4	3.86	21.36	25.67	99.95
5	3.44	19.91	21.37	48.46	5	3.43	21.45	26.08	99.95
6	3.44	19.93	21.40	48.49	6	3.43	21.45	26.10	99.97
7	3.00	20.16	21.74	48.51	7	3.00	21.57	26.61	99.94
8	3.00	20.18	21.77	48.48	8	3.00	21.58	26.63	99.93
9	2.52	20.35	22.12	48.50	9	2.51	21.82	27.38	99.98
10	2.52	20.37	22.13	48.44	10	2.51	21.84	27.40	100.04
11	1.97	20.57	22.58	48.50	11	1.97	22.05	28.39	99.98
12	1.97	20.57	22.59	48.48	12	1.97	22.06	28.40	99.92
13	1.49	20.79	23.12	48.44	13	1.49	22.36	29.71	99.99
14	1.49	20.79	23.12	48.44	14	1.49	22.35	29.71	100.01
15	1.16	21.02	23.70	48.51	15	1.16	22.58	31.07	99.97
16	1.16	21.02	23.69	48.45	16	1.16	22.62	31.10	99.97
17	4.41	20.30	21.53	48.53	17	4.40	21.95	26.00	100.06
18	4.41	20.30	21.54	48.52	18	4.40	21.94	25.99	100.02

TABLE 20

RAW DATA FOR FIN SPACING 0.5 MM TUBE WITH POROUS TRIANGULAR SHAPED STRIP (THICKNESS = 2.6 MM)

Tube Number: 04
File Name: UPF04V1
Pressure Condition: Vacuum
Steam Velocity: 2.0 (m/s)

Data #	Vw (m/s)	Tin (C)	Tout (C)	Ts (C)
1	4.41	19.95	21.13	48.45
2	4.41	19.99	21.18	48.42
3	3.87	20.15	21.45	48.51
4	3.87	20.18	21.48	48.53
5	3.44	20.33	21.73	48.43
6	3.44	20.34	21.74	48.47
7	3.00	20.45	21.99	48.51
8	3.00	20.46	21.99	48.50
9	2.51	20.58	22.39	48.50
10	2.51	20.70	22.40	48.51
11	1.97	20.85	22.82	48.50
12	1.97	20.89	22.85	48.44
13	1.49	21.10	23.37	48.44
14	1.49	21.11	23.38	48.41
15	1.16	21.30	23.89	48.46
16	1.16	21.33	23.93	48.47
17	4.41	20.67	21.87	48.52
18	4.41	20.68	21.88	48.48

Tube Number: 04
File Name: UPF04A1
Pressure Condition: Atmospheric
Steam Velocity: 1.0 (m/s)

Data #	Vw (m/s)	Tin (C)	Tout (C)	Ts (C)
1	4.40	21.57	25.55	100.03
2	4.40	21.62	25.60	99.78
3	3.86	21.73	25.86	100.05
4	3.86	21.74	26.07	100.09
5	3.43	21.85	26.50	100.01
6	3.43	21.85	26.52	100.00
7	3.00	21.93	26.96	100.00
8	3.00	21.93	26.96	99.98
9	2.51	22.05	27.60	99.94
10	2.51	22.07	27.62	99.96
11	1.97	22.27	28.61	99.99
12	1.97	22.29	28.64	100.00
13	1.49	22.49	29.77	99.99
14	1.48	22.51	29.78	100.00
15	1.16	22.76	31.03	99.95
16	1.16	22.75	31.01	99.92
17	4.40	22.13	26.13	100.01
18	4.40	22.11	26.10	100.05

TABLE 21

RAW DATA FOR FIN SPACING 0.5 MM TUBE WITH STRIP HAVING AN AIR GAP

Tube Number: 04
File Name: BF04V1
Pressure Condition: Vacuum
Steam Velocity: 2.0 (m/s)

Data #	Vw (m/s)	Tin (C)	Tout (C)	Ts (C)
1	4.41	19.50	20.76	48.49
2	4.41	19.52	20.78	48.48
3	3.87	19.72	21.10	48.46
4	3.87	19.73	21.11	48.50
5	3.44	19.86	21.35	48.48
6	3.44	19.87	21.35	48.51
7	3.00	20.01	21.63	48.50
8	3.00	20.03	21.65	48.51
9	2.52	20.15	21.95	48.48
10	2.52	20.17	21.96	48.48
11	1.98	20.32	22.36	48.51
12	1.98	20.35	22.39	48.56
13	1.49	20.66	23.01	48.53
14	1.49	20.68	23.04	48.53
15	1.16	20.84	23.52	48.48
16	1.16	20.87	23.54	48.49
17	4.41	20.26	21.54	48.47
18	4.41	20.28	21.54	48.53

Tube Number: 04
File Name: BF04A1
Pressure Condition: Atmospheric
Steam Velocity: 1.0 (m/s)

Data #	Vw (m/s)	Tin (C)	Tout (C)	Ts (C)
1	4.40	21.28	25.22	99.98
2	4.40	21.32	25.37	100.01
3	3.86	21.44	25.81	99.98
4	3.86	21.47	25.84	99.92
5	3.43	21.62	26.31	99.98
6	3.43	21.64	26.31	99.97
7	3.00	21.83	26.90	99.96
8	3.00	21.84	26.90	99.93
9	2.51	22.00	27.58	99.94
10	2.51	22.03	27.60	99.99
11	1.97	22.23	28.57	99.95
12	1.97	22.25	28.58	99.90
13	1.49	22.49	29.83	100.00
14	1.49	22.50	29.83	99.98
15	1.16	22.82	31.17	99.97
16	1.16	22.84	31.19	99.95
17	4.40	22.19	26.25	99.98
18	4.40	22.19	26.26	99.94

TABLE 22

RAW DATA FOR FIN SPACING 0.5 MM TUBE WITH SOLID STRIP (HEIGHT = 8 MM, THICKNESS = 3.0 MM)

Tube Number: 04
File Name: DSF04V1
Pressure Condition: Vacuum
Steam Velocity: 2.0 (m/s)

Data #	Vw (m/s)	Tin (C)	Tout (C)	Ts (C)
1	4.41	20.01	21.16	48.48
2	4.41	20.02	21.18	48.41
3	3.87	20.13	21.43	48.46
4	3.87	20.14	21.43	48.43
5	3.44	20.26	21.67	48.47
6	3.44	20.31	21.71	48.42
7	3.00	20.41	21.95	48.41
8	3.00	20.42	21.96	48.41
9	2.52	20.57	22.27	48.45
10	2.52	20.59	22.30	48.44
11	1.97	20.75	22.71	48.43
12	1.97	20.76	22.73	48.43
13	1.49	20.93	23.22	48.50
14	1.49	20.97	23.26	48.48
15	1.16	21.22	23.82	48.49
16	1.16	21.22	23.83	48.53
17	4.41	20.52	21.71	48.48
18	4.41	20.52	21.72	48.41

Tube Number: 04
File Name: DSF04A1
Pressure Condition: Atmospheric
Steam Velocity: 1.0 (m/s)

Data #	Vw (m/s)	Tin (C)	Tout (C)	Ts (C)
1	4.40	21.37	25.16	100.00
2	4.40	21.40	25.19	99.97
3	3.86	21.54	25.67	99.98
4	3.86	21.56	25.68	99.95
5	3.43	21.66	26.10	99.95
6	3.43	21.65	26.09	99.96
7	3.00	21.77	26.62	100.00
8	3.00	21.77	26.64	99.92
9	2.51	21.97	27.35	99.93
10	2.51	21.98	27.37	99.90
11	1.97	22.17	28.33	99.99
12	1.97	22.22	28.37	99.94
13	1.49	22.42	29.53	99.97
14	1.49	22.43	29.54	99.89
15	1.16	22.74	30.90	99.91
16	1.16	22.71	30.88	99.86
17	4.40	22.08	25.37	99.92
18	4.40	22.06	25.84	99.88

TABLE 23

RAW DATA FOR FIN SPACING 0.5 MM TUBE WITH SOLID STRIP (HEIGHT = 8 MM, THICKNESS = 4.5 MM)

Tube Number: 04
File Name: TSF04V5
Pressure Condition: Vacuum
Steam Velocity: 2.0 (m/s)

Data #	Vw (m/s)	Tin (C)	Tout (C)	Ts (C)
1	4.40	21.32	22.49	48.39
2	4.40	21.32	22.48	48.42
3	3.86	21.36	22.64	48.41
4	3.86	21.36	22.63	48.48
5	3.43	21.39	22.78	48.49
6	3.43	21.39	22.79	48.49
7	3.00	21.45	22.98	48.49
8	3.00	21.45	22.99	48.45
9	2.51	21.54	23.25	48.46
10	2.51	21.55	23.25	48.37
11	1.97	21.70	23.66	48.39
12	1.97	21.70	23.65	48.42
13	1.49	21.90	24.17	48.44
14	1.49	21.92	24.17	48.44
15	1.16	22.16	24.73	48.44
16	1.16	22.16	24.73	48.32
17	4.40	21.42	22.62	48.38
18	4.40	21.41	22.62	48.44

Tube Number: 04
File Name: TSF04AF
Pressure Condition: Atmospheric
Steam Velocity: 1.0 (m/s)

Data #	Vw (m/s)	Tin (C)	Tout (C)	Ts (C)
1	4.39	23.38	27.19	99.94
2	4.39	23.48	27.19	100.11
3	3.85	23.57	27.71	99.99
4	3.85	23.61	27.75	99.98
5	3.42	23.81	28.25	99.96
6	3.42	23.87	28.32	100.03
7	2.99	24.12	28.96	99.98
8	2.99	24.16	29.01	100.01
9	2.50	24.46	29.81	99.92
10	2.50	24.50	29.86	99.93
11	1.96	24.69	30.81	100.05
12	1.96	24.71	30.84	100.05
13	1.48	24.95	32.01	100.01
14	1.48	24.97	32.04	100.06
15	1.16	25.23	33.29	99.89
16	1.16	25.25	33.34	99.89
17	4.38	24.56	28.36	99.85
18	4.38	24.60	28.39	99.66

TABLE 24

RAW DATA FOR FIN SPACING 0.5 MM TUBE WITH STRIP (HEIGHT = 8 MM AND PORE DIAMETER = 0.0025-0.013 MM)

Tube Number: 04
File Name: 100P8F4V1
Pressure Condition: Vacuum
Steam Velocity: 2.0 (m/s)

Data #	Vw (m/s)	Tin (C)	Tout (C)	Ts (C)
1	4.41	20.82	21.94	48.48
2	4.41	20.81	21.93	48.48
3	3.86	20.83	22.07	48.47
4	3.86	20.83	22.07	48.45
5	3.43	20.80	22.15	48.42
6	3.43	20.79	22.15	48.47
7	3.00	20.82	22.30	48.41
8	3.00	20.81	22.30	48.44
9	2.51	20.87	22.53	48.47
10	2.51	20.86	22.53	48.48
11	1.97	20.95	22.86	48.48
12	1.97	20.94	22.85	48.47
13	1.49	21.10	23.33	48.48
14	1.49	21.10	23.33	48.47
15	1.16	21.29	23.84	48.45
16	1.16	21.29	23.83	48.45
17	4.41	20.50	21.67	48.49
18	4.41	20.50	21.66	48.49

Tube Number: 04
File Name: 100P8F04AA
Pressure Condition: Atmospheric
Steam Velocity: 1.0 (m/s)

Data #	Vw (m/s)	Tin (C)	Tout (C)	Ts (C)
1	4.40	22.05	25.70	99.94
2	4.40	22.09	25.74	99.96
3	3.86	22.16	26.13	99.99
4	3.86	22.19	26.17	99.89
5	3.43	22.33	26.62	100.03
6	3.43	22.35	26.63	99.98
7	2.99	22.53	27.20	100.00
8	2.99	22.60	27.27	99.98
9	2.51	22.73	27.92	99.98
10	2.51	22.80	27.99	99.96
11	1.97	23.03	28.95	99.89
12	1.97	23.04	28.96	99.89
13	1.48	23.33	30.26	99.93
14	1.48	23.34	30.28	100.00
15	1.16	23.67	31.61	99.99
16	1.16	23.69	31.63	100.01
17	4.39	23.03	26.73	99.97
18	4.39	23.03	26.73	99.90

APPENDIX B
UNCERTAINTY ANALYSIS

There is always an uncertainty associated with any measurement which is dependent on the measuring device accuracy, calibration of the device, and the operator's experience. Numerical data collected during this thesis effort were used together with theoretical formulations, so final values of the steam-side heat transfer coefficient may be distorted due to uncertainty propagation during calculations. In cases where the final results show large uncertainties, it may be unwise to accept the experimental results. The uncertainty on a computation can be determined using the following equation proposed by Kline and McClintok [Ref. 30] shown below:

$$W_r = [(\frac{\partial R}{\partial x_1} W_1)^2 + (\frac{\partial R}{\partial x_2} W_2)^2 + \bullet\bullet\bullet\bullet\bullet + (\frac{\partial R}{\partial x_n} W_n)^2]^{1/2} \qquad \text{(eqn B.1)}$$

where

R is the result

w_r is the uncertainty of the desired dependent variable

$x_1, x_2, \ldots\ldots, x_n$ are the measured independent variables

$w_1, w_2, \ldots\ldots, w_n$ are the uncertanties in the measured variables

A complete discussion covering the developement of the uncertainty analysis used for this investigation is given by Georgiadis [Ref. 5]. The uncertainties associated with various quantities during this experiment were obtained using the program "UNA7" which is listed in [Ref. 7].

File Name:		F04V4
Pressure Condition:		Vacuum (11 kPa)
Steam Temperature	=	48.51 (Deg C)
Water Flow Rate (%)	=	80.00
Water Velocity	=	4.40 (m/s)
Heat Flux	=	3.028E+05 (W/m^2)
Tube-metal thermal conduc.	=	385.0 (W/m.K)
Sieder-Tate constant	=	0.0710

UNCERTAINTY ANALYSIS:

VARIABLE	PERCENT UNCERTAINTY
Mass Flow Rate, Md	.79
Reynolds Number, Re	1.11
Heat Flux, q	1.64
Log-Mean-Tem Diff, LMTD	1.37
Wall Resistance, Ru	2.67
Overall H.T.C., Uo	[illegible]
Water-Side H.T.C., Hi	1.19
Steam-Side H.T.C., Ho	4.56

DATA FOR THE UNCERTAINTY ANALYSIS:

File Name:		F04V4
Pressure Condition:		Vacuum (11 kPa)
Steam Temperature	=	48.41 (Deg C)
Water Flow Rate (%)	=	20.00
Water Velocity	=	1.16 (m/s)
Heat Flux	=	1.819E+05 (W/m^2)
Tube-metal thermal conduc.	=	385.0 (W/m.K)
Sieder-Tate constant	=	0.0710

UNCERTAINTY ANALYSIS:

VARIABLE	PERCENT UNCERTAINTY
Mass Flow Rate, Md	3.00
Reynolds Number, Re	3.10
Heat Flux, q	3.09
Log-Mean-Tem Diff, LMTD	0.61
Wall Resistance, Ru	2.67
Overall H.T.C., Uo	3.15
Water-Side H.T.C., Hi	2.61
Steam-Side H.T.C., Ho	17.37

DATA FOR THE UNCERTAINTY ANALYSIS:

File Name:		F04AT5
Pressure Condition:		Atmospheric (101 kPa)
Steam Temperature	=	99.94 (Deg C)
Water Flow Rate (%)	=	80.00
Water Velocity	=	4.40 (m/s)
Heat Flux	=	1.004E+06 (W/m^2)
Tube-metal thermal conduc.	=	385.0 (W/m.K)
Sieder-Tate constant	=	0.0675

UNCERTAINTY ANALYSIS:

VARIABLE	PERCENT UNCERTAINTY
Mass Flow Rate, Md	1.79
Reynolds Number, Re	1.12
Heat Flux, q	1.00
Log-Mean-Tem Diff, LMTD	0.41
Wall Resistance, Rw	3.67
Overall H.T.C., Uo	1.08
Water-Side H.T.C., Hi	1.22
Steam-Side H.T.C., Ho	3.03

DATA FOR THE UNCERTAINTY ANALYSIS:

File Name:		F04AT5
Pressure Condition:		Atmospheric (101 kPa)
Steam Temperature	=	99.97 (Deg C)
Water Flow Rate (%)	=	20.00
Water Velocity	=	1.16 (m/s)
Heat Flux	=	5.030E+05 (W/m^2)
Tube-metal thermal conduc.	=	385.0 (W/m.K)
Sieder-Tate constant	=	0.0675

UNCERTAINTY ANALYSIS:

VARIABLE	PERCENT UNCERTAINTY
Mass Flow Rate, Md	3.00
Reynolds Number, Re	3.12
Heat Flux, q	3.04
Log-Mean-Tem Diff, LMTD	0.18
Wall Resistance, Rw	3.67
Overall H.T.C., Uo	3.05
Water-Side H.T.C., Hi	2.63
Steam-Side H.T.C., Ho	23.19

DATA FOR THE UNCERTAINTY ANALYSIS:

File Name:		30P8F04A1
Pressure Condition:		Atmospheric (101 kPa)
Steam Temperature	=	99.99 (Deg C)
Water Flow Rate (%)	=	80.00
Water Velocity	=	4.39 (m/s)
Heat Flux	=	1.058E+06 (w/m^2)
Tube-metal thermal conduc.	=	385.0 (W/m.K)
Sieder-Tate constant	=	0.0645

UNCERTAINTY ANALYSIS:

VARIABLE	PERCENT UNCERTAINTY
Mass Flow Rate, Mc	.75
Reynolds Number, Re	1.13
Heat Flux, q	0.99
Log-Mean-Tem Diff, LMTD	1.39
Wall Resistance, Rw	2.67
Overall H.T.C., Uo	1.06
Water-Side H.T.C., Hi	1.25
Steam-Side H.T.C., Ho	3.55

DATA FOR THE UNCERTAINTY ANALYSIS:

File Name:		30P8F04A1
Pressure Condition:		Atmospheric (101 kPa)
Steam Temperature	=	99.90 (Deg C)
Water Flow Rate (%)	=	20.00
Water Velocity	=	1.16 (m/s)
Heat Flux	=	5.073E+05 (W/m^2)
Tube-metal thermal conduc.	=	385.0 (W/m.K)
Sieder-Tate constant	=	0.0645

UNCERTAINTY ANALYSIS:

VARIABLE	PERCENT UNCERTAINTY
Mass Flow Rate, Mc	3.01
Reynolds Number, Re	3.14
Heat Flux, q	3.05
Log-Mean-Tem Diff, LMTD	0.18
Wall Resistance, Rw	2.67
Overall H.T.C., Uo	3.06
Water-Side H.T.C., Hi	2.66
Steam-Side H.T.C., Ho	35.29

File Name:		30PSF04V'
Pressure Condition:		Vacuum (' kPa)
Steam Temperature	=	48.42 (Deg C)
Water Flow Rate (%)	=	80.00
Water Velocity	=	4.40 (m/s)
Heat Flux	=	2.324E+05 (W/m 2)
Tube-metal thermal conduc.	=	385.0 (W/m.K)
Sieder-Tate constant	=	0.0698

UNCERTAINTY ANALYSIS:

VARIABLE	PERCENT UNCERTAINTY
Mass Flow Rate, Md	.79
Reynolds Number, Re	'.'0
Heat Flux, q	:.54
Log-Mean-Tem Diff, LMTD	'.24
Wall Resistance, Rw	:.67
Overall H.T.C., Uo	'.39
Water-Side H.T.C., Hi	'.2'
Steam-Side H.T.C., Ho	4.87

DATA FOR THE UNCERTAINTY ANALYSIS:

File Name:		30PSF04V'
Pressure Condition:		Vacuum (' kPa)
Steam Temperature	=	48.39 (Deg C)
Water Flow Rate (%)	=	20.00
Water Velocity	=	'.'5 (m/s)
Heat Flux	=	1.946E+05 (W/m'2)
Tube-metal thermal conduc.	=	385.0 (W/m.K)
Sieder-Tate constant	=	0.0698

UNCERTAINTY ANALYSIS:

VARIABLE	PERCENT UNCERTAINTY
Mass Flow Rate, Md	3.00
Reynolds Number, Re	3.10
Heat Flux, q	3.08
Log-Mean-Tem Diff, LMTD	0.57
Wall Resistance, Rw	2.67
Overall H.T.C., Uo	3.13
Water-Side H.T.C., Hi	2.51
Steam-Side H.T.C., Ho	25.53

LIST OF REFERENCES

1. Honda, H., Nozu, and S., Mitsumori, K., "Augmentation of Condensation on Horizontal Finned Tubes By Attaching Porous Drainage Plates," *Proc. ASME-JSME Thermal Engineering Conference*, Hawaii, pp. 289-295, 1983.

2. Yau, K. K., Cooper, J. R., and Rose, J. W., "Effects of Drainage Strips and Fin Spacing on Heat Transfer and Condensate Retention for Horizontal Finned and Plain Condenser Tubes," *Fundamentals of Phase Change: Boiling and Condensation*, C. T. Avedisian and T. M. Rudy (Eds.), ASME, pp. 151-156, 1984.

3. Honda, H. and Nozu, S., "Effect of Drainage Strips on the Condensation Heat Transfer Performance of Horizontal Finned Tubes," *International Symposium on Heat Transfer*, Vol. 2, Beijing, 85-ISHI-11-32, 1985.

4. Wanniarachchi, A. S., Marto, P. J., and Rose, J. W., "Filmwise Condensation of Steam on Externally-Finned Horizantal Tubes," *Fundamentals of Phase Change: Boiling and Condensation*, HTD-Vol. 38, C. T. Avedisian and T. M. Rudy (Eds.), pp. 133-141, 1984.

5. Georgiadis, I. V., *Filmwise Condensation of Steam on low Integral-Finned Tubes*, M. S. Thesis, Naval Postgraduate School, Monterey, California, September 1984.

6. Flook, F. V., *Filmwise Condensation of Steam on Low Integral-Finned Tubes*, M. S. Thesis, Naval Postgraduate School, Monterey, California, March 1985.

7. Mitrou, E. S., *Film Condensation of Steam on Externally Enhanced Horizontal Tubes*, M. S. Thesis, Naval Postgraduate School, Monterey, California, March 1986.

8. Katz, D. L., Hope, R. E., and Dasko, S. C., *Liquid Retension on Finned Tubes*, Dept. of Eng. Research, University of Michigan, Ann Arbor, Michigan, Project M 592, 1946.

9. Rudy, T. M. and Webb, R. L., "Condensate Retention of Horizontal Integral-Fin Tubes," *Advances in Enhanched Heat-Transfer*, HTD-Vol. 18, Presented at 20th National Heat-Transfer Conference, Milwaukee, Wisconsin, August 1981.

10. Beatty, B. O. and Katz, D. L., "Condensation of Vapors on Outside of Finned Tubes," *Chemmical Engineering Process*, Vol. 44, No.1, pp. 55-69, January 1948.

11. Karkhu, V. A. and Borovkov, V. P., "Film Condensation of Vapor at Finely-Finned Horizontal Tubes," *Heat Transfer-Soviet Research*, Vol. 3, No. 2, pp. 183-191, March-April 1971.

12. Carnavos, T. C., "An experimental study: Condensation R-11 on Augmented Tubes," Asme paper No. 80-HT-54, 19th National Heat Transfer Conference, Milwaukee, Wisconsin, August 1981.

13. Krohn, R. L., *An Experimental Apparatus to Study Enhanced Condensation Heat-Transfer of Steam on Horizontal Tubes*, M. S. Thesis, Naval Postgraduate School, Monterey, California, June 1982.

14. Graber, K. A., *Condensation Heat Transfer of Steam on a Single Horizontal Tube*, M. S. Thesis, Naval Postgraduate School, Monterey, California, June 1983.

15. Poole, W. M., *Filmwise Condensation of Steam on Externally-Finned Horizontal Tubes*, M. S. Thesis, Naval Postgraduate School, Monterey, California, December 1983.

16. Wanniarachchi, A. S., Marto, P. J., and Rose, J. W., "Filmwise condensation of Steam on Horizontal Finned Tubes: Effect of Fin spacing, Thickness and Height," *Multiphase Flow and Heat Transfer*, HTD-Vol. 47, V. K. Dhir, J. C. Chen, and O. C. Jones (Eds.), pp. 93-99, 1985.

17. Mori, Y., Hijikata, K., Hirasawa, S., and Nakayama, W., "Optimized performance of Condensers with Outside Condensing Surface," *Condensation Heat-Transfer*, Presented at 20th National Heat Transfer Conference, San Diego, California, pp. 59-62, August 1979.

18. Gregorig, R., "Film Condensation on Finely Rippled Surfaces with Condensation of Surfaces Tension," *Zeitschrift fur Angewantde Mathematik und Physic*, Vol. V, pp. 36-49. (Translation by D. K. Edwards), 1954.

19. Rudy, T. M. and Webb, R. L., "An analytical Model to Predict Condensate Retention on Horizontal Integral-Fin Tubes," *ASME/JSME THERMAL Engrg. Joint Conf.*, Vol. 1, pp. 373-378, March 20-24, 1983.

20. Rudy, T. M. and Webb, R. L., "An analytical Model to Predict Condensate Retention on Horizontal Integral-Fin Tubes," *Journal of Heat Transfer*, Vol. 107, pp. 361-368, 1985.

21. Oven, R. G., Sardesai, R. G., Smith, R. A., and Lee W. C., "Gravity Controlled Condensation on a low-Fin Tube," *I. Chem. E. Symposium*, Series No. 75, pp. 415-428, 1985.

22. Rifert, V. G., "A New Method for Calculating Rates of Condensation on Finned Tubes," *Heat Transfer -Soviet Research*, Vol. 12, No. 3, May-June 1980.

23. Rudy, T. M. and Webb, R. L., "Theoretical Model for Condensation on Horizontal,Integral-Fin Tubes," *Heat Transfer*, Seattle, AIChE Symp. Ser., Vol. 79, No. 225, pp. 11-18, 1983.

24. Honda, H. and Nozu, S., "A Prediction Method for Heat-Transfer During Film Condensation in Horizontal Low Integral-Fin Tubes," *Fundamentals of Phase Change: Boiling and Condensation*, C. T. Avedisian and T. M. Rudy (Eds.), ASME, pp. 107-114, 1984.

25. Webb, R. L., Rudy, T. M., and Kedrizierski, M. A., "Prediction of the Condensation Coefficient on Horizontal Integral-Fin Tubes," *Journal of Heat Transfer*, Vol. 107, pp. 369-376, 1985.

26. Rudy, T. M., Kedzierski, M. A., and Webb, R. L., "Investigation of Integral-fin Type Condenser Tubes for Process Industry Applications," *First U. K. National Conference on Heat Transfer*, The Institution of Chemical Engineers Symposium Series No. 86, pp. 633-648, 1984.

27. Adamek, T., "Bestimmung der Kondensationgrossen auf feingewellten Oberflachen zur Auslegung aptimaler Wandprofile," *Warme und Stoffubertrangung*, Vol. 15, pp. 255-270, 1981.

28. Wanniarachchi, A. S., Marto, P. J., and Rose, J. W., "Film Condensation of Steam on Horizontal Finned Tubes: Effect of Fin Spacing," *Journal of Heat Transfer*, Vol. 108, pp. 960-966, November 1986.

29. Holman, J. P., *Heat Transfer*, 4th ed., McGraw-Hill Book Company, New York, p. 38, 1976.

30. Kline, S. J. and McClintok, F. A., "Describing Uncertainties in Single-Sample Experiments," *Mechanical Engineering*, Vol. 74, pp. 3-8, January 1953.

INITIAL DISTRIBUTION LIST

		No. Copies
1.	Defense Technical Information Center Cameron Station Alexandria, Virginia 22304-6145	2
2.	Library, Code 0142 Naval Postgraduate School Monterey, California 93943-5002	2
3.	Chairman, Code 69He Mechanical Engineering Department Naval Postgraduate School Monterey, California 93943-5000	1
4.	Professor P. J. Marto, Code 69Mx Department of Mechanical Engineering Naval Postgraduate School Monterey, California 93943-5000	5
5.	Professor A. S. Wanniarachchi, Code 69Wa Department of Mechanical Engineering Naval Postgraduate School Monterey, California 93943-5000	3
6.	Dr. John W. Rose Department of Mechanical Engineering Queen Mary College London E1 4NS England	1
7.	Dr. E. M. Sparrow Program Director Thermal Systems and Engineering Program National Science Foundation Washington, D. C. 20550	1
8.	LTJG Oguz Cakan Cevizli Dragos Acelya sok No:10 Kartal, Istanbul, Turkey	2
9.	Dz. K. Komutanligi Okullar ve Kurslar Dairesi Bakanliklar, Ankara, Turkey	5
10.	Deniz Harp Okulu Kutuphanesi Tuzla, Istanbul, Turkey	1
11.	Istanbul Teknik Universitesi Makine Fakultesi Kutuphanesi Istanbul, Turkey	1
12.	Istanbul Bogazici Universitesi Makine Fakultesi Kutuphanesi Istanbul, Turkey	1
13.	Ortadogu Teknik Universitesi Makine Fakultesi Kutuphanesi Ankara, Turkey	1

14. LT. Mitrou Evagelos, H. N.
19, Filikis Eterias St, Koridalos
Athens, Attiki, Greece 1

TITLE NUMBER _____ CUSTOMER NUMBER: _____

LIBRARY: Dudley Knox Library, Naval Postgraduate School
Monterey, Ca 93943

ROSWELL BOOKBINDING
LIBRARY DIVISION
2614 NORTH 29th AVENUE
PHOENIX, ARIZONA 85009
PHONE (602) 272-9338

Binding in Everything ☐

	F	B	NP
CONTENTS	☐	☐	☐
INDEX	☐	☐	☐
Bind without Index	☐	☐	☐

ISSUE CONTENTS

Discard	☐
Bind in Place	☐
Gather at Front	☐

	IN	OUT
Advertisements	☐	☐
Front Covers	☐	☐
Back Covers	☐	☐
1st only	☐	☐
Accents	☐	☐
Imprints	☐	☐

Special Instructions:

OGUZ CAKAN

C1855

Thesis C1855

Buck Color	598
Print Color	Gold
Trim Height	
Ht. Inches	
Over Thick	
For Title	
Extra Lines	
Extra Coll	
Hand Sew	
Slit	
Rules	
1st Slot No	
Vol Slot No	
Year Slot No	
Call # Slot	
Imp Slot No	
Type Face	
Price	
Mending	
Map Pockets	
2 Vols in 1	

ACTUAL TRIM	DATE
SPINE	JOB
BOARD DIM.	LOT
CLOTH DIM	ROUTE
CLOTH BIN	SEQ NO

Thesis
C1855
c.1

Cakan
Film condensation of steam on low-integral finned tubes with dr
age strips.